A DISSERTATION FOR
THE DEGREE OF DOCTOR OF PHILOSOPHY

# Identification of a *spotted leaf sheath* Gene and Proteomic Analysis of Rice Seedlings Exposed to Cold and Heat Stresses


BY

DONGRYUNG LEE


AUGUST, 2018


MAJOR IN CROP SCIENCE AND BIOTECHNOLOGY
DEPARTMENT OF PLANT SCIENCE
THE GRADUATE SCHOOL OF SEOUL NATIONAL UNIVERSITY

# Identification of a *spotted leaf sheath* Gene and Proteomic Analysis of Rice Seedlings Exposed to Cold and Heat Stresses

**UNDER THE DIRECTION OF DR. HEE-JONG KOH**
**SUBMITTED TO THE FACULTY OF THE GRADUATE SCHOOL**
**OF SEOUL NATIONAL UNIVERSITY**

**BY**
**DONGRYUNG LEE**

**MAJOR IN CROP SCIENCE AND BIOTECHNOLOGY**
**DEPARTMENT OF PLANT SCIENCE**

**APPROVED AS QUALIFIED DISSERTATION OF DONGRYUNG LEE**
**FOR THE DEGREE OF DOCTOR OF PHILOSOPHY**
**BY THE COMMITTEE MEMBERS**
**JULY, 2018**

**CHAIRMAN** Nam-Chon Paek, Ph.D.

**VICE-CHAIRMAN** Hee-jong Koh, Ph.D.

**MEMBER** Tae-Jin Yang, Ph.D.

**MEMBER** Kwang Soo Kim, Ph.D.

**MEMBER** Joohyun Lee, Ph.D

# Identification of a *spotted leaf sheath* Gene and Proteomic Analysis of Rice Seedlings Exposed to Cold and Heat Stresses

**DONGRYUNG LEE**

## GENERAL ABSTRACT

During the life span, plants are exposed to many stresses. Since plants, unlike animals, are incapable of maintaining the optimum condition for their growth, a slight change, even transiently, may affect physiological and biochemical processes crucial for plant growth and its production. Therefore, understanding the molecular mechanisms in response to biotic and abiotic stresses is important to develop cultivars with tolerance to various stress constraints.

In this study, we identified *spotted leaf sheath* (*sles*), a MAP kinase kinase kinase (MAPKKK) gene that is required for resistance against *Magnaporthe oryzae*. Two day after inoculation, the development of infectious hyphae (IH) were mostly restricted to primary infected cells with dark brown granules in *sles*

mutant while IH actively grew in wild type. ROS content was elevated in *sles* mutant, corresponding to increased expression of genes encoding ROS-generating enzymes. Moreover, the *sles* mutant showed lesion mimic spots on the leaf sheath rather than on leaves which differed from that of other lesion mimic mutants (LMMs). The *sles* mutant also displayed early senescence, as shown, by color loss in the mesophyll cells, a decrease in chlorophyll content, and upregulation of chlorophyll degradation-related and senescence-associated genes. Taken together, our results revealed that *SLES* is involved in ROS homeostasis resulting resistance against pathogen infection and formation of lesion mimic spots on the leaf sheath.

We also identified proteins differentially expressed in response to temperature stresses, including cold and heat, followed by recovery. Two rice cultivars with contrasting levels of tolerance to cold and heat stress, Koshihikari and Samnam, were used in this study. Proteomic responses of typical and healthy three-leaf old seedlings to sudden temperature changes were investigated. Rice seedling grown at 28/25° C (day/night) were subjected to 5 day exposure to 4° C (day/night) for cold stress, and 42° C (day/night) for heat stress, followed by 5 days of recovery. Mature leaves were harvested from plants from each treatment for protein extraction and subsequent triple TOF MS/MS analysis. Out of over 1192

proteins identified in one or more temperature treatment, more than 500 were found to be responsive to temperature stresses. Of these, 82, 159, 254, and 250 proteins were expressed in both cultivars at cold stress, recovery after cold stress, heat stress, and recovery after heat stress, respectively. In addition, 197 and 278 proteins were exclusively found in Koshihikari under cold stress and recovery and 104, and 155 proteins exclusively found in Samnam under heat stress and recovery, respectively. This study has provided a number of valuable molecular insights into temperature stress responses in rice and generated large number of candidate proteins that can form the basis of further detailed study.

**Keyword:** MAP kinase kinase kinase (MAPKKK), legion mimic mutants (LMMs), ROS homeostasis, defense response, proteomic analysis, temperature stresses

**Student Number:** 2012-30985

# CONTENTS

# LIST OF TABLES

# LIST OF FIGURES

# LIST OF ABBREVIATIONS

| | |
|---|---|
| LMM | Lesion mimic mutant |
| SLES | Spotted leaf sheath |
| HR | Hypersensitive response |
| ROS | Reactive oxygen species |
| LCD | Localized cell death |
| PR | Pathogenesis-related |
| MAPKKK | Mitogen-activated protein kinase kinase kinase |
| KD | Kinase domain |
| Chl | Chlorophyll |
| Car | Carotenoid |
| NBT | Nitro blue tetrazolium |
| DAB | 3, 3' –diaminobenzidine |
| BSA | Bulked segregant analysis |
| STS | Sequence-tagged site |
| CDS | Coding sequence |
| PB1 | Phox and Bem1p |
| DEP | Differentially expressed protein |
| FC | Fold-change |

# LITERATURE REVIEW

## Lesion mimic mutants

Lesion mimic mutants (LMMs) spontaneously form brown spots on leaves, which are caused by cell death, similar to lesions induced by pathogens. LMMs can be divided into two classes according to the mechanisms involved in controlling cell death: i) initiation mutants and ii) feedback or propagation mutants. Initiation mutants form localized necrotic spots of determined size whereas formation rate and lesion extent are not controlled in propagation mutants. Since some LMMs exhibit resistance to some pathogens, they are expected to be useful for investigating mechanisms of disease resistance. LMMs have been isolated and studies in many plant species, including *Arabidopsis*, maize, barley, and also in rice. Since Sekiguchi (1965) had isolated the first lesion mimic mutant in 1965, many others have been identified. Various phenotypes of mature leaves of LMMs are shown below (Mizobuchi et al., 2002; Wu et al., 2008). To the best of our knowledge, no LMMs in which lesion mimic spots are found on the leaf sheath have been identified in rice to date. The *sles* mutant identified in this study exhibited lesion mimic spots on the leaf sheath.

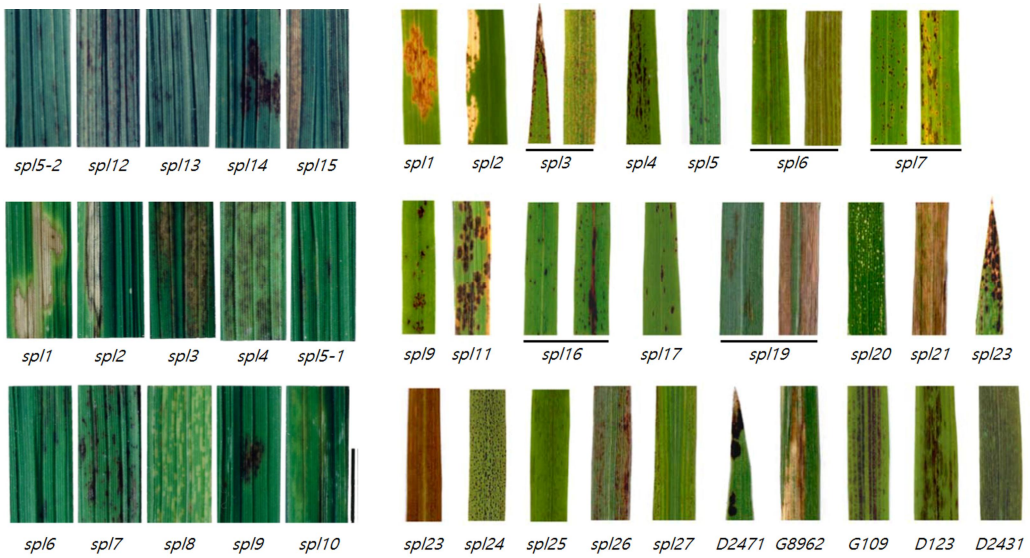


Plant Science (2002) Mol Genet Genomics (2008)

**MAPK cascades and MAPKKKs in plants**

Mitogen-activated protein kinase (MAPK) cascades mediate the intracellular transmission and amplification of extracellular stimuli, resulting in the induction of appropriate biochemical and physiological cellular responses (Lewis et al., 1998). They are conserved modules of signal transduction in all eukaryotes. These protein cascades are composed of the three classes of enzymes: MAPK kinase kinase (MAPKKKor MEKKs), MAPK kinase (MAPKK or MEKs), and MAPK. Upstream signals activate MAPKKKs, which then phosphorylate MAPKKs through phosphorylation of conserved serine and/or threonine residues in their activation loop (T-loop): MAPKKs in turn activate a specific MAPK via dual phosphorylation of conserved threonine and tyrosine residues in the motif TxY located in the T-loop between kinase subdomain VII and VIII. The downstream targets of MAPKs can be transcription factors, phospholipases, or cytoskeletal proteins (Lin et al., 1993; Sturgill and Ray, 1986; Tian et al., 2017).

In rice (*Oryza sativa*), there are 16 MAPKs, 8 MAPKKs, and 75 MAPKKKs (Hamel et al., 2006; Rao et al., 2010). Compared with MAPKs and MAPKKs, MAPKKKs have more complex and variable primary structures and domain compositions. MAPKKKs from higher plants can be divided into three distinct

categories, which include Raf, ZIK and MEKK subfamilies. There were 43 MAPKKKs grouped under Raf subfamily, 22 MAPKKKs grouped into MEKK subfamily, whereas only 10 MAPKKKs were grouped under ZIK subfamily. Most of the Raf subfamily proteins have a C-terminal kinase domain and a long N-terminal regulatory domain. In contrast, ZIK subfamily members have N-terminal kinase domain whereas members of MEKK subfamily has less conserved protein structure with kinase domain.

Several studies revealed that MAPKKK played an important role in regulating a range of biological processes, such as plant hormone signaling (Kieber et al., 1993; Wang et al., 2015), plant cytokinesis (Krysan et al., 2002), stomatal development (Kim et al., 2012), and responses to various stresses (Gao and Xiang, 2008). In recent years, the roles of individual plant MAPKKK proteins in defense responses and innate immunities also have been explored. Overexpression *NbMAPKKKα* in *N. benthamiana* leaves activated MAPKs and caused pathogen-independent cell death which restricted further pathogen growth (del Pozo et al., 2004). The tobacco *NPK1*, a homologs of human *MEKK1*, functions in the regulation of *N*-, *Bs2*-, and *Rx*-mediated resistance responses and regulates multiple cellular processes (Jin et al., 2002). However, biological functions of MAPKKKs involved in defense responses and innate immunities are yet to be clarified.

**Proteomic analysis**

Numerous studies investigating response to various stimuli by transcriptomics has been reported over the past years. Although this gene expression profiling under various stimuli has deepened our knowledge a great deal, changes in transcriptome are not always closely correlated with protein species (Gygi et al., 1999). Thus, molecular mechanisms underlying in cells coping with environmental change can only be interpreted through integration of both proteomics and transcriptomics.

Proteomic analysis (proteomics) refers to the systematic identification and quantification of the complete complement of proteins of a biological system (cell, tissue, organ, biological fluid, or organism) at a specific point in time. It became popular since 1990s and has greatly evolved to a mature stage today. The most frequently used proteomic technique was two-dimensional polyacrylamide gel electrophoresis (2D-PAGE) technique, which differentially expressed spots were excised and analyzed by mass spectrometry (MS). However, for certain groups of proteins, such as proteins with high molecular weights and isoelectric points and basic, hydrophobic membrane spanning proteins, and low abundant proteins, 2D-PAGE technique gives low resolution.

In recent years, a number of higher throughput and more sensitive liquid chromatography (LC) based approaches have been developed to profile plant proteomes. LC-based quantitative proteomic analysis methods are subdivided into two categories i) stable isotope labelling and ii) label-free approaches. Labelling approaches use mass tags, such as iTRAQ (isobaric tags for relative and absolute quantitation), SILAC (stable isotope labelling of amino acids in culture), ICAT (isotope coded affinity tagging), $^{15}N$ metabolic labelling. Label-free approaches include peak area integration and spectral counting. In this study, differentially expressed proteins under temperature stresses has been investigated by Triple Time of Flight Tandem Mass Spectrometer (Triple TOF MS/MS).

# CHAPTER I

# Identification of a *spotted leaf sheath* Gene Involved in Early Senescence and Defense Response in Rice

## ABSTRACT

Lesion mimic mutants (LMMs) commonly exhibit spontaneous cell death similar to the hypersensitive defense response that occurs in plants in response to pathogen infection. Several lesion mimic mutants have been isolated and characterized, but their molecular mechanisms remain largely unknown. Here, a *spotted leaf sheath* (*sles*) mutant derived from *japonica* cultivar Koshihikari is described. The *sles* phenotype differed from that of other LMMs in that lesion mimic spots were observed on the leaf sheath rather than on leaves. The *sles* mutant displayed early senescence, as shown, by color loss in the mesophyll cells, a decrease in chlorophyll content, and upregulation of chlorophyll degradation-related and senescence-associated genes. ROS content was also elevated, corresponding to increased expression of genes encoding ROS-generating enzymes. Pathogenesis-related genes were also activated and showed improved resistance to pathogen infection on the leaf sheath. Genetic analysis revealed that

the mutant phenotype was controlled by a single recessive nuclear gene. Genetic mapping and sequence analysis showed that a single nucleotide substitution in the sixth exon of *LOC_Os07g25680* was responsible for the *sles* mutant phenotype and this was confirmed by T-DNA insertion line. Taken together, our results revealed that *SLES* was associated with the formation of lesion mimic spots on the leaf sheath resulting early senescence and defense responses. Further examination of *SLES* will facilitate a better understanding of the molecular mechanisms involved in ROS homeostasis and may also provide opportunities to improve pathogen resistance in rice.

**Keyword:** Rice (*Oryza sativa* L.), lesion mimic spots, leaf sheath, early senescence, reactive oxygen species (ROS), Mitogen-Activated Protein Kinase Kinase Kinase (MAPKKK), defense

# INTRODUCTION

Leaf senescence, the final stage of leaf development, is primarily governed by leaf age. However, leaf senescence is also influenced by various internal and environmental signals that are integrated with the age information (Lim et al., 2007). Lesion mimic mutants (LMMs) are often associated with early leaf senescence. An *spl5* mutant continuously developed small reddish-brown necrotic lesions on leaves, leading to early senescence (Chen et al., 2012). An *lmes1* mutant also exhibited early senescence, with tiny brown spots developing initially at the leaf tip and spreading to the entire leaf surface (Li et al., 2014). Red-brown lesion spots on the leaf tips of a *vsl1* mutant led to plant death before the heading stage (Yin et al., 2015).

LMMs can be divided into two classes according to the mechanisms involved in controlling cell death: i) initiation mutants and ii) feedback or propagation mutants (Lorrain et al., 2003). Initiation mutants, such as *acd5*, *cpn1*, and *cpr5*, form localized necrotic spots of determinate size whereas formation rate and lesion extent are not controlled in propagation mutants, such as, *acd2*, *lsd1*, and *svn1* (Boch et al., 1998; Bowling et al., 1997; Dietrich et al., 1994; Greenberg et al., 1994, 2000; Jambunathan et al., 2001; Lin and De Wit, 1999; Mach et al., 2001; Rustérucci et al., 2001).

The necrotic spots formed in LMMs resemble those formed during the pathogen infection-induced hypersensitive response (HR). HR is an important resistance mechanism that prevents pathogen spread to adjacent cells by inducing cell death in infected regions (Lam et al., 2001). Reactive oxygen species (ROS) are thought to prime the orchestration of the HR (Zurbriggen et al., 2010). During HR, rapid production of ROS, such as hydrogen peroxide ($H_2O_2$), superoxide ($O_2^-$) and its more toxic derivatives, hydroxyl radicals ($OH^-$), and singlet oxygen ($^1O_2$), is stimulated in mitochondria and chloroplast as well as the cytoplasmic level (Zurbriggen et al., 2010). Recent observations suggest that chloroplast-derived ROS play a key role in localized cell death (LCD) during HR (Zurbriggen et al., 2010).

Plants use two types of defense mechanisms to combat oxidative stress. These mechanisms involve non-enzymatic antioxidants such as ascorbate and glutathione, or enzymatic antioxidants such as catalase, superoxide dismutase, and ascorbate peroxidase (Navabpour et al., 2003). Either over-accumulation of ROS or the failure of these oxidative stress defense mechanisms will result in cell death. HR is usually accompanied by the activation of pathogenesis-related (*PR*) genes. Expression of *PR1a* and *PR1b*, which encoded acidic and basic proteins, respectively, was induced upon infection with rice blast fungus

(Agrawal et al., 2000). Expression of *PR5* family genes, which encode thaumatin-like proteins, was induced in plants in response to infection by plant pathogens, elicitors, stress, and developmental signals (Bryngelsson and Green, 1989). Proteins of the PR10 family were involved in multiple anti-pathogen processes, and are generally localized in the intracellular spaces, in contrast to the extracellular nature of most PR proteins (Jwa et al., 2001; Van Loon and Van Strien, 1999).

LMM genes encode wide range of functional protein types, such as phenolic compounds (Gray et al., 1997), porphyrin (Ishikawa et al., 2001), heat stress transcription factor (Yamanouchi et al., 2002), U-Box/Armadillo repeat protein (Zeng et al., 2004), zinc finger proteins (Wang et al., 2005), membrane-associated proteins (Noutoshi et al., 2006), ion channel family member (Mosher et al., 2010), clathrin-associated adaptor protein (Qiao et al., 2010), and splicing factor 3b subunit 3 (Chen et al., 2012), indicating the involvement of complex and diverse molecular mechanisms in lesion mimic spot formation.

Recently, (Wang et al., 2015) showed that Mitogen-Activated Protein Kinase Kinase Kinase (MAPKKK) was also involved in the formation of lesion mimic spots. Several studies revealed that MAPKKK played an important role in

regulating a range of biological processes, such as responses to various stresses (Gao and Xiang, 2008; Mizoguchi et al., 1998), plant cytokinesis (Krysan et al., 2002; Nishihama et al., 2001), stomatal development (Kim et al., 2012), ethylene signaling (Kieber et al., 1993), ABA signaling (Wang et al., 2015), innate immunity (Asai et al., 2002), and defense responses (Frye et al., 2001; Suarez-Rodriguez et al., 2007). However, the relationship between HR and MAPK cascades remains poorly understood.

In this study, a new lesion mimic mutant (*sles*) was identified. In contrast to other LMMs, which exhibited necrotic spots on leaves, lesion mimic spots in the *sles* mutant covered the leaf sheath resulting in early senescence. Fine-mapping and sequence analysis revealed that the *sles* locus encoded a kinase domain (KD) containing protein of the Raf MAPKKK family. Greenness and chlorophyll content were adversely affected in mesophyll cells in the *sles* mutant. Expression of genes encoding ROS-generating enzymes was induced in the *sles* mutant and ROS accumulation increased accordingly. Defense response genes were also activated, suggesting that resistance to pathogen infection of the leaf sheath might be enhanced in the *sles* mutant. These results are relevant to future research into the mechanisms involved in the formation of lesion mimic spots, ROS homeostasis, and resistance to diseases in plants.

# MATERIALS AND METHODS

**Plant material and growth conditions**

The *sles* mutant was isolated through EMS treatment of the *japonica* cultivar Koshihikari and was maintained at the Rice Gene Bank of the Department of Plant Science, Seoul National University, Seoul, Korea. The *sles* mutant was crossed with Koshihikari (*japonica*) and Milyang 23 (M.23). M.23 is a *Tongil*-type rice derived from a *japonica* × *indica* cross. The M.23 genetic background is similar to that of *indica*. For phenotypic characterization and genetic mapping, plants were grown by conventional culture at the Experimental Farm of Seoul National University. $F_2$ populations and parents were seeded in a plastic tunnel seedbed. Forty-day-old seedlings were then transplanted, one plant per hill, into a paddy field. The two-tailed Student *t*-test was used to compare the agronomic traits of *sles* mutant and wild type plants. 10 independent plants were measured to calculate the means values.

**Anatomical characterization**

For light microscopic study, thin sections of 100-day-old wild-type penultimate leaf sheath and non-spotted and spotted regions of the sles mutant leaf sheath were cut using a sharp blade and observed using an Olympus CX31 dissecting

microscope (Olympus, Japan) under white light. Photographs were taken using an Olympus eXcope T500 digital camera (Olympus, Japan). Three independent plants were used for the anatomical characterization.

**Chlorophyll and carotenoid content measurements**

Chlorophyll (Chl) a, Chlb, and carotenoid contents were assessed in the penultimate leaf sheath from 120-day-old wild-type and *sles* mutant plants. Absorption values were measured as described by (Arnon, 1949) using UV/Vis spectrophotometer (Biochrom Libra S22, USA). The two-tailed Student t-test was used to compare the pigment intensity between *sles* mutant and wild type plants. Three biological replicates were used for the experiment.

**Histochemical characterization**

For $O_2^-$ determination, penultimate leaves and leaf sheath samples from 100-day old plants were vacuum-infiltrated (three cycles of 10 min) in 0.5 mg $ml^{-1}$ nitro blue tetrazolium (NBT) in 10 mM potassium phosphate buffer (pH 7.8) for 16 h. For $H_2O_2$ detection, samples were vacuum-infiltrated (three cycles of 10 min) in 1 mg $ml^{-1}$ 3,3′-diaminobenzidine (DAB) containing 10 mM MES (pH 6.5) for 16 h. Reactions were stopped by transferring tissue to 90% ethanol and incubating at 70°C until chlorophyll was completely removed. The cleared leaves and leaf

sheaths were examined and photographed after a 2-4 h incubation period. Trypan blue staining was performed on fresh leaf and leaf sheath as previously described by Qiao et al. (2010). Samples were submerged in lactic acid-phenol-trypan blue solution (LPTB; 2.5 mg $ml^{-1}$ trypan blue, 25% (w/v) lactic acid, 23% water-saturated phenol and 25% glycerol in $H_2O$) at 70°C, infiltrated by slow-release vacuum for 4 min, and then re-infiltrated. Samples in LPTB were heated in boiling water for 2 min and then cooled for 1.5 h before LPTB solution was replaced with visikol for destaining. The cleared leaves and leaf sheaths were examined and photographed after 3 d incubation period. All the experiments were performed in 10 biological replicates.

**Blast resistance evaluation**

The *Magnaporthe oryzae* strain KJ201 was provided by Department of Agricultural Biotechnology, College of Agriculture and Life Sciences, Seoul National University, Seoul, Korea. The *sles* mutant and wild type plants were grown in the greenhouse at 28/25°C, day/night, and were inoculated with KJ201 suspension into the leaf sheath of 50-day-old seedlings in a procedure described by Koga et al. (2004). The blast resistance evaluation was determined 2 days after inoculation by the invasive hyphae on inoculated leaf sheath.

**RNA isolation and Real-Time RT-PCR**

Total RNA was extracted from the penultimate leaf sheath of *sles* mutant and wild-type plants after heading using Iso-Plus reagent (Takara Bio, Japan) according to the manufacturer's instructions. RNA was then treated with RNA-free DNase I (Promega, USA) to remove any remaining genomic DNA. DNase-treated RNA was reverse transcribed to first-strand cDNA using M-MLV reverse transcriptase (Promega, USA). Real-time PCR was performed using a CFX96 Real-time PCR detection system with SYBR Premix Ex Taq (Takara Bio, Japan). Primer3web (http://bioinfo.ut.ee/ primer3/) was used to design primers that spanned an intron to enhance specific amplification of target fragments. Primers used for gene-specific PCR are listed in **Table 1-1**. Data were analyzed using the comparative Ct method. The two-tailed Student *t*-test was used to compare the expression level between *sles* mutant and wild type plants.

**Table 1-1** Primers used in this study

| Purpose | Primer name | Forward primer (5' → 3') | Reverse primer (5' → 3') |
|---|---|---|---|
| Mapping | S07050a | CTCCACTTATGGCAGCGAAT | CAAGTGAAGTGGGAGCAGGT |
| | S07053 | CGAAACTTTGGGACGAAATG | CGTCCACCATTCACTGTCAC |
| | 147-1 | GCCAGTACATCCTCGTTCGT | GAGCATGGAGGATCCAAAGA |
| | 147-1-1 | AACCATGCATTGCAACAGAC | GCTGAATCAAACAGGGCTTT |
| | 147-2 | CTTGTGCGCCTGGAATATG | TCGATAAACTCATCCGACGTA |
| Real-time | SGR | GGCCTCCGCTACTACATCTT | GGGAGGTTGGAGTGGAAGTA |
| PCR | NYC3 | TGTGCTCCAAAGGGACAAAT | GATTCTGGCACCTGCTGTTT |
| | NYC1 | GCTTGCCTTGGTTACTGCAT | TTCAGCCCAATTACGGATTC |
| | NOL | ACATCCGTTTTCTCACAGGC | GGCAGCAAAACGGACACTAA |
| | WRKY23 | TACCGATGGAGGAAGTACGG | CTTGCTTCTTCACGTTGCAC |
| | WRKY72 | GCTTCCCACATGTTCCAGTAG | TTTTCCTGCTAACATCCATCG |
| | Osl2 | GCAGACAACAAATCGCCAAAT | TCTCCAGCAACTCTAACCAGCAT |
| | Osl30 | GAGAAATCCCTTGAAGCCAA | CACAAAGCAGTGAAAGCACA |
| | Osl43 | TGTGACAAGTGCTAATAATACATACGA | CCAGACCTTCCAAAGAATCCAAC |
| | Osl85 | TCCAGGATGTGATGAGGATTATTC | GCGTGCTGTAGTTCAGTCTGTAAAG |
| | Osh36 | GTGCACCATGCACTTAATCC | CACCGACCCTTCCTGTAGTT |
| | Osh69 | ACGAGCTACACGCCTACCTT | ACTTCCTTGCCAGAAGCACT |
| | PAO | CCTAGCCAAGAAGTGTTGCC | TCGCTCCCATGAAGACCTTT |
| | NOX1 | AGGCCGACTGCTTCCTCT | CACTGACAATTGCAGCAGGT |
| | NOX2 | ACTGCTTCCTCTTCGCCTCT | CTCTGTCAGCCCAGCAGTT |
| | SODA | ATCTGGATGGGTGTGGCTAGCTTT | AGTACGCATGCTCCCAGACATCAA |
| | SODB | TCCGCCGTATAAACTTGATGCCCT | TGGGTTGCCGTTGTTGTATGCTTC |
| | SodCc1 | GTGCATGCCGATCCTGATG | CTGGGAGATGGAAGGTGAGT |
| | SodCc2 | TGTGACGGGAAGTGTCTCTG | AGTAAGGGGGATCTGGCTGT |
| | CATA | CAACCGCAACGTCGACAACTTCTT | TTCACCGGCAGCATCAGGTAGTTT |
| | CATB | GCTTGCTTTCTGCCCAGCGATAAT | AAATAGTTTGGGCCAAGACGGTGC |
| | CATC | CCACGAGATCAGGAGCATCT | TCCGTGACTGAAGCAGATTG |

| | | | |
|---|---|---|---|
| | APX1 | AGGTGCCACAAGGAAAGATCTGGT | TCAGCAGGGCTTTGTCACTAGGAA |
| | APX2 | TGGGAAGATGCCACAAGGAGAGAT | TCCGCAGCATATTTCTCCACCAGT |
| | APX4 | GAAGCTCCCAACTGACAAGG | TTGTGCGATTCAGCGTAGTC |
| | APX5 | CTGAAGCTCATGCCAAACTG | TATCACTCGCCAAAATGCAG |
| | APX6 | CTGAAGCTCATGCCAAACTG | CTTGTTCATTCGCCAAAATG |
| | APX7 | TACGCAGAGGACCAAGAAGC | ACTTCAGCGATCTGGCTCAT |
| | APX8 | CAGTAACGGTAGGAGCAGCA | TACTCCGCCCTGATCTTCTG |
| | PR1a | TTCATCACCTGCAACTACTCG | TGCATAAACACGTAGCATAGCAT |
| | PR5 | ATCGACGGCTACAACGTC | GTGTCTTGGTGTTGTCTTCG |
| | PR10 | CACCATCTACACCATGAAGC | AGCACATCCGACTTTAGGAC |
| | eEF1a | AGCACGCTCTTCTTGCTTTC | TGTAGCCGACCTTCTTCAGG |
| dCAPS | HphI | GGGACTCTCCCATGGGTG | GCCAAAGGAAAATACATCAACC |
| T-DNA | 11526 | CGATCGGGATTGTTAGCTGT | TTCAGCAACACGTACTAAAATGA |
| insertion | 2715 | AGCACCCCAAGTTAGTCATGT | |

**Genetic analysis and molecular mapping of *sles***

For genetic analysis, $F_2$ populations were developed from two crosses: *sles* mutant × M.23 and *sles* mutant × Koshihikari. Genomic DNA samples were extracted from young leaves of each parent and $F_2$ individuals using the CTAB method. Bulked segregant analysis (BSA) was performed for preliminary genetic mapping using sequence-tagged site (STS) markers designed at the Crop Molecular Breeding Lab, Seoul National University (Chin et al., 2007). Two molecular markers flanking the primary candidate region were used to screen recombination events from 628 $F_2$ individuals. To fine map *sles*, new STS

markers between the two flanking markers were designed based on the sequence difference between japonica variety Nipponbare and the indica variety 93-11. Primers used for genetic mapping are listed in **Table 1-1**.

**Sequence analysis of candidate genes**

Gene prediction analysis was performed using the Gramene database (http://www.gramene.org) and *sles* candidate genes were analyzed further. The sequence of the AP005101 BAC clone was used to design 28 specific primers for sequence analysis of *sles* candidate genes. PCR-amplified products were purified using Inclone$^{TM}$ Gel & PCR purification kit (Inclone Biotec, Republic of Korea), TA-cloned into the pGEM-T Easy Vector (Promega, Madison, USA), and transformed into *E. coli* strain DH5α for sequencing.

**Genotyping of T-DNA insertion mutants**

To select T-DNA insertion lines, 20 dehulled $T_1$ seeds were surfaced-sterilized, placed on 1/2 MS media containing 50 mg/ml hygromycin, and allowed to germinate in the dark at 37°C. To genotype T-DNA insertion lines, three primers were designed based on sequence information for T-DNA insertion positions available at RiceGE (http://signal.salk.edu/cgi-bin/RiceGE). Primers used for PCR are listed in **Table 1-1**. PCR was used to test co-segregation between

flanking sequences and the mutation phenotype. Primers 11526-F and 11526-R were designed using rice genome sequences containing the T-DNA inserted region, and primer 2715-F was designed to the right border sequence of the T-DNA.

**Amino acid sequence alignment and phylogenetic relationship**

Homologs of SLES were identified in other species using search functions at the NCBI website. Multiple sequence alignments were conducted using Clustal X (http://www.clustal.org/) and edited with BOXSHADE (http://www.ch.embnet.org/software/BOX_form.html). Sequence homology searches in GenBank were carried out using BLAST (http://blast.ncbi.nlm.nih.gov/Blast.cgi). NCBI web-based searches were used for conserved domain prediction of the SLES protein (https://www.ncbi.nlm.nih.gov/cdd).

# RESULTS

**Phenotypic characterization of the *sles* mutant**

Wild-type and mutant plants were phenotypically and agronomically compared. The mutant exhibited lesion mimic spots on the leaf sheath (**Figure 1-1A**). Sparse spots appeared initially at the two-leaf stage and later expanded to cover the entire leaf sheath, resulting in earlier senescence than in wild type (**Figure 1-1B**). Lesion mimic spots were restricted to the leaf sheath and were not observed on leaves. Based on these observations, the mutant was designated *spotted leaf sheath* (*sles*). Lesion mimic spots also appeared on *sles* mutant roots (**Figure 1-1C**), initiating at the same growth stage as spot appearance on the leaf sheath.

Wild-type and *sles* mutant plants were significantly different with respect to agronomic traits (**Table 1-2**). Seed germination rate was substantially lower in the mutant, at 52.7% compared to wild-type rate of 86.5%. Seedling vigor at the 3-leaf-seedling stage, as determined by shoot length, root length, fresh weight, and dry weight, was significantly reduced in the *sles* mutant compared to wild type. Leaf emergence was also slower in the *sles* mutant than in wild type. In the reproductive stage, plant height and number of tillers were significantly reduced in the *sles* mutant compared to wild type. Grains were smaller and thinner in the

*sles* mutant than in wild-type. However, grain shape, which was determined by the grain length/width ratio, was similar between wild type and the *sles* mutant. Heading was delayed by a week in the *sles* mutant compared to wild type. Nevertheless, the *sles* mutant senesced more rapidly than wild type and *sles* leaves yellowed 4 weeks after heading while wild-type plants remained green (**Figure 1-1B**). Yield-related agronomic traits such as spikelet number per panicle, seed-setting rate, and 1,000-grain weight were all significantly adversely impacted compared to wild type.

**Table 1-2.** Agronomic traits of *sles* mutant and wild type plants

| Traits | GR (%) | SL (cm) | RL (cm) | FW (mg) | DW (mg) | PH (cm) | TN (No.) | GL (mm) | GW (mm) | GWR | SN (No.) | SF (%) | KGW (g) |
|---|---|---|---|---|---|---|---|---|---|---|---|---|---|
| WT | 86.5 | 16.2 | 12.7 | 123.6 | 22.0 | 113. | 11.1 | 0.71 | 0.33 | 2.2 | 122. | 90.7 | 25.0 |
| *sles* | 52.7 | 13.8 | 11.2 | 91.4 | 15.2 | 97.3 | 6.1 | 0.67 | 0.30 | 2.2 | 100.8 | 69.4 | 17.4 |
| Difference | ** | ** | * | ** | ** | ** | ** | ** | ** | NS | * | ** | ** |

GR, germination rate; SL, shoot length; RL, root length; FW, fresh weight; DW, dry weight; PH, plant height; TN, tiller number; GL, grain length; GW, grain weight; GWR, GL/GW ratio; SN, number of spikelets per panicle; SF, spikelet fertility; KGW, 1000-grain weight; NS, not significant. 10 independent plants were measured to calculate the means value. Asterisks indicate statistical significance level according to Student's *t* test: **P<0.01 and *P<0.05.

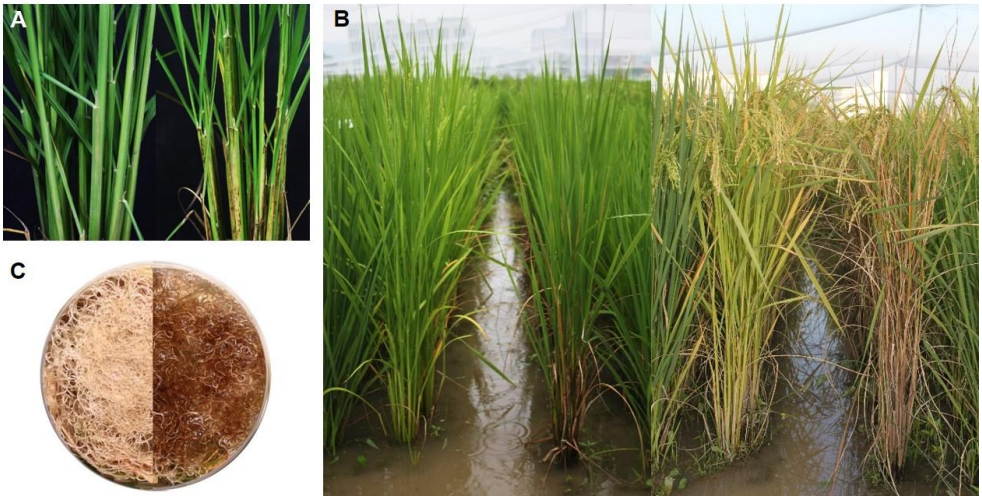


**Figure 1-1. Morphological comparisons between wild-type and *sles* mutant plants. (A)** Wild type (left) and *sles* mutant (right) at 60 day after germination. **(B)** 90-day-old and 120-day-old wild type (left) and *sles* mutant (right). **(C)** Root color in wild type (left) and *sles* mutant (right).

**Anatomical characterization of the *sles* mutant**

Leaf sheath anatomical features were examined in wild-type and *sles* plants using a light microscope (**Figure 1-2**). Differences in mesophyll greenness level were apparent between wild type and *sles* mutant tissues. Palisade parenchyma of mesophyll cells were green and filled with chloroplast in leaf sheath sections from wild type and non-spotted regions close to spots in the *sles* mutant. However, although the palisade parenchyma of mesophyll cells from non-spotted *sles* regions were green, dark brown areas were sometimes observed in the spongy parenchyma of the mesophyll cells **(Figures 1-2A, B, D, E)**. In the spotted region of *sles* mutant leaf sheath, however, mesophyll cells were completely dark brown **(Figures 1-2C, F)**, indicating their death.

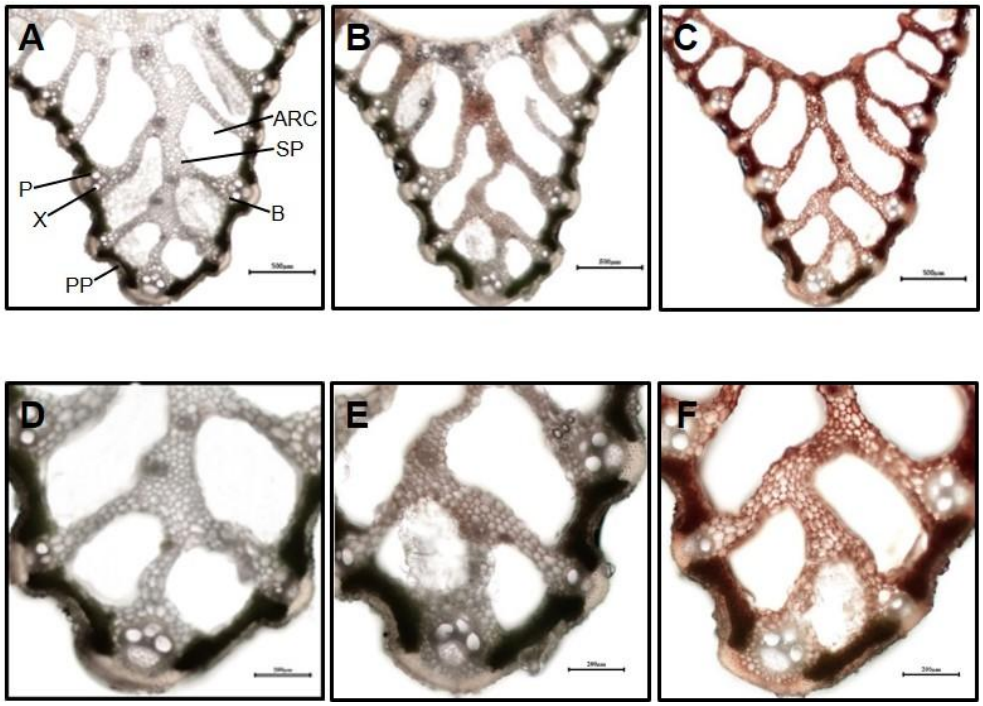


**Figure 1-2. Light microscopic analysis of spotted and non-spotted leaf sheath from *sles* mutant and wild type plants.** Transverse sections of penultimate leaf sheaths were observed under white light. **(D)**, **(E)**, and **(F)** are magnified view of **(A)**, **(B)**, and **(C)**, respectively. **(A)** and **(D)** are wild type leaf sheath sections. **(B)** and **(E)** are non-spotted and **(C)** and **(F)** are spotted leaf sheath sections from the *sles* mutant. Indications in **(A)** are ARC, aerenchyma; B, bundle sheath; P, phloem; PP, palisade parenchyma; SP, spongy parenchyma; X, xylem.

**Leaf sheath chlorophyll and carotenoid content in the *sles* mutant**

Lesion mimic spots on the leaf sheath were not green in the *sles* mutant. To quantify this, contents of chlorophyll and carotenoid, the two most important pigments in rice, were compared between *sles* mutant and wild type (**Figure 1-3A**). Total chlorophyll content and Chla and Chlb levels were significantly lower in *sles* spotted regions than in wild type. The Chla/Chlb ratio was also significantly lower in the *sles* mutant than in wild type, indicating that Chla content had decreased to a greater extent than Chlb content in the *sles* mutant. The Chla/Chlb ratio was also significantly different between the non-spotted region of the *sles* mutant and the wild type, but there were no apparent differences in total chlorophyll content or Chla and Chlb levels. Carotenoid content was also significantly lower in the spotted region of the *sles* mutant leaf sheath than in wild type. Overall, the dark brown spotted regions of the *sles* mutant leaf sheath correlated with reductions in chlorophyll content.

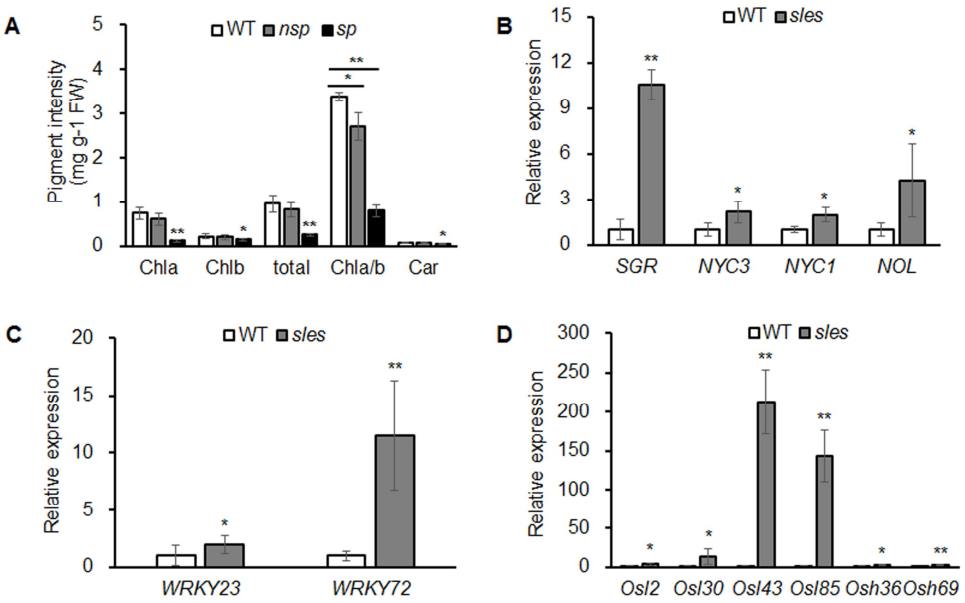


**Figure 1-3. Early senescence in the *sles* mutant leaf sheath. (A)** Abundance of major plant pigments in non-spotted (*nsp*) and spotted (*sp*) leaf sheaths from the *sles* mutant and wild-type (WT) leaf sheaths. **(B)** Expression of chlorophyll degradation-related genes. **(C)** Expression of senescence transcription factors. **(D)** Expression of senescence-associated genes. Real-time PCR (three biological replicates and three technical replicates) was performed with WT leaf sheath samples and *sles* leaf sheath samples from regions with legion mimic spots. Asterisks indicate the statistical significance levels according to Student's *t* test: **P<0.01 and *P<0.05.

**Senescence-related gene expression in the *sles* mutant**

Significantly lower chlorophyll content were observed in the sles mutant than in wild type, and we thus examined the expression of chlorophyll degradation-related genes such as *SGR*, *NYC1*, *NYC3*, and *NOL*. *STAY GREEN* (*SGR*) was reported to regulate chlorophyll degradation by inducing the disassembly of light-harvesting chlorophyll binding protein II (LHCP II) (Park et al., 2007). *NON-YELLOW COLORING* (*NYC1*) and *NYC1-like* (*NOL*) were shown to regulate Chlb degradation (Kusaba et al., 2007; Sato et al., 2009). *NON-YELLOW COLORING3* (*NYC3*) was implicated in chlorophyll breakdown (Morita et al., 2009; Tanaka and Tanaka, 2011). Expression analysis showed that the chlorophyll degradation-related genes, particularly *SGR*, were dramatically upregulated in the sles mutant compared to wild type **(Figure 1-3B)**. To confirm that senescence occurred in the leaf sheath of the sles mutant, expression of senescence transcription factors (*OsWRKY23* and *OsWRKY72*) and senescence-associated genes (*Osl2*, *Osl30*, *Osl43*, *Osl85*, *Osh36*, and *Osh69*) were examined using real-time PCR **(Figures 1-3C, D)**. All eight genes, particularly *Osl43* and *Osl85*, exhibited elevated expression in the leaf sheath of the sles mutant, compared to wild type, consistent with the early senescence phenotype.

**HR-like lesions in the *sles* mutant**

Histochemical markers were examined to investigate putative mechanisms underlying the development of lesion mimic spots in the *sles* mutant **(Figure 1-4A)**. The leaf sheath of *sles* mutant exhibited strong blue color of cells compared to that of wild type after staining with trypan blue, which is a histochemical indicator of irreversible membrane damage or cell death. There was no evidence of ROS production in the wild-type leaf sheath, but the pattern of NBT staining, an indicator of $O_2^-$ accumulation, correlated strongly with lesion formation on the *sles* mutant leaf sheath. In leaves, there were negligible differences in ROS production between *sles* mutant and wild type. Similar results were obtained with 3,3′-diaminobenzidine (DAB) staining, which indicated $H_2O_2$ accumulation. These results confirmed that ROS accumulation in the leaf sheath of *sles* mutant lead to cell death and ultimately accelerated senescence.

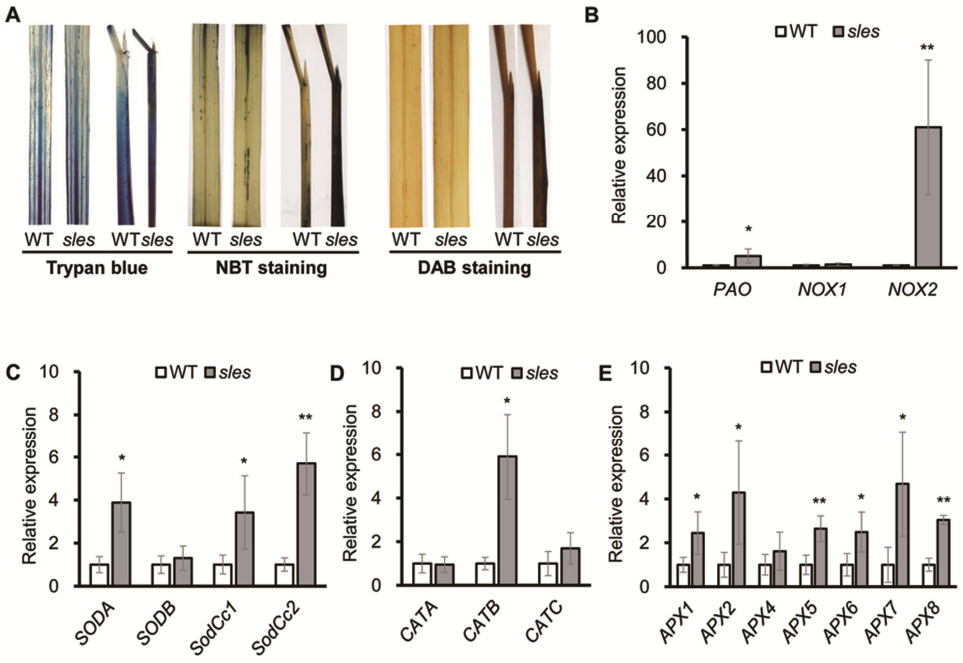


**Figure 1-4. ROS accumulation and expression of ROS homeostasis-related genes. (A)** Trypan blue, NBT and DAB staining of penultimate leaves and leaf sheaths in wild-type and *sles* mutant plants after heading. **(B)** Expression of genes encoding ROS-generating enzymes in wild-type and *sles* mutant **(C, D, E)** Expression levels of ROS detoxification-related genes in wild-type and *sles* mutant. Real-time PCR (three biological replicates and three technical replicates) was performed with leaf sheath samples form wild type and from areas with legion mimic spots in the *sles* mutant. Asterisks indicate the statistical significance level according to Student's *t* test: **P<0.01 and *P<0.05.

**ROS homeostasis-related gene expression in the *sles* mutant**

NADPH oxidase (NOX) and polyamine oxidase (PAO) are major ROS sources. Expression of *NOX1*, *NOX2*, and *PAO* was significantly increased in the spotted region of *sles* mutant leaf sheath (**Figure 1-4B**). Complex antioxidant systems in diverse subcellular compartments tightly regulate the abundance of intercellular ROS. These ROS scavenging systems include major enzymes, such as superoxide dismutase (SOD), catalase (CAT), and ascorbate peroxidase (APX), that coordinately function in ROS detoxification (Mittler et al., 2004). As *sles* mutants exhibited enhanced ROS accumulation, we next examined gene expression of ROS scavenging genes (*SODA*, *SODB*, *SodCc1*, *SodCc2*, *CATA*, *CATB*, *CATC*, *APX1*, *APX2*, *APX3*, *APX4*, *APX5*, *APX6*, *APX7*, and *APX8*) (**Figure 1-4 C, D, E**) and found that most were significantly upregulated in the *sles* mutant compared to wild type.

**Blast resistance in the *sles* mutant**

ROS contribute to accelerated transcriptional activation of *PR* genes, leading to production of antimicrobial secondary metabolites and localized cell death (LCD) (Zurbriggen et al., 2010). As ROS accumulation was observed in the spotted region of the *sles* mutant leaf sheath, expression of three *PR* marker genes (*PR1a*, *PR5*, and *PR10*) associated with the defense response was

examined (**Figure 1-5A**). All the *PR* genes were significantly upregulated in the *sles* mutant compared to wild type.

To evaluate response of the *sles* mutant to rice blast, the development of infectious hyphae (IH) within the host cells was observed using an excised leaf sheath assay (**Figure 1-5B**). IH actively grew and occupied 5-7 cells neighboring the primary infected cells by 48 h after inoculation in wild type. However, IH were mostly restricted to the primary infected cell, and there was an abundant accumulation of dark brown granules along IH in *sles* mutant. These results indicated that *sles* mutant conferred significantly enhanced resistance to rice blast compared to wild type.

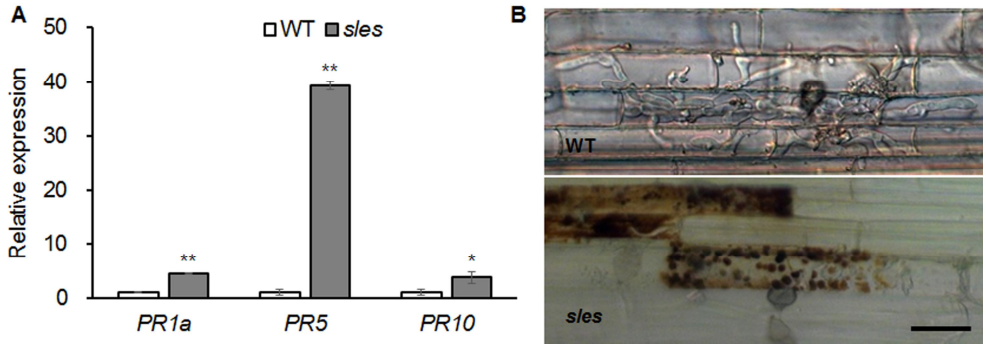


**Figure 1-5. Blast resistance in the *sles* mutant. (A)** Expression of pathogenesis-related marker genes. Real-time PCR (three biological replicates and three technical replicates) was performed with leaf sheath samples from wild type and from areas with legion mimic spots in the *sles* mutant. Asterisks indicate the statistical significance level according to Student's *t* test: **P<0.01 and *P<0.05. **(B)** The excised leaf sheath from 50-day-old rice seedlings of WT and *sles* mutant was inoculated with conidial suspension ($1 \times 10^4$ conidia/ml). Samples were harvested and observed 48 h after inoculation. Bar = 25μm.

**Genetic analysis of the *sles* mutant**

$F_1$ and $F_2$ plants from crosses between the *sles* mutant and M.23 were used to determine whether the phenotype was dominant or recessive, and whether the *sles* mutant phenotype was controlled by multiple genes or by a single gene. $F_1$ plants exhibited the wild-type phenotype, indicating that the *sles* mutant phenotype was recessive. The $F_2$ population contained 492 wild-type plants and 136 plants with the *sles* phenotype, fitting a 3:1 ratio ($\chi^2_{(3:1)}=3.75<\chi^2_{0.05}=3.84$, $P=0.06$). In another population of 55 $F_2$ individuals derived from *sles* mutant/Koshihikari, the phenotype of 46 plants were wild type and 9 plants were *sles* mutant phenotype, matching a 3:1 ratio ($\chi^2_{(3:1)}=2.19<\chi^2_{0.05}=3.84$, $P=0.14$). This indicated that the *sles* phenotype was controlled by a single recessive nuclear gene.

**Genetic mapping and identification of the *SLES* gene**

An $F_2$ population derived from a cross between the *sles* mutant and M.23 was used to map the locus responsible for the *sles* mutant phenotype. Bulked segregant analysis (BSA) using 60 polymorphic STS markers evenly distributed across the 12 rice chromosomes was used for preliminary genetic mapping. BSA mapped the *sles* locus to the interval between STS markers S07050a and S07053 **(Figure 1-6A)**. To fine map the *sles* locus, new STS markers were designed

between the two flanking markers based on the differences in DNA sequence between *indica* and *japonica* rice varieties. Using 628 $F_2$ individuals, the *sles* locus was mapped to the interval between markers 147-1 and 147-2, an approximately 66 kb physical distance in Nipponbare **(Figure 1-6A)**. Eight predicted candidate genes were located within the 66 kb candidate region, and the region was encompassed by BAC clone AP005101 **(Table 1-3)**.

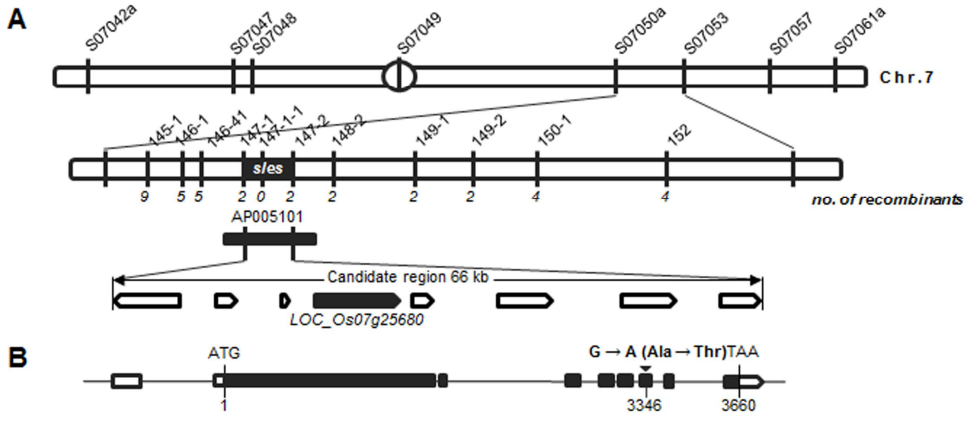


**Figure 1-6. Fine-mapping and identification of *SLES*.** **(A)** Fine-mapping of *SLES*. The *sles* locus was mapped to a 66 kb region on chromosome 7. **(B)** Schematic diagram of *SLES*. Black rectangles represent exons and the black inverted triangle represents the mutation site. **(D)** Seedling. **(E)** Leaf sheath. **(F)** Root. Real-time PCR (three biological replicates and three technical replicates) was performed. Asterisks indicate the statistical significance levels according to Student's *t* test: **P<0.01 and *P<0.05.

**Table 1-3** Predicted genes in the mapped *sles* region (66 kb)

| Gene name | Size (bp) | Predicted function |
|---|---|---|
| *LOC_Os07g25650* | 1890 | Predicted expressed protein |
| *LOC_Os07g25660* | 345 | Predicted expressed protein |
| *LOC_Os07g25670* | 726 | Predicted expressed protein |
| *LOC_Os07g25680* | 3660 | Protein kinase domain containing protein |
| *LOC_Os07g25690* | 354 | Subtilisin N-terminal region family protein |
| *LOC_Os07g25700* | 591 | Predicted expressed protein |
| *LOC_Os07g25710* | 1281 | myb-like DNA-binding domain containing protein |
| *LOC_Os07g25730* | 213 | Predicted expressed protein |

Sequence comparisons of candidate genes between wild type and the *sles* mutant revealed a single point mutation in the 6$^{th}$ exon of the *LOC_Os07g25680* candidate gene. Guanine (G) in the wild-type gene was changed to adenine (A) in the *sles* mutant gene, resulting in a single amino acid change from alanine to threonine at position 3,346 (**Figure 1-6B**). For coding regions, no other DNA sequence differences were detected in any other candidate genes. To verify the SNP, dCAPS markers were designed and used to screen the $F_2$ mapping population. Primers used for PCR are listed in **Table 1-1**. The genotype exhibited complete co-segregation with the matching phenotypes **(Figure 1-7A)**. To examine whether the SNP was present as a natural variant in other cultivars,

dCAPS analysis of eight *japonica* and five *indica* rice cultivars was performed. None of the 13 cultivars exhibited an additional restriction fragment **(Figure 1-7B)**.

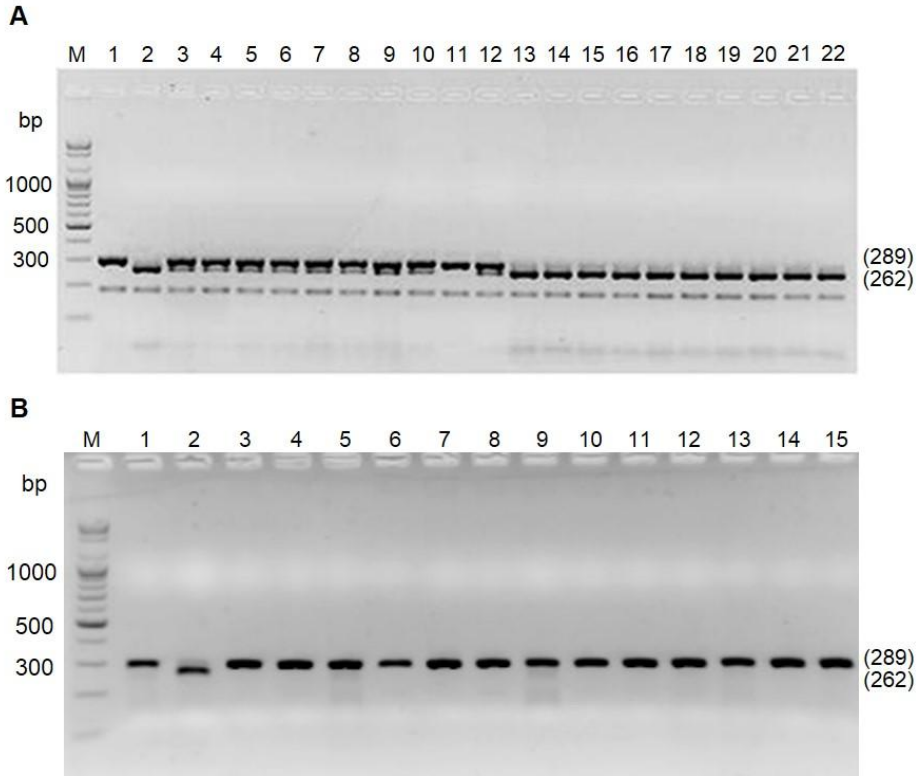


**Figure 1-7. Co-segregation analysis using dCAPS maker analysis. (A)** Co-segregation with the *sles* mutant phenotype was analyzed by size comparison of PCR products from the $F_2$ population. Lanes 1-2, WT and *sles* mutant, respectively; lanes 3-12, normal homozygotes and heterozygotes; 13-22, *sles* mutant homozygotes. **(B)** Confirmation of the splice variation in *SLES* gene by analysing PCR product size in *sles* mutant and 14 rice varieties. Lanes 1-2, WT and *sles* mutant, respectively; lanes 3-10 *japonica* rice varieties (Hwachong, Dongjin, Nipponbare, Ilpum, Hapcheon, Kunmingxiaobaigu, Dainxi4, Tong88-7) and lanes 11-15 *indica* rice varieties (M.23, Dasan, IR64, Unkwang, Giza178).

To understand the possible role of *SLES* in premature senescence with lesion mimic spots, we examined the transcriptional level of *SLES* during the formation of lesion mimic spots on the leaf sheath in *sles* mutant. The results showed that the *SLES* exhibited significantly elevated expression in the leaf sheath of the *sles* mutant compared to wild type (**Figure 1-8**). However, there was no remarkable difference of the expression level in the leaf between wild type and *sles* mutant.

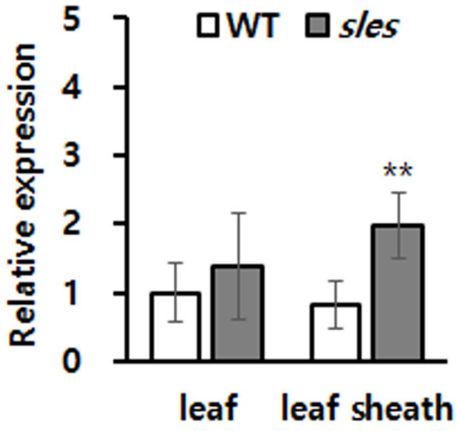


**Figure 1-8. Expression of *SLES* gene on leaf and leaf sheath.**

**Validation of the mutation causing *sles* mutant phenotype**

A T-DNA insertion line (3A-11526.R) from the Crop Biotech Institute, Department of Plant Systems Biotech, Kyung Hee University, was used to confirm that a single functional base substitution in *SLES* gene was responsible for the abnormal phenotype of *sles* mutants. This line has a T-DNA inserted into the first intron of *LOC_Os07g25680* **(Figure 1-9A)**, which was confirmed by PCR analysis. Seven homozygous and five heterozygous T-DNA tagging mutants were identified **(Figure 1-9B)**. As with the *sles* mutant, even severer, lesion mimic spots appeared on leaf sheaths and roots in the homozygous T-DNA insertion lines, and seedling height was shorter than the wild type (the cultivar Dongjin) (**Figure 1-9C, D, E**). Homozygous T-DNA insertion lines exhibited weak growth vigor compared to wild type and eventually died within 4 weeks after germination. These results confirmed that the mutation in *SLES* was responsible for the *sles* mutant phenotype.

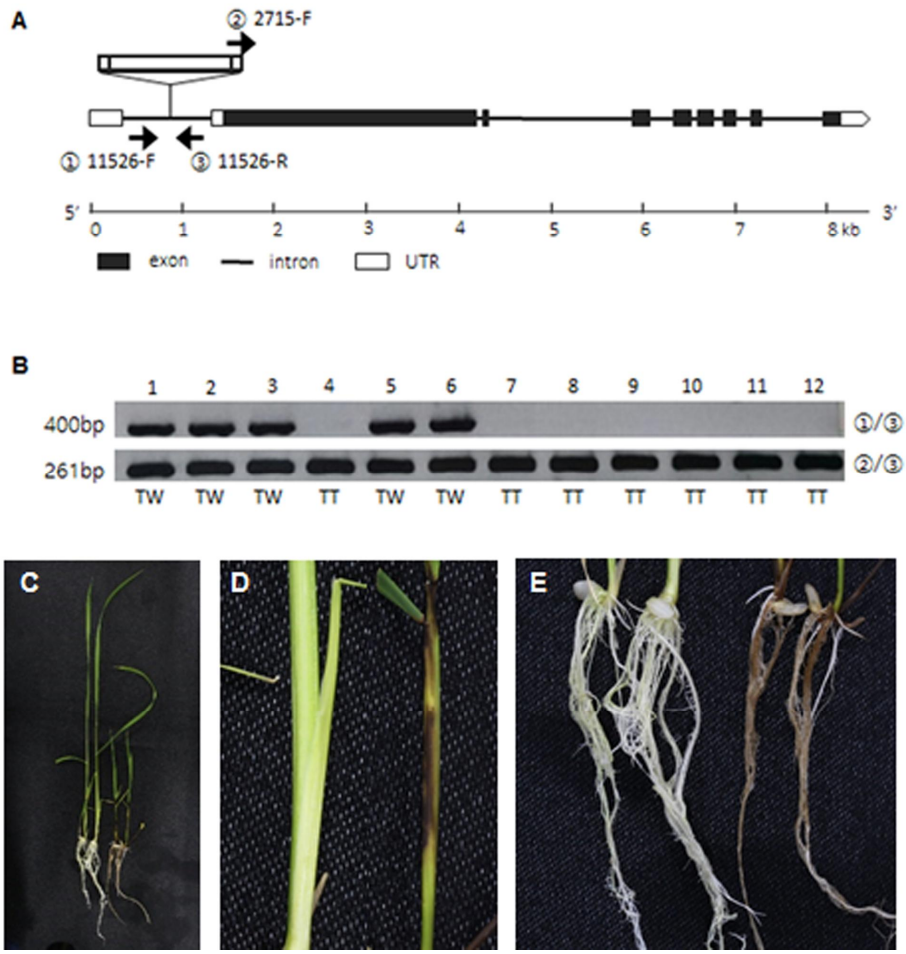


**Figure 1-9. T-DNA insertion line (A)** Schematic diagram of the T-DNA insertion. *Arrows* indicate primers. **(B)** Genotype of the $T_1$ plants evaluated by the PCR amplification with primer combinations of 11526-F/11526-R and 2715-F/11526-R. *TT* homozygous mutant, *TW* heterozygous. **(C-E)** Phenotypic comparison of wild-type Dongjinbyeo (left) and the homozygous T-DNA insertion line (right).

**SLES protein structure prediction**

Examination of the rice genome database revealed that the coding sequence (CDS) of *SLES* consisted of 3,660 nucleotides over 8 exons, and encoded a putative 1,219-amino acid protein. SLES contained Phox and Bem1p (PB1) domain at the N terminus and KD at the C terminus (**Figure 1-10A**). The SLES KD contained all 11 subdomains common to known protein kinases (Hanks and Quinn, 1991) (**Figure 1-10B**). Bioinformatic analysis and multiple amino acid sequence alignment of the predicted KD indicated a conserved catalytic and RAF-specific signature GTXX (W/Y) MAPE, which classified SLES as a Raf MAPKKK (**Figure 1-10B**) (Rao et al., 2010). SLES homologs were identified within monocots such as *Oryza brachyantha*, *Setaria italica*, *Brachypodium distachyon*, *Sorghum bicolor*, and *Zea mays* with 60-92% amino acid identity. However, no clear co-orthologues were identified in eudicots. None of these predicted proteins have been characterized to date.

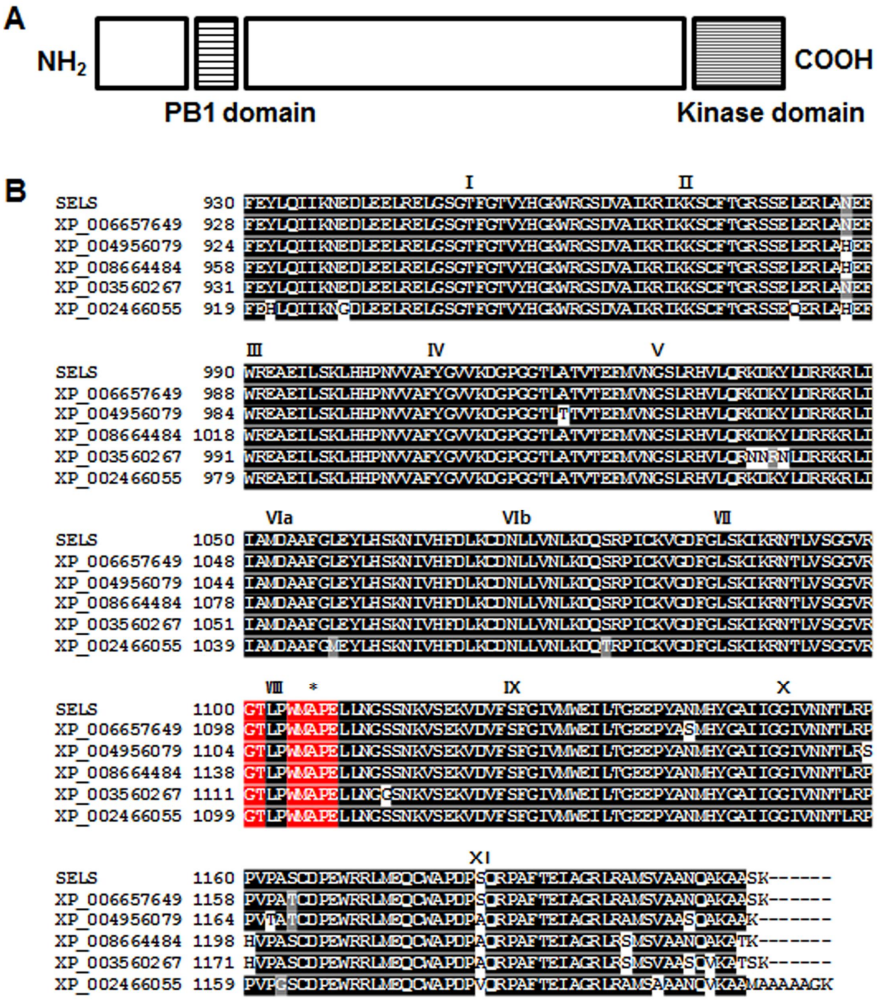


**Figure 1-10. Alignment of SLES from multiple organisms. (A)** Predicted schematic of the SLES protein. **(B)** Amino acid sequence alignment of the SLES kinase domain with that of other proteins indicated that SLES had a highly conserved kinase domain. Black boxes indicate identical residues and gray boxes indicate conservative substitutions. Roman numerals indicate the 11 characteristic sub-domains of protein kinases. The Raf specific motif is shown in red boxes. Asterisk indicates the position where a single amino acid change occurred in the *sles* mutant. Shown are: *Oryza brachyantha* (XP_006657649), *Setaria italic* (XP_004956079), *Zea mays* (XP_008664484), *Brachypodium distachyon* (XP_003560267), and *Sorghum bicolor* (XP_002466055).

# DISCUSSION

Several rice mutants associated with lesion mimic spots that result in early senescence, such as *spl5*, *lmes1*, and *lmes2*, have been identified (Chen et al., 2012; Li et al., 2014; Xing et al., 2016). However, to the best of our knowledge, no LMMs in which lesion mimic spots are found on the leaf sheath have been identified in rice to date. The *sles* mutant identified in this study exhibited lesion mimic spots on the leaf sheath. Further analysis revealed that these lesion mimic spots were attributable to ROS accumulation.

In the *sles* mutant, total chlorophyll content and Chla and Chlb levels were significantly lower in the spotted region than in wild type, whereas chlorophyll levels in non-spotted regions in the *sles* mutant did not differ from wild type. The ratios of Chla/Chlb in the non-spotted regions and in wild type were in the 2.5-4.0 range. The Chla/Chlb ratio in the *sles* mutant spotted regions was significantly lower than that in wild type, indicating that Chla levels in the mutant were relatively more diminished than Chlb levels. *SGR*, *NYC1*, *NYC3*, and *NOL* play important roles in chlorophyll degradation. Overexpression of *SGR* and *NYC3* accelerated chlorophyll degradation in developing leaves. Moreover, Chlb content was slightly lowered at the late stage of senescence in

*nol-1*, *nyc1-2*, and *nol-1 nyc1-2* mutants (Park et al., 2007; Sato et al., 2009; Wei et al., 2013). In the *sles* mutant, expression of chlorophyll degradation genes, particularly *SGR*, was markedly higher than in wild type. These results suggest that chlorophyll content in the *sles* mutant was reduced by activation of chlorophyll degradation genes resulting in senescence of the leaf sheath. Leaf senescence is mediated by a large number of genes, such as senescence transcription factors (*WRKY23* and *WRKY72*) and *SAGs* (*Osl2*, *Osl30*, *Osl43*, *Osl85*, *Osh36*, and *Osh69*) (Lee et al., 2001; Zhou et al., 2013). Expression of *WRKYs* and *SAGs*, particularly *Osl43* (stress response) and *Osl85* (fatty acid metabolism), was significantly increased in the leaf sheath of the *sles* mutant compared to wild type. Moreover, a large amount of irreversible membrane damage or cell death were observed in the leaf sheath of *sles* mutant. Taken together, the phenotypic, physiological, biochemical and molecular observations indicate that early senescence occurs in the leaf sheath of the *sles* mutant.

The results outlined above showed that HR-like cell death, leading to early senescence, occurred in the *sles* mutant; however, the cause of the lesion mimic spots on the leaf sheath remained unclear. Substantial ROS accumulation (superoxide ($O_2^-$) and hydrogen peroxide ($H_2O_2$)) was detected in leaf sheath of the *sles* mutant. In contrast, no significant difference was shown between leaves of wild type and *sles* mutant.

NADPH oxidase (NOX) and polyamine oxidase (PAO) are the main ROS sources (Langebartels et al., 2002). An *OsSRFP1* overexpression line with enhanced levels of *NOX* showed high levels of ROS accumulation (Fang et al., 2015). Overexpression of *AtPAO3* also resulted in increased production of ROS (Sagor et al., 2016). Expression of *NOX2* and *PAO* was substantially elevated in the spotted leaf sheath of the *sles* mutant compared to wild type. These results reveal that the elevated expression of genes encoding ROS-generating enzymes may have led to ROS accumulation in spotted regions of the *sles* mutant leaf sheath. As a large amounts of hydrogen peroxide and superoxide anion accumulated in the spotted region of the *sles* mutant leaf sheath, the expression of gene encoding scavenging enzymes, especially those located in the chloroplast, such as *SodCc1*, *SodCc2*, *APX5*, *APX6*, *APX7*, and *APX8*, was significantly higher than in wild type.

ROS accumulation not only triggers senescence but also activates the expression of defense genes such as *PR* genes (Dangl and Jones, 2001; Zentgraf and Hemleben, 2008). Overexpression of these *PR* genes may enhance plant tolerance to pathogen infections. For instance, overexpression of *OsPR1* in tobacco showed enhanced host tolerance to *Phytophthora nicotianae*, *Palstonia solanacearum*, and *Pseudomonas syringae* (Sarowar et al., 2005);

overexpression of *JIOsPR10* in rice enhanced tolerance to *Magnaporthe oryzae* (Wu et al., 2016a); and overexpression of *PR5* in rice enhanced tolerance to *Rhizoctonia solani* (Datta et al., 1999). Expression of *PR* genes, especially *PR5*, was significantly higher in the leaf sheath of the *sles* mutant than in wild type and showed significantly enhanced disease resistance to *M. oryzae* by restricting the development of infectious hyphae.

A database search and sequence analysis suggested that SLES contained a conserved protein KD and was a member of the Raf MAPKKK family. Although MAPK cascades have been identified and characterized in rice, little is known about members of the MAPKKK gene family and their functions and regulation in rice. MAPKKKs act upstream of MAPK cascade composed of three classes of enzymes: MAPKKK, MAPKK, and MAPK. Upstream signals activate MAPKKKs, which then phosphorylate MAPKKs. MAPKKs in turn activate a specific MAPK. The downstream targets of MAPKs can be transcription factors, phospholipases, or cytoskeletal proteins (Lin et al., 1993; Sturgill and Ray, 1986; Tian et al., 2017). In general, substrates of kinase are found at relatively constant level in most tissues. However, Gould et al., (1984) revealed that some kinase substrates are only expressed at high level in certain tissues. Since sles protein loses the normal function of kinase activity, we suggest that a specific protein

kinase substrate regulating ROS homeostasis specifically in leaf sheath might not regularly conduct its normal function, resulting in ROS accumulation in the leaf sheath of *sles* mutant. However, further experiments are necessary.

Several studies reveal that MAPKKK gene family is involved in plant defense/stress responses as well as ROS homeostasis regulation. Studies of MEKK1, the MAPKKK of the flagellin cascade, revealed that MEKK1 conferred resistance to both bacterial and fungal pathogens (Asai et al., 2002). Overexpression of *TaFLR* (a wheat MAPKKK gene) activated *PR* genes, such as *PR2a* and *PR3*, and resulted in increased resistance to *Fusarium graminearum* (Gao et al., 2016). In the *sles* mutant, markedly increased ROS accumulation was observed in accordance with induced expression of genes encoding ROS generating enzymes. Moreover, pathogenesis-related genes, especially *PR5*, were activated and pathogen resistance was enhanced in the *sles* mutant compared to wild type. Taken together, we suggest that SLES might suppress production of ROS associated with pathogen defense mechanism, thus leading to HR-like cell death on the leaf sheath and prevents the further pathogen infection of the *sles* mutant (**Figure 1-11**).

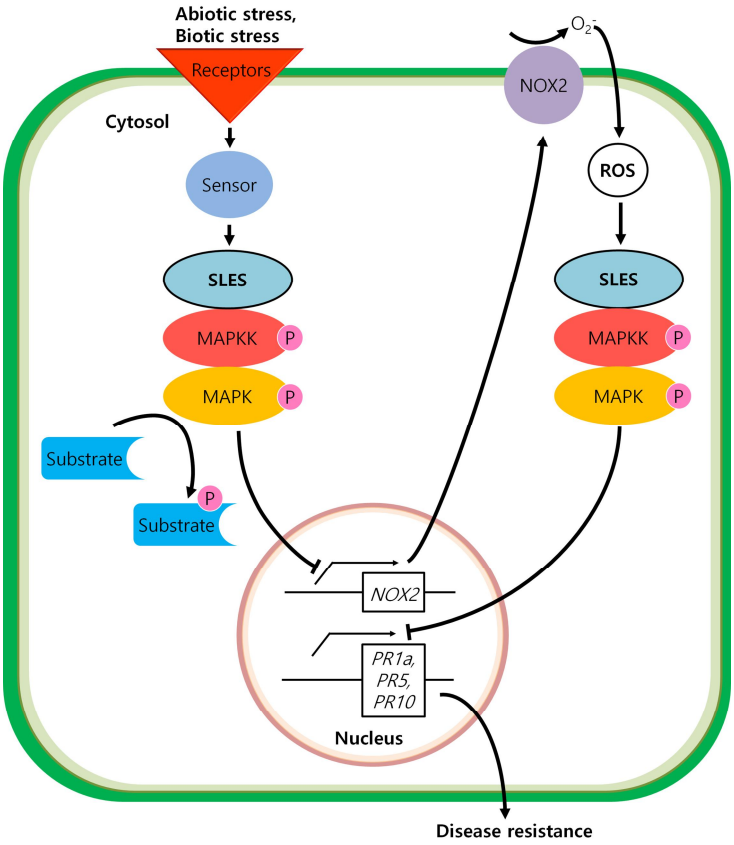


**Figure 1-11. The hypothetical model of mitogen-activated protein kinase (MAPK) cascade associated with disease resistance through ROS homeostasis.** Arrows indicate activation and bars indicate inhibition.

In this study, the *SLES* gene was characterized and isolated. Further examination of *SLES* will facilitate a better understanding of the molecular mechanisms involved in ROS homeostasis and may also provide opportunities to improve pathogen resistance in rice. Furthermore, as *SLES* is a Raf MAPKKK, the *sles* mutant is ideal for studies of MAPK cascades.

# CHAPTER II

## Comparative Proteomic Analysis of Differentially Expressed Proteins in Rice Seedlings Exposed to Cold and Heat Stresses

## ABSTRACT

During 21th century, global-average surface temperature of the earth are likely to increase by 1.8 to 4°C, accompanied by increasing climate variability and more frequent extreme temperature events such as cold snaps and hot days. Plants have developed complex regulatory mechanism to cope with various stress constraints. Therefore, understanding the molecular response of rice to temperature stresses will help us to develop rice cultivars better adapted to non-optimal temperatures. Two rice cultivars with contrasting levels of tolerance to temperature stresses, Koshihikari and Samnam, were used in this study. Three-leaf old seedlings of both cultivars grown at 28/25°C (day/night) were subjected to 5 day exposure to 4°C (day/night) for cold stress, or 42°C (day/night) for heat stress, followed by 5 days of recovery, respectively. Mature leaves were harvested from plants from each treatment for protein extraction and subsequent

triple TOF MS/MS analysis. In total, 1192 proteins were identified and Gene Ontology (GO) information was used to categorize the biological processes of identified proteins. Our data indicate that Koshihikari appears to be better able to cope with cold stress by upregulating proteins involved in translation, chlorophyll biosynthesis and translocation targeted to chloroplast, which were shown less abundance in Samnam. On the other hand, Samnam appears to be better able to cope with heat stress by upregulating proteins involved in oxidation-reduction process and energy metabolism process, which were decreased in Koshihikari.

**Keyword:** Rice, proteomic analysis, temperature stress, seedling, NanoLC-MS/MS

# INTRODUCTION

Rice is one of the world's most important staple food crop and a primary source of food for more than half of the world's population. According to UN estimates, the global population is predicted to grow from seven to nine billion by 2050. To satisfy the growing demand, crop production has to increase by 1% annually until 2050 (Carriger and Vallée, 2007; Smith and Gregory, 2013). Therefore, increasing grain yield has been the primary objective in current rice breeding programs. However, plants are exposed to many stresses which causes tremendous reduction of its production during the life span.

During the 21th century, global-average surface temperature of the earth are likely to increase by 1.8 to 4°C, accompanied by increasing climate variability and more frequent extreme temperature events such as cold snaps and hot days (Change, 2007; Cohen et al., 2014; Salinger, 2005). Both cold and heat stress, even when occurring for just a few hours, can drastically reduce the production of important food crops (Vara Prasad et al., 2000). In 2007, a month-long cold snap that occurred in Vietnam destroyed at least 53,000 hectares of rice (Mitin, 2009). An extraordinary heat wave over Russia during a month in 2010 decreased crop production by 20-30% relative to 2009 levels (Grumm, 2011).

Temperature stresses including chilling (0-20°C), freezing (<0°C), and high temperatures, often adversely affects plant growth and development resulting significant crop yield losses. Some common cold stress injuries include poor germination, reduced leaf expansion, yellowing and withering, reduced tillering, stunted growth (Kaneda, 1974), and sterility due to failure of microspore development (Satake, 1989) or a decrease in the number of pollen grains per anther (Murai et al., 1991). Plants affected by heat stress also appeared severe seedling loss, stunted growth, reduced leaf expansion, leaf number, rooting, tillering (Yang et al., 1993), high sterility (Prasad et al., 2006), and decreased grain quality (Zhong et al., 2005).

Since plants, unlike animals, are incapable of maintaining the optimum condition for their growth, they have developed complex regulatory mechanisms to cope with various stress constraints. Therefore, understanding the regulatory mechanisms will help confronting the yield reduction by various abiotic stresses result in meeting the needs of the world's population. Numerous studies investigating response to various stresses have been proceeded over the past years to understand these regulatory mechanisms.

Proteomic analysis is a powerful tool to study plant stress responses and it has been carried out recently to the systematic study of the proteomic responses to particular stress such as temperature stresses (Cui et al., 2005; Gammulla et al., 2010, 2011; Han et al., 2009; Hashimoto and Komatsu, 2007; Ji et al., 2017; Lee et al., 2007; Neilson et al., 2011b; Sarkar et al., 2014; Yang et al., 2006; Zou et al., 2011). Most of these proteomic studies compared single stress treatment with an optimal temperature and a few have examined the response to multiple stress temperatures to either cold or heat stress (Cui et al., 2005; Han et al., 2009). However, except for Gammulla et al. (2010, 2011), protein expression profiling has not been conducted for both temperature stresses.

Attempts have also been made to understand the molecular mechanisms conferring stress tolerance using varieties with different sensitivity to stress condition (Chen et al., 2015; Jagadish et al., 2009; Sarhadi et al., 2012; Sengupta and Majumder, 2009; Song et al., 2013; Wu et al., 2011, 2016b; Xu and Huang, 2008). Most of these proteomic studies were conducted other than temperature stresses such as salinity and copper tolerance. However there was few studies for heat tolerance (Jagadish et al., 2009; Wu et al., 2016b) and none of them were for cold tolerance.

In general, stress tolerance includes the direct response to stress and the ability to recover from stress. To understand the molecular basis of each phase, proteomic analysis during stress treatment and recovery were conducted (Badowiec and Weidner, 2014, 2014; de Abreu et al., 2014; Echevarría-Zomeño et al., 2009; Gazanchian et al., 2007, 2007; Hao et al., 2015; Liu et al., 2014; Mirzaei et al., 2012; Salekdeh et al., 2002; Sengupta et al., 2011, 2011). However, most of the studies were examined for drought stress and the response of rice to temperature stresses have not been performed.

Addressing the molecular mechanisms conferring temperature tolerance during seedling stage will help us to develop rice cultivars capable of adapting extreme temperature events. Therefore, experiments were carried out under control (28/25°C), cold stress (4°C), and heat stress (42°C), respectively, during stress treatment and recovery: (i) to identify expression patterns of stress-responsive proteins at varying temperatures, (ii) to identify and compare stress-responsive proteins in rice cultivars, (iii) and to understand the molecular mechanisms conferring stress tolerance in rice.

# MATERIALS AND METHODS

**Plant materials and growth condition**

Two rice genotypes with contrasting sensitivity to temperature stresses (cold and heat) in opposite way were used in this study. Koshihikari, a *japonica* rice variety, shows tolerance in cold stress but it exhibits heat sensitivity compared to Samnam (a *japonica* rice variety). Samnam is relatively tolerant to heat stress and sensitive to cold stress, respectively, compared to Koshihikari. Seedlings used in this study were grown by hydroponic culture in Yoshida solution (pH 5.8) in the growth chamber with an average day/night temperature of 28°C/25°C with a 14-h photoperiod at 70% relative humidity.

**Temperature stress treatment**

Typical and healthy three-leaf old seedlings were selected for the further experiment. Seedlings were directly transferred to growth chamber maintained at 4°C for cold stress treatment and 42°C for heat stress treatment. After 5d of exposure to each stress, all the remaining seedlings were returned to normal growth conditions for recovery. Leaf samples from twenty selected seedlings were collected and pooled into a bulk from each stage: (i) 21 d after sowing (DAS), (ii) 5 d after stress treatment (DAT), (iii) and 5 d after recovery (DAR).

Samples were stored immediately at -80°C for protein extraction. Each treatment comprised two biological replicates.

**Protein extraction**

Samples were grounded pulverized in pre-chilled pestle and mortar using liquid nitrogen and homogenized with 20 ml solution comprising TCA (10%) in acetone with 2-mercaptoethanol (ME) (0.07%). The total protein was left overnight at −20°C. The precipitate was vortexed and centrifuged at 13,000 rpm at 4°C for 15 min. The pellet obtained was rinsed thrice with acetone supplemented with 2 ME (0.07%), and 1 tablet of complete EDTA free protease inhibitor. For every washing, 20 ml chilled wash buffer was added, vortexed briskly and centrifuged at 13,000 rpm at 4°C for 15 min. Final washing was carried out with pre-chilled acetone (100%). Air-dried pellet was re-suspended with 10 ml SDS-extraction buffer (30% Sucrose, 2 % SDS, 5% 2 ME, 0.1 M Tris-Cl (pH 7.5)) and incubated with continuous shaking at 4°C. An equal volume of Tris-buffered phenol was then added and the solution was again incubated on a shaker for 10 min at 4°C. The aqueous and organic phases were separated by centrifugation at 13,000 rpm for 15 min at 4°C. The phenolic phase was carefully recovered and re-extracted with equal volume of SDS-extraction buffer. The samples were vigorously vortexed and centrifuged for phase

separation at 13,000 rpm for 15 min at 4°C. The phenolic layer was transferred to a fresh tube for precipitation of proteins by addition of ammonium acetate (0.1 M) in cold methanol with subsequent overnight incubation at −20°C. The precipitate/protein pellet was washed thrice with precipitation solution (stored at −20°C) and final washing was done with pre-chilled pure acetone. The pellet was air-dried and then dissolved in rehydration buffer (7 M urea, 2 M thiourea and 2% (w/v) CHAPS).

**Trypsin in-gel digestion**

Proteins are separated by the 10% SDS-PAGE electrophoresis. The gel is stained with the 0.25% solution of Commassie Blue G-250 for overnight, and destained in water then excised by 2 slices each lane. Excised gels were destained with 50% ACN, shrunk with 100% ACN. Proteins in gels were then reduced for 45 minutes at RT by addition of 1M DTT to a final concentration of 1 mM DTT and then alkylated for 30 minutes by addition of 550 mM IAA solution to a final concentration of 5.5 mM. The gels were then digested with sequence grade modified trypsin for overnight at 30°C in 0.1 M $NH_4HCO_3$. About 2 μg of protease was used for one gel band. Peptides were extracted from the gel slices with 66% ACN, 5% FA. The extracts were dried by speedvac and stored at -80ºC before analysis.

**Triple TOF MS/MS Analysis**

Each dried peptide sample was dissolved in 5% formic acid and analyzed by nanoLC-MS/MS using an Ekspert nanoLC 400 system coupled to an AB Sciex 6600 triple TOF system. After the sample was loaded, peptide was trapped (ChromXP C18CL, 120 Å, 0.5 mm x 350 μm) and eluted into a reverse-phase C18 column (3 μm, ChromXP C18CL, 120 Å, 15 cm x 75 μm) at a flow rate of 300 nL/min using a linear gradient of acetonitrile (5–40%) in 0.1% formic acid for 150 min. MS and MS/MS spectra were recorded in the "high-sensitivity" and positive-ion mode with a resolution of ~35000 full width at half-maximum. After each survey MS1 scan (typically allowing 250 ms of acquisition per MS/MS), advanced information-dependent acquisition was used on the 6600 triple TOF to obtain MS/MS spectra for the 10 most abundant and multiple-charged ($z$ = 2, 3, or 4) precursor ions. For the parameters for instrument, the spray voltage and curtain gas were set to 1.5 kV and 20L/min, respectively. Nitrogen gas was used as the collision gas and dynamic exclusion was set for 30 s after two repetitive occurrences. For reproducibility of data, the spectra acquired through nanoHPLC-MS and MS/MS using 3μL of 25 fmol of digested β-galactosidasewere automatically calibrated after acquisition of five or six samples.

**Protein identification and quantification**

Raw data files of nanoLC-MS/MS were converted to Mascot generic format (MGF) by tools obtained from AB SCIEX. The MGF files were searched against UniRice_20170926 database (unknown version, 86632 entries) using Mascot 2.5 (Matrix Science, London, UK; version 2.5.1) software. The search parameters were as follows: (i) a maximum of two trypsin miss-cleavages were allowed; (ii) fixed modification were set for carbamidomethylation of cysteine and variable modifications were set for oxidation of methionine; (iii) fragment ion mass tolerance and a parent ion tolerance was set at ± 0.20 Da, respectively. Scaffold (version Scaffold_4.8.4, Proteome Software Inc., Portland, OR) was used to validate MS/MS based peptide and protein identifications. Peptide identifications were accepted if they could be established at greater than 95.0% probability by the Peptide Prophet algorithm (Keller et al., 2002) with Scaffold delta-mass correction. Protein identifications were accepted if they could be established at greater than 95.0% probability and contained at least 1 identified peptide. Protein probabilities were assigned by the Protein Prophet algorithm (Nesvizhskii et al., 2003). Proteins that contained similar peptides and could not be differentiated based on MS/MS analysis alone were grouped to satisfy the principles of parsimony.

The 24 lists of identified proteins were further filtered using two criteria. A protein was retained only if it fulfilled both criteria: for at least one stage (1) the protein should be present and (2) the average of the protein in replicates should have a total spectral count greater than 5 (Mirzaei et al., 2011; Neilson et al., 2011a; Voelckel et al., 2010). Protein abundance data were calculated based on normalized total spectra, including addition of a spectral fraction of 0.5 to all counts to compensate for null values.

**Criterion for differentially expressed proteins**

To identify significant differentially expressed proteins (DEPs) for temperature stresses, a series of *t*-test was performed between two distinct conditions: (i) control versus stress treatment, and (ii) control versus recovery stage after stress treatment. The *t*-test were performed on log-transformed normalized total spectra data, and proteins with a *t*-tests *p*-value less than 0.05 were regarded as differentially expressed.

**GO enrichment analysis**

Gene ontology (GO) information was used to categorize the biological processes of identified proteins. GO annotations were extracted from the UniProt database and matched to the list of identified proteins. For GO categories of interest, normalized total spectra data were merged and plotted to obtain an image of overall protein abundance change for biological process categories.

# RESULTS AND DISCUSSION

**Survival rate under cold and heat stresses**

Koshihikari and Samnam showed opposite results under cold and heat stresses **(Figure 2-1A, C).** After cold stress treatment at three-leaf stage, the survival rate of Koshihikari was 84%, whereas that of Samnam was 4% seven-day after recovery (**Figure 2-1B**). After heat stress treatment at three-leaf stage, none of the seedlings survived in Koshihikari, whereas the survival rate of Samnam was 80% seven-day after recovery (**Figure 2-1D**). These findings indicated that temperature stresses, including cold and heat stresses, imparted different effects on Koshihikari and Samnam, respectively.

**Protein identification and quantification**

After nanoLC-MS/MS analysis, a total of 1 224 989 spectra were detected, and 524 038 exclusive spectrum were identified, and 97 996 and 93 462 were unique spectra and unique peptides, respectively (**Figure 2-2**). In total, 1192 proteins were identified using the *Oryza sativa* UniRice database with a FDR < 0.01 as stated in the methods.

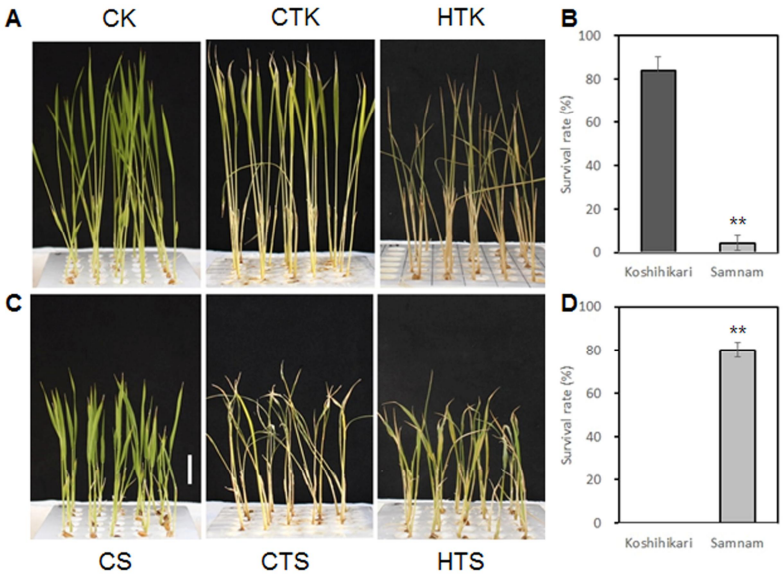


**Figure 2-1. Survival rate exposed to cold and heat stress.** Indications in **(A, C)** are CCK, cold control Koshihikari; CTK, cold treatment Koshihikari; CRK, cold recovery Koshihikari; HCS, heat control Samnam; HTS, heat treatment Samnam; HRS, heat recovery Samnam

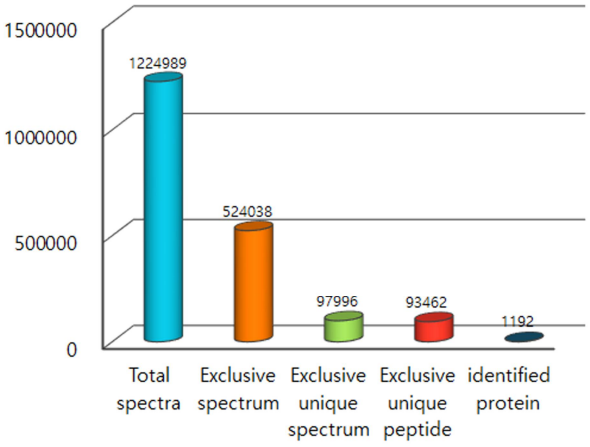


**Figure 2-2. Basic information statistics.** Total spectra, exclusive spectrum, exclusive unique spectrum, exclusive unique peptides and identified proteins by searching against Uniprot database

**Table 2-1** shows a numerical summary of protein and peptide identification data from leaves of seedlings grown under normal, temperature stress treatments, and recovery conditions. There were 867 non-redundant proteins reproducibly identified at high stringency across all three conditions in Koshihikari against cold stress treatment. In Samnam, there were 833 non-redundant proteins reproducibly identified at high stringency across all three treatments. For heat stress treatment, there were 873 non-redundant proteins reproducibly identified at high stringency across all three treatment in Koshihikari. In Samnam, there were 831 non-redundant proteins reproducibly identified at high stringency across all three treatments. The peptide FDR was less than 0.4% while the protein FDR was below 0.7%.

**Table 2-1** Proteins identified in Koshihikari and Samnam under different conditions

| | cold stress | | heat stress | |
|---|---|---|---|---|
| | Koshihikari | Samnam | Koshihikari | Samnam |
| control | 607 | 620 | 613 | 565 |
| stress | 541 | 517 | 634 | 629 |
| recovery | 577 | 564 | 532 | 652 |
| non-redundant proteins across three conditions | 867 | 833 | 873 | 831 |

**Proteins found in both Koshihikari and Samnam exposed to cold stress**

83 and 196 proteins in Koshihikari and 74 and 141 proteins in Samnam were respectively up- and downregulated for cold stress treatment (**Figure 2-3A**).

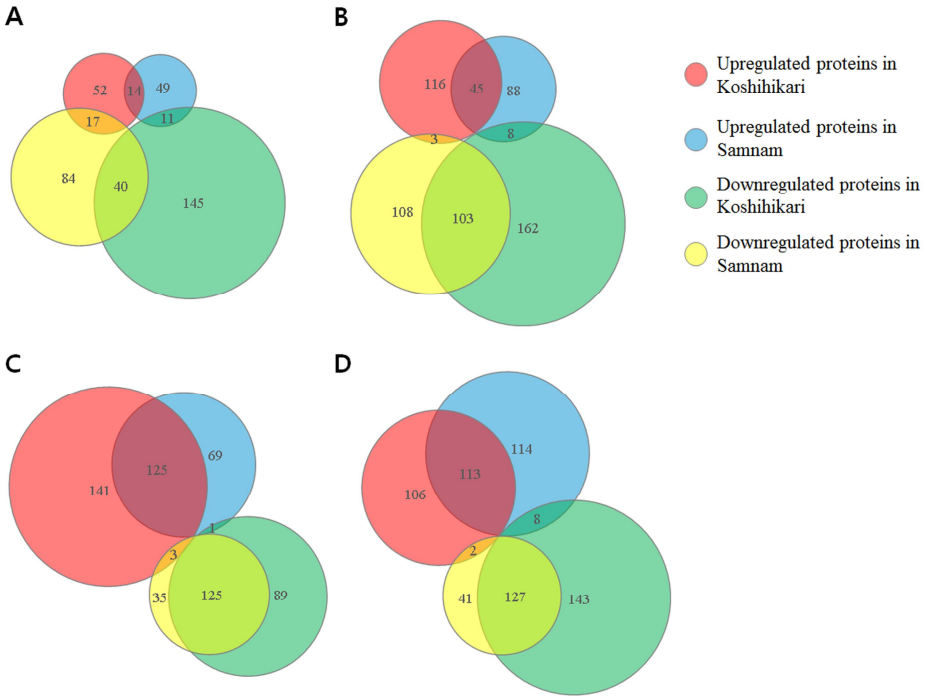


**Figure 2-3. Venn diagram of the up- and downregulated proteins between Koshihikari and Samnam. (A)** exposed to cold stress. **(B)** under recovery after cold stress. **(C)** exposed to heat stress. **(d)** under recovery after heat stress.

Cold stress resulted in 14 upregulated and 40 downregulated proteins found in common between Koshihikari and Samnam (**Table 2-2**). The major differentially expressed proteins found in both cultivars were involved in metabolic process

(28%) and oxidation-reduction process (15%). A decrease in abundance was observed mostly in oxidation-reduction process (27%) and metabolic process (24%). In contrast, GRAM domain containing protein, adenosylhomocysteinase, glutathione S-transferase, fructose-1,6-bisphosphatase, ribosomal proteins, and peroxidases were all increased in both cultivars.

**Table 2-2** DEPs found in both Koshihikari and Samnam exposed to cold stress

| Identified Proteins | Accession Number | Alternate ID | dCTK | dCTS |
|---|---|---|---|---|
| GRAM domain containing protein (Fragment) | C7JA48_ORYSJ | Os12g0478200 | 69.80 | 21.86 |
| Adenosylhomocysteinase (Fragment) | A0A0P0Y1Y5_ORYSJ | Os11g0455500 | 69.04 | 4.52 |
| Uncharacterized protein | A2ZAT7_ORYSI (+2) | OsI_34873 | 48.78 | 18.94 |
| DUF538 domain containing protein (Fragment) | A0A0P0WXJ2_ORYSJ | Os06g0538900 | 28.89 | 13.56 |
| Glutathione S-transferase protein | Q8LR62_ORYSJ | Os01g0933900 | 23.74 | 12.58 |
| Fructose-1,6-bisphosphatase, cytosolic | F16P2_ORYSI (+1) | OsI_04558 | 21.40 | 14.68 |
| 30S ribosomal protein S8, chloroplastic | RR8_ORYSI (+1) | rps8 | 15.74 | 19.87 |
| Peroxiredoxin-2E-2, chloroplastic | PR2E2_ORYSJ | PRXIIE-2 | 19.00 | 13.70 |
| Peroxidase | B8APG3_ORYSI | OsI_11487 | 16.64 | 13.62 |
| 60S ribosomal protein L36 | A2Y5F8_ORYSI (+1) | OsI_20226 | 16.64 | 12.50 |
| Uncharacterized protein | A2WX82_ORYSI (+1) | OsI_04525 | 13.22 | 15.75 |
| Uncharacterized protein | A2Z9M2_ORYSI (+1) | OsI_34432 | 13.25 | 13.56 |
| Uncharacterized protein | A2YHC5_ORYSI (+1) | OsI_24591 | 14.99 | 11.54 |
| Peroxidase | Q6ER49_ORYSJ | prx29 | 3.80 | 3.79 |
| Uncharacterized protein | A2XUR5_ORYSI (+1) | OsI_16352 | 0.46 | 0.02 |
| Uncharacterized protein | B8AN77_ORYSI (+1) | OsI_14277 | 0.08 | 0.09 |
| Os02g0117100 protein | Q6ZGM0_ORYSJ | Os02g0117100 | 0.07 | 0.09 |
| Os02g0792800 protein | Q6K689_ORYSJ | Os02g0792800 | 0.07 | 0.08 |
| Os03g0390700 protein | Q7XXQ9_ORYSJ | LOC_Os03g27320 | 0.06 | 0.09 |
| Uncharacterized protein | A2YHF9_ORYSI (+1) | OsI_24624 | 0.06 | 0.09 |
| Uncharacterized protein | A2YLI3_ORYSI (+1) | OsI_26080 | 0.06 | 0.08 |
| Uncharacterized protein | A2XU31_ORYSI | OsI_16109 | 0.07 | 0.06 |
| Citrate synthase | Q7F8R1_ORYSJ | P0437H03 | 0.05 | 0.08 |
| Peptidylprolyl isomerase | A2X9U8_ORYSI (+1) | OsI_09019 | 0.05 | 0.08 |
| Uncharacterized protein | A2WWU4_ORYSI (+1) | OsI_04374 | 0.07 | 0.06 |
| NADH dehydrogenase iron-sulfur protein 3 | NDUS3_ORYSJ (+1) | NAD9 | 0.05 | 0.07 |
| Uncharacterized protein | A2XN31_ORYSI (+1) | OsI_13961 | 0.03 | 0.09 |
| DNA binding protein PF1 | Q69MW7_ORYSJ | Os09g0402100 | 0.04 | 0.07 |
| Uncharacterized protein | B8AWQ3_ORYSI | OsI_20971 | 0.05 | 0.06 |
| Os06g0264300 protein | Q5Z6P9_ORYSJ | Os06g0264300 | 0.05 | 0.06 |
| Os04g0117800 protein | A3AQC6_ORYSJ (+1) | Os04g0117900 | 0.02 | 0.09 |
| Uncharacterized protein | A2XPF9_ORYSI (+1) | OsI_14471 | 0.05 | 0.06 |
| Uncharacterized protein | A2XLM8_ORYSI (+1) | OsI_13379 | 0.05 | 0.05 |
| Chitinase 1, putative, expressed | Q7XEL9_ORYSJ | Os10g0416800 | 0.05 | 0.05 |
| Probable aldo-keto reductase 2 | AKR2_ORYSI (+1) | OsI_15387 | 0.04 | 0.06 |
| Os11g0592200 protein | Q941F5_ORYSJ | PR4 | 0.02 | 0.08 |
| Os06g0687800 protein | Q653F5_ORYSJ | Os06g0687800 | 0.04 | 0.06 |
| Os06g0157000 protein | Q0DEF1_ORYSJ | KMK0024M20 | 0.04 | 0.05 |
| NADH-cytochrome b5 reductase | Q5VR12_ORYSJ | Os01g0174300 | 0.03 | 0.06 |
| Os01g0139200 protein | Q5ZDH9_ORYSJ | Os01g0139200 | 0.03 | 0.05 |
| Uncharacterized protein | B8AWM3_ORYSI | OsI_19471 | 0.04 | 0.03 |

| | | | | |
|---|---|---|---|---|
| Probable linoleate 9S-lipoxygenase 4 | LOX4_ORYSJ | Os03g0700700 | 0.05 | 0.02 |
| Uncharacterized protein | A2ZIM1_ORYSI (+1) | OsI_37672 | 0.02 | 0.05 |
| Uncharacterized protein | A2ZLT9_ORYSI (+1) | OsI_38783 | 0.03 | 0.04 |
| Os04g0685600 protein | A0A0N7KJY7_ORYSJ (+1) | Os04g0685600 | 0.03 | 0.03 |
| Uncharacterized protein | A2ZBF1_ORYSI (+1) | OsI_35100 | 0.03 | 0.03 |
| Os07g0671800 protein (Fragment) | A0A0P0XAA0_ORYSJ | Os07g0671800 | 0.02 | 0.04 |
| Pyrophosphate--fructose 6-phosphate 1-phosphotransferase subunit alpha | B8B9Z2_ORYSI (+1) | PFP-ALPHA | 0.03 | 0.03 |
| Uncharacterized protein | A2XEP1_ORYSI (+1) | OsI_10803 | 0.04 | 0.02 |
| Os10g0436800 protein | A0A0P0XV01_ORYSJ | Os10g0436800 | 0.02 | 0.03 |
| Uncharacterized protein | A2YE41_ORYSI (+1) | OsI_23386 | 0.03 | 0.02 |
| Os09g0572900 protein | Q650Z3_ORYSJ | Os09g0572900 | 0.01 | 0.03 |
| 26S proteosome regulatory subunit-like | Q6Z8F7_ORYSJ | Os02g0697600 | 0.01 | 0.02 |
| Peroxidase | Q7XSU7_ORYSJ | Os04g0688500 | 0.01 | 0.02 |
| Uncharacterized protein | B8A8D4_ORYSI (+1) | OsI_03471 | 93.82 | 0.02 |
| Uncharacterized protein | B8B7Y3_ORYSI (+1) | OsI_25188 | 47.99 | 0.04 |
| Uncharacterized protein | B8B8E9_ORYSI (+1) | OsI_25360 | 43.18 | 0.05 |
| Uncharacterized protein | B8BB36_ORYSI (+1) | OsI_29378 | 37.96 | 0.06 |
| Uncharacterized protein | A2XDB9_ORYSI (+1) | OsI_10302 | 35.39 | 0.04 |
| Uncharacterized protein | B8AY06_ORYSI (+1) | OsI_19859 | 33.69 | 0.06 |
| Uncharacterized protein | A2WLL2_ORYSI | OsI_00727 | 24.89 | 0.04 |
| Uncharacterized protein | B8BG64_ORYSI | OsI_33051 | 20.06 | 0.07 |
| Os06g0550000 protein (Fragment) | A0A0P0WXQ4_ORYSJ (+3) | Os06g0550000 | 19.65 | 0.06 |
| Uncharacterized protein | A2WPB5_ORYSI (+2) | OsI_01687 | 18.69 | 0.02 |
| OSJNBa0072K14.5 protein | Q7XVM2_ORYSJ | Os04g0394200 | 18.63 | 0.05 |
| Phosphoserine aminotransferase | Q8LMR0_ORYSJ | OJ1134F05 | 17.49 | 0.05 |
| Uncharacterized protein | A2Y3J4_ORYSI (+1) | OsI_19576 | 15.76 | 0.07 |
| Os09g0442300 protein (Fragment) | A0A0P0XNI7_ORYSJ | Os09g0442300 | 13.56 | 0.04 |
| Elongation factor 1-gamma 2 | EF1G2_ORYSJ | Os02g0220500 | 13.27 | 0.05 |
| Proteasome subunit beta type | A2XKY8_ORYSI (+1) | OsI_13132 | 11.44 | 0.07 |
| Uncharacterized protein | B8AXN6_ORYSI (+1) | OsI_18361 | 11.44 | 0.07 |
| Cytochrome b559 subunit alpha | PSBE_ORYSI (+2) | psbE | 0.24 | 3.90 |
| Uncharacterized protein | A2XV80_ORYSI | OsI_16517 | 0.09 | 15.72 |
| 30S ribosomal protein S7, chloroplastic | RR7_ORYSI (+1) | rps7-A | 0.09 | 18.81 |
| Uncharacterized protein | B8AKU1_ORYSI (+1) | OsI_12278 | 0.08 | 13.51 |
| Uncharacterized protein | A2X7M2_ORYSI (+1) | OsI_08214 | 0.08 | 11.51 |
| Uncharacterized protein | A2YVK0_ORYSI (+3) | OsI_29358 | 0.07 | 17.85 |
| Uncharacterized protein | B8AUD0_ORYSI (+1) | OsI_16063 | 0.05 | 15.22 |
| Uncharacterized protein | B8ACE5_ORYSI (+1) | OsI_03049 | 0.04 | 34.18 |
| Photosystem I assembly protein Ycf4 | YCF4_ORYSI (+1) | ycf4 | 0.04 | 16.53 |
| Uncharacterized protein | A2YGA4_ORYSI | OsI_24205 | 0.03 | 17.33 |
| Os01g0106200 protein | Q657Y8_ORYSJ | Os01g0106200 | 0.02 | 44.17 |

**Proteins found in both Koshihikari and Samnam under recovery after cold stress**

164 and 273 proteins in Koshihikari and 141 and 214 proteins in Samnam were respectively up- and down regulated during recovery condition after cold stress (**Figure 2-3B**). Among those, there were 45 upregulated and 103 downregulated

proteins found in common between Koshihikari and Samnam (**Table 2-3**). The major differentially expressed proteins found in both cultivars were involved in metabolic process (33%) and oxidation-reduction process (16%). A decrease in abundance was observed mostly in metabolic process (27%), oxidation-reduction process (16%), and cell part / cellular component / cellular component organization (23%). In contrast, glyceraldehyde-3-phosphate dehydrogenase and alpha-dioxygenase related to oxidation-reduction process were mostly increased in both cultivars. Interestingly, proteins related to stress response, such as heat shock protein, pathogenesis-related proteins and cold shock protein and a few proteasome subunits were also upregulated.

**Table 2-3** DEPs found in both Koshihikari and Samnam under recovery after cold stress

| Identified Proteins | Accession Number | Alternate ID | dCRK | dCRS |
|---|---|---|---|---|
| Glyceraldehyde-3-phosphate dehydrogenase | A2XC18_ORYSI (+1) | OsI_09835 | 253.83 | 457.24 |
| Uncharacterized protein | A2Y2Y4_ORYSI | OsI_19374 | 263.95 | 258.44 |
| Oryzain alpha chain | ORYA_ORYSJ | Os04g0650000 | 44.23 | 143.94 |
| Heat shock protein STI, putative, expressed | Q6H660_ORYSJ | Os02g0644100 | 108.58 | 68.87 |
| Alpha-dioxygenase, putative, expressed | Q2QRV3_ORYSJ | LOC_Os12g26290 | 71.61 | 86.91 |
| Uncharacterized protein | A2WPB5_ORYSI (+2) | OsI_01687 | 108.19 | 2.27 |
| Probable plastid-lipid-associated protein 2, chloroplastic | PAP2_ORYSJ | PAP2 | 36.05 | 65.25 |
| carboxyvinyl-carboxyphosphonate phosphorylmutase | Q0IPL3_ORYSJ | Os12g0189300 | 14.51 | 68.98 |
| Uncharacterized protein | B8AIX1_ORYSI | OsI_06111 | 47.96 | 32.85 |
| Pathogenesis-related protein | B8BMF9_ORYSI (+1) | PR10a | 14.34 | 64.55 |
| PTAC16, putative, expressed | A0A0P0WKD6_ORYSJ (+1) | Os05g0291700 | 15.78 | 59.60 |
| Uncharacterized protein | A2XNF7_ORYSI (+1) | OsI_14096 | 28.65 | 46.62 |
| Adenosylhomocysteinase (Fragment) | A0A0P0Y1Y5_ORYSJ | Os11g0455500 | 66.12 | 5.85 |
| Uncharacterized protein | B8BLP4_ORYSI | OsI_36917 | 39.21 | 31.77 |
| Peroxiredoxin-2E-2, chloroplastic | PR2E2_ORYSJ | PRXIIE-2 | 19.10 | 45.17 |
| Uncharacterized protein | A2Z9V6_ORYSI (+1) | OsI_34517 | 20.18 | 41.68 |
| Uncharacterized protein | A2YXJ3_ORYSI (+1) | OsI_30061 | 59.58 | 1.37 |
| Cysteine synthase | Q5UJF9_ORYSI (+1) | CAS | 26.59 | 32.75 |
| Aspartate aminotransferase | Q0JJ47_ORYSJ | Os01g0760600 | 36.05 | 22.45 |
| GDP-mannose 3,5-epimerase 1 | GME1_ORYSI (+1) | OsI_032456 | 27.49 | 30.98 |
| Alpha-L-arabinofuranosidase C-terminus family protein, expressed | Q2QY88_ORYSJ | Os12g0128700 | 28.47 | 29.99 |
| Cold shock domain protein 2 | Q84UR8_ORYSJ | P0582D05 | 37.21 | 20.85 |
| Alanine--tRNA ligase | Q10A14_ORYSJ | LOC_Os10g10244 | 39.29 | 18.36 |
| pathogenesis-related Bet v I family protein, putative, expressed | Q2QNS7_ORYSJ | LOC_Os12g36880 | 13.89 | 43.18 |
| Protein THYLAKOID FORMATION1, chloroplastic | THF1_ORYSJ | THF1 | 22.71 | 29.30 |
| Uncharacterized protein | B8B9C4_ORYSI (+1) | OsI_30128 | 37.23 | 13.16 |
| Proteasome subunit beta type | A2XA20_ORYSI (+1) | OsI_09094 | 22.79 | 27.29 |

| | | | | |
|---|---|---|---|---|
| Uncharacterized protein | A2ZAT7_ORYSI (+2) | OsI_34873 | 22.44 | 27.31 |
| Proteasome subunit alpha type | B8B9D7_ORYSI (+2) | OsI_30159 | 26.67 | 19.61 |
| Probable glucan 1,3-alpha-glucosidase | GLU2A_ORYSJ | Os03g0216600 | 19.97 | 24.62 |
| Uncharacterized protein | B8BGM4_ORYSI | OsI_33417 | 23.52 | 20.44 |
| Uncharacterized protein | B8B8E9_ORYSI (+1) | OsI_25360 | 38.84 | 4.55 |
| Succinate--CoA ligase [ADP-forming] subunit alpha, mitochondrial | B8B7R8_ORYSI | OsI_26601 | 21.00 | 22.09 |
| Uncharacterized protein | A2Y2C8_ORYSI (+1) | OsI_19158 | 35.12 | 7.33 |
| Pyruvate dehydrogenase E1 component subunit alpha-1, mitochondrial | ODPA1_ORYSJ | Os02g0739600 | 19.56 | 19.13 |
| Proteasome subunit beta type | B8B2Z5_ORYSI (+1) | OsI_21721 | 14.42 | 23.35 |
| Proteasome subunit beta type-1 | PSB1_ORYSJ | PBF1 | 11.91 | 23.82 |
| Uncharacterized protein | A2WYX5_ORYSI (+2) | OsI_05141 | 14.24 | 21.34 |
| Uncharacterized protein | B8AU70_ORYSI (+1) | OsI_17346 | 18.75 | 15.88 |
| glutathione S-transferase, putative, expressed | Q8LR62_ORYSJ | Os01g0933900 | 11.72 | 18.36 |
| Porphobilinogen deaminase, chloroplastic | HEM3_ORYSJ | HEMC | 16.05 | 11.41 |
| Uncharacterized protein | B8AT02_ORYSI | OsI_15572 | 11.45 | 13.91 |
| Xylose isomerase | B8B5T6_ORYSI (+1) | OsI_27268 | 12.53 | 11.68 |
| Cold shock domain protein 1 | Q6YUR8_ORYSJ | CSP1 | 12.90 | 11.17 |
| Glyceraldehyde-3-phosphate dehydrogenase 1, cytosolic | G3PC1_ORYSJ (+1) | GAPC1 | 7.08 | 2.71 |
| Flavone 3'-O-methyltransferase 1 | OMT1_ORYSJ | COMT | 0.58 | 0.30 |
| Cytochrome b6-f complex iron-sulfur subunit | A2YMJ8_ORYSI (+1) | OsI_26450 | 0.26 | 0.57 |
| Uncharacterized protein | B8AMB1_ORYSI (+1) | OsI_14091 | 0.30 | 0.45 |
| Peptidylprolyl isomerase | Q653Z1_ORYSJ | Os06g0663800 | 0.19 | 0.53 |
| Os02g0816800 protein | Q6K6A4_ORYSJ | Os02g0816800 | 0.53 | 0.04 |
| Os06g0130900 protein (Fragment) | A0A0P0WRT9_ORYSJ | Os06g0130900 | 0.51 | 0.02 |
| Uncharacterized protein | B8B8Z2_ORYSI | OsI_28519 | 0.47 | 0.06 |
| Photosystem II CP47 reaction center protein | PSBB_ORYSJ | psbB | 0.20 | 0.32 |
| Chitinase 4 | CHI4_ORYSJ (+1) | Cht4 | 0.44 | 0.02 |
| Uncharacterized protein | A2Y2Y3_ORYSI (+1) | OsI_19373 | 0.41 | 0.02 |
| Methylenetetrahydrofolate reductase | A2XNC0_ORYSI (+1) | OsI_14054 | 0.07 | 0.35 |
| Os07g0468100 protein | Q69RL1_ORYSJ | Os07g0468100 | 0.39 | 0.04 |
| Chitinase III-like protein | Q69RN2_ORYSJ | Os07g0500300 | 0.18 | 0.24 |
| Uncharacterized protein | A2XM46_ORYSI (+1) | OsI_13588 | 0.35 | 0.03 |
| Uncharacterized protein | B8BM99_ORYSI | OsI_38581 | 0.00 | 0.32 |
| Os07g0671800 protein (Fragment) | A0A0P0XAA0_ORYSJ | Os07g0671800 | 0.26 | 0.04 |
| Chaperonin protein | Q6ASR1_ORYSJ | Os05g0147400 | 0.01 | 0.26 |
| Os02g0196800 protein | Q6H7M1_ORYSJ | Os02g0196800 | 0.24 | 0.03 |
| Os10g0100300 protein | Q10A77_ORYSJ | LOC_Os10g01044 | 0.00 | 0.26 |
| Delta-aminolevulinic acid dehydratase, chloroplastic | HEM2_ORYSJ | HEMB | 0.24 | 0.03 |
| Uncharacterized protein | Q8HCR5_ORYSJ | orf25 | 0.24 | 0.01 |
| Uncharacterized protein | B8AMC4_ORYSI (+1) | OsI_14111 | 0.21 | 0.04 |
| Os06g0232600 protein | Q67UK9_ORYSJ | Os06g0232600 | 0.16 | 0.03 |
| Uncharacterized protein | B8AN77_ORYSI (+1) | OsI_14277 | 0.08 | 0.09 |
| Os02g0117100 protein | Q6ZGM0_ORYSJ | Os02g0117100 | 0.07 | 0.09 |
| Os02g0792800 protein | Q6K689_ORYSJ | Os02g0792800 | 0.07 | 0.08 |
| Os03g0390700 protein | Q7XXQ9_ORYSJ | LOC_Os03g27320 | 0.06 | 0.09 |
| Uncharacterized protein | A2X835_ORYSI (+1) | OsI_08388 | 0.12 | 0.03 |
| Uncharacterized protein | A2YHF9_ORYSI (+1) | OsI_24624 | 0.06 | 0.09 |
| 30S ribosomal protein S4, chloroplastic | RR4_ORYSI (+1) | rps4 | 0.07 | 0.07 |
| Uncharacterized protein | A2YLI3_ORYSI (+1) | OsI_26080 | 0.06 | 0.08 |
| Uncharacterized protein | A2XU31_ORYSI | OsI_16109 | 0.07 | 0.06 |
| Uncharacterized protein | A2YZX0_ORYSI (+1) | OsI_30905 | 0.07 | 0.07 |
| Dirigent protein | A2Y986_ORYSI | OsI_21624 | 0.07 | 0.06 |
| Os10g0470900 protein | Q7XDI5_ORYSJ | LOC_Os10g33230 | 0.05 | 0.08 |
| Uncharacterized protein | B8AR34_ORYSI (+1) | OsI_13422 | 0.06 | 0.08 |
| Os01g0144100 protein | Q9ARP1_ORYSJ | Os01g0144100 | 0.05 | 0.09 |
| Uncharacterized protein | A2XXG3_ORYSI | OsI_17369 | 0.05 | 0.08 |
| Citrate synthase | Q7F8R1_ORYSJ | P0437H03 | 0.05 | 0.08 |
| Peptidylprolyl isomerase | A2X9U8_ORYSI (+1) | OsI_09019 | 0.05 | 0.08 |
| Uncharacterized protein | A2WWU4_ORYSI (+1) | OsI_04374 | 0.07 | 0.06 |
| NADH dehydrogenase [ubiquinone] iron-sulfur protein 3 | NDUS3_ORYSJ (+1) | NAD9 | 0.05 | 0.07 |
| Nitrogen regulatory protein P-II homolog | GLNB_ORYSJ | GLB | 0.04 | 0.08 |
| Uncharacterized protein | A2XN31_ORYSI (+1) | OsI_13961 | 0.03 | 0.09 |
| 4-alpha-glucanotransferase DPE1, chloroplastic/amyloplastic | DPE1_ORYSJ | DPE1 | 0.00 | 0.11 |
| Eukaryotic translation initiation factor isoform 4G-1 | IF4G1_ORYSJ | Os04g0499300 | 0.10 | 0.01 |
| Hsp20/alpha crystallin family protein, expressed | Q7G754_ORYSJ | LOC_Os10g07210 | 0.04 | 0.07 |
| DNA binding protein PF1 | Q69MW7_ORYSJ | Os09g0402100 | 0.04 | 0.07 |
| Uncharacterized protein | B8AWQ3_ORYSI | OsI_20971 | 0.05 | 0.06 |
| Os06g0264300 protein | Q5Z6P9_ORYSJ | Os06g0264300 | 0.05 | 0.06 |

| | | | | |
|---|---|---|---|---|
| Uncharacterized protein | B8BE24_ORYSI (+1) | OsI_32232 | 0.04 | 0.07 |
| Uncharacterized protein | A2XPF9_ORYSI (+1) | OsI_14471 | 0.05 | 0.06 |
| Uncharacterized protein | B8B5M9_ORYSI (+1) | OsI_25803 | 0.04 | 0.06 |
| Uncharacterized protein | A2XLM8_ORYSI (+1) | OsI_13379 | 0.05 | 0.05 |
| Probable aldo-keto reductase 2 | AKR2_ORYSI (+1) | OsI_15387 | 0.04 | 0.06 |
| Os11g0592200 protein | Q941F5_ORYSJ | PR4 | 0.02 | 0.08 |
| 3-isopropylmalate dehydrogenase (Fragment) | A0A0P0W1E6_ORYSJ | Os03g0655700 | 0.03 | 0.06 |
| Os06g0687800 protein | Q653F5_ORYSJ | Os06g0687800 | 0.04 | 0.06 |
| Pyrophosphate--fructose 6-phosphate 1-phosphotransferase subunit alpha | B8AHL5_ORYSI (+1) | PFP-ALPHA | 0.05 | 0.04 |
| Probable aquaporin PIP2-2 | PIP22_ORYSJ | PIP2-2 | 0.03 | 0.06 |
| Cytochrome b559 subunit alpha | PSBE_ORYSI (+2) | psbE | 0.01 | 0.07 |
| Os03g0214600 protein | Q10Q05_ORYSJ | Os03g0214600 | 0.03 | 0.06 |
| Uncharacterized protein | B8ALV6_ORYSI (+1) | OsI_09743 | 0.02 | 0.07 |
| NADH-cytochrome b5 reductase | Q5VR12_ORYSJ | Os01g0174300 | 0.03 | 0.06 |
| Os01g0139200 protein | Q5ZDH9_ORYSJ | Os01g0139200 | 0.03 | 0.05 |
| GTP-binding protein Rab6 | Q8H4Q9_ORYSJ | OJ1457_D07 | 0.03 | 0.05 |
| Probable V-type proton ATPase subunit H | VATH_ORYSJ | Os07g0549700 | 0.02 | 0.05 |
| Uncharacterized protein | B8AWM3_ORYSI | OsI_19471 | 0.04 | 0.03 |
| Uncharacterized protein | A2XHV1_ORYSI (+1) | OsI_11989 | 0.03 | 0.05 |
| Acetyltransferase component of pyruvate dehydrogenase complex | Q654L9_ORYSJ | Os06g0499900 | 0.05 | 0.02 |
| Uncharacterized protein | A2ZIF8_ORYSI | OsI_37606 | 0.02 | 0.05 |
| Glucose-6-phosphate isomerase | B8BCM8_ORYSI (+1) | OsI_31689 | 0.05 | 0.02 |
| Uncharacterized protein | A2ZIM1_ORYSI (+1) | OsI_37672 | 0.02 | 0.05 |
| Uncharacterized protein | B8BMN2_ORYSI | OsI_38846 | 0.02 | 0.04 |
| Uncharacterized protein | A2ZLT9_ORYSI (+1) | OsI_38783 | 0.03 | 0.04 |
| Os04g0685600 protein | A0A0N7KJY7_ORYSJ (+1) | Os04g0685600 | 0.03 | 0.03 |
| Os02g0106800 protein | Q6ETC8_ORYSJ | Os02g0106800 | 0.01 | 0.05 |
| Os06g0320700 protein | Q5ZA96_ORYSJ | Os06g0320700 | 0.02 | 0.04 |
| Uncharacterized protein | B8AVZ8_ORYSI (+1) | OsI_17824 | 0.02 | 0.04 |
| Eukaryotic translation initiation factor 3 subunit A | Q5ZEN1_ORYSJ | P0684C01 | 0.03 | 0.03 |
| Uncharacterized protein | A2ZBF1_ORYSI (+1) | OsI_35100 | 0.03 | 0.03 |
| Cytochrome b-c1 complex subunit Rieske, mitochondrial | A2X5F8_ORYSI (+1) | OsI_07438 | 0.02 | 0.04 |
| Gamma interferon inducible lysosomal thiol reductase family protein, expressed | Q10MT8_ORYSJ | Os03g0295800 | 0.03 | 0.03 |
| 40S ribosomal protein S26 | B8ABD0_ORYSI (+1) | OsI_04251 | 0.02 | 0.03 |
| Pyrophosphate--fructose 6-phosphate 1-phosphotransferase subunit alpha | B8B9Z2_ORYSI (+1) | PFP-ALPHA | 0.03 | 0.03 |
| Uncharacterized protein | B8AD25_ORYSI (+1) | OsI_00236 | 0.02 | 0.04 |
| Uncharacterized protein | A2XEP1_ORYSI (+1) | OsI_10803 | 0.04 | 0.02 |
| Uncharacterized protein | B8A8X4_ORYSI | OsI_02153 | 0.02 | 0.04 |
| Os01g0784800 protein | Q8LQN2_ORYSJ | Os01g0784800 | 0.02 | 0.03 |
| Reticulon-like protein | B8B2W6_ORYSI | OsI_23118 | 0.01 | 0.04 |
| Os10g0436800 protein | A0A0P0XV01_ORYSJ | Os10g0436800 | 0.02 | 0.03 |
| Sucrose transport protein SUT2 | SUT2_ORYSI (+1) | SUT2 | 0.01 | 0.04 |
| Pyrophosphate--fructose 6-phosphate 1-phosphotransferase subunit alpha | Q0DCI1_ORYSJ | Os06g0326400 | 0.02 | 0.03 |
| Uncharacterized protein | A2YQP2_ORYSI (+1) | OsI_27611 | 0.02 | 0.03 |
| Uncharacterized protein | B8AIS2_ORYSI (+1) | OsI_08964 | 0.01 | 0.03 |
| Os08g0559600 protein | Q6YZH8_ORYSJ | Os08g0559600 | 0.01 | 0.03 |
| Uncharacterized protein | B8B1T1_ORYSI | OsI_24243 | 0.02 | 0.01 |
| Uncharacterized protein | A2YFJ3_ORYSI (+1) | OsI_23875 | 0.02 | 0.02 |
| Hydroxyproline-rich glycoprotein family protein, putative, expressed | Q8LNU2_ORYSJ | OSJNBa0041P03 | 0.01 | 0.02 |
| Uncharacterized protein | A2WL57_ORYSI (+1) | OsI_00570 | 0.01 | 0.02 |
| Uncharacterized protein | A2YI72_ORYSI (+1) | OsI_24908 | 0.01 | 0.02 |
| Plasma membrane ATPase | B8B893_ORYSI (+1) | OsI_25220 | 0.01 | 0.01 |
| Phenylalanine ammonia-lyase | A2XVK1_ORYSI (+1) | OsI_16658 | 0.00 | 0.00 |
| Uncharacterized protein | B8B5K7_ORYSI (+1) | OsI_27219 | 54.97 | 0.17 |
| Os01g0185200 protein | Q5VRX8_ORYSJ | P0510F03 | 34.67 | 0.03 |
| Elongation factor 1-gamma 2 | EF1G2_ORYSJ | Os02g0220500 | 31.10 | 0.05 |
| Uncharacterized protein | A2XNY1_ORYSI (+1) | OsI_14280 | 0.07 | 1.46 |
| Chlorophyll a-b binding protein, chloroplastic | A2YCB9_ORYSI (+1) | OsI_22755 | 0.07 | 17.87 |
| Glutathione S-transferase | Q6WSC2_ORYSI | gstu4 | 0.06 | 16.14 |
| ATP synthase subunit b, chloroplastic | ATPF_ORYSI (+1) | atpF | 0.06 | 33.20 |
| Uncharacterized protein | A2XBY3_ORYSI (+1) | OsI_09799 | 0.06 | 13.67 |
| Os03g0219200 protein (Fragment) | Q0DTX5_ORYSJ | Os03g0219200 | 0.04 | 13.40 |
| Ribosome-recycling factor, chloroplastic | RRFC_ORYSI (+1) | OsI_26546 | 0.03 | 15.39 |
| Cysteine proteinase inhibitor (Fragment) | A0A0P0V179_ORYSJ (+1) | Os01g0270100 | 0.03 | 11.41 |

**Proteins found in both Koshihikari and Samnam exposed to heat stress**

269 and 215 proteins in Koshihikari and 195 and 163 proteins in Samnam were respectively up- and downregulated exposed to heat stress (**Figure 2-3C**). Among those, there were 125 upregulated and 125 downregulated proteins found in common between Koshihikari and Samnam (**Table 2-4**). The major differentially expressed proteins found in both cultivars were involved in metabolic process (32%), oxidation-reduction process (21%) and response to stimulus (10%). A decrease in abundance was observed mostly in metabolic process (41%), oxidation-reduction process (20%). In contrast, an increase in abundance was observed not only in oxidation-reduction process (22%) and metabolic process (21%) but also in response to stimulus (16%). Among these proteins, DnaK family protein was mostly increased in both cultivars. Moreover, a number of heat shock proteins were also highly expressed in both cultivars.

**Table 2-4** DEPs found in both Koshihikari and Samnam exposed to heat stress

| Identified Proteins | Accession Number | Alternate ID | dHTK | dHTS |
|---|---|---|---|---|
| DnaK family protein, putative, expressed | Q6L509_ORYSJ | Os05g0460000 | 487.25 | 676.69 |
| 26.7 kDa heat shock protein, chloroplastic | HS26P_ORYSJ | HSP26 | 206.23 | 134.04 |
| Phosphoenolpyruvate carboxylase, putative, expressed | A0A0P0XLG1_ORYSJ | Os09g0315700 | 188.60 | 142.31 |
| Uncharacterized protein | A2Y2C8_ORYSI (+1) | OsI_19158 | 281.73 | 8.69 |
| Uncharacterized protein | A2X9T6_ORYSI (+1) | OsI_09007 | 141.57 | 115.27 |
| Ubiquinol oxidase | A2XX54_ORYSI (+1) | OsI_17254 | 170.08 | 85.28 |
| Glutathione S-transferase, N-terminal domain containing protein, expressed | Q945W6_ORYSJ | Os10g0527800 | 184.36 | 55.34 |
| Uncharacterized protein | B8A9R2_ORYSI | OsI_03777 | 186.41 | 52.42 |
| Os01g0754500 protein | Q5JML5_ORYSJ | Os01g0754500 | 182.38 | 46.82 |
| Ubiquinol oxidase | A2XX55_ORYSI (+1) | OsI_17255 | 174.61 | 53.75 |
| Mitochondrial Rho GTPase | A2XN85_ORYSI (+1) | OsI_14016 | 139.44 | 87.36 |
| Alpha-dioxygenase, putative, expressed | Q2QRV3_ORYSJ | LOC_Os12g26290 | 154.26 | 35.21 |
| Uncharacterized protein | A2XE02_ORYSI (+1) | OsI_10547 | 126.01 | 55.23 |
| Aldehyde dehydrogenase | Q69P84_ORYSJ | OJ1344_B01 | 105.24 | 73.35 |
| Uncharacterized protein | A2Y861_ORYSI (+1) | OsI_21235 | 143.20 | 35.36 |
| Uncharacterized protein | A2XZ94_ORYSI | OsI_18034 | 78.66 | 84.19 |

| | | | | |
|---|---|---|---|---|
| Os09g0379900 protein | Q6H5B5_ORYSJ | Os09g0379900 | 101.37 | 56.10 |
| Hydroxyproline-rich glycoprotein family protein | Q8LNU2_ORYSJ | OSJNBa0041P03 | 122.65 | 30.02 |
| Uncharacterized protein | A2XEW1_ORYSI (+1) | OsI_10878 | 85.60 | 64.95 |
| Os03g0840200 protein | Q6AVR6_ORYSJ | LOC_Os03g62370 | 26.21 | 120.90 |
| Uncharacterized protein | A2WKD5_ORYSI (+1) | OsI_00285 | 79.29 | 60.95 |
| Hsp18.0 | A2XEW8_ORYSI (+1) | Hsp18 | 77.74 | 58.55 |
| 18.0 kDa class II heat shock protein | HSP18_ORYSJ (+1) | HSP18 | 68.34 | 64.14 |
| Uncharacterized protein | A2Y534_ORYSI (+1) | OsI_20107 | 62.68 | 64.14 |
| Uncharacterized protein | B8BGM4_ORYSI | OsI_33417 | 69.81 | 55.29 |
| Sucrose synthase | B8APD5_ORYSI (+1) | OsI_11498 | 84.04 | 38.06 |
| Uncharacterized protein | A2X753_ORYSI (+1) | OsI_08047 | 69.14 | 52.15 |
| 17.7 kDa class I heat shock protein | HS177_ORYSJ | HSP17 | 65.53 | 55.35 |
| Uncharacterized protein | A2XEW6_ORYSI (+2) | OsI_10881 | 66.23 | 53.75 |
| Uncharacterized protein | B8AMC4_ORYSI (+1) | OsI_14111 | 64.18 | 50.55 |
| Uncharacterized protein | A2X9V8_ORYSI | OsI_09029 | 18.30 | 86.80 |
| Uncharacterized protein | A2ZKG0_ORYSI | OsI_38312 | 69.19 | 34.57 |
| Probable linoleate 9S-lipoxygenase 4 | LOX4_ORYSJ | Os03g0700700 | 86.39 | 14.06 |
| Catalase | B8B2L5_ORYSI (+2) | OsI_24526 | 54.65 | 44.19 |
| Os07g0638100 protein | Q8GVH2_ORYSJ | OJ1340_C08 | 82.63 | 15.15 |
| Os01g0947000 protein | Q8GT15_ORYSJ | Os01g0947000 | 84.24 | 12.99 |
| Uncharacterized protein | B8ACF1_ORYSI | OsI_04454 | 60.47 | 34.56 |
| Superoxide dismutase [Mn], mitochondrial | SODM_ORYSJ | SODA | 59.83 | 32.17 |
| Uncharacterized protein | B8AI32_ORYSI (+1) | OsI_08851 | 56.17 | 34.56 |
| Glycosyltransferase | A2WUT6_ORYSI (+1) | OsI_03644 | 75.82 | 12.99 |
| Os10g0491000 protein | Q9FWU4_ORYSJ | Os10g0491000 | 62.66 | 21.78 |
| Uncharacterized protein | A2Z9M2_ORYSI (+1) | OsI_34432 | 49.07 | 30.57 |
| Os12g0478100 protein (Fragment) | C7JA48_ORYSJ | Os12g0478200 | 44.76 | 34.57 |
| V-type proton ATPase subunit C | B8AXG9_ORYSI (+1) | OsI_21221 | 44.68 | 32.97 |
| Plasma membrane ATPase | A2XYF8_ORYSI (+1) | OsI_17734 | 52.21 | 20.96 |
| Thioredoxin H1 | TRXH1_ORYSJ (+1) | TRXH | 36.91 | 35.38 |
| Probable plastid-lipid-associated protein 2, chloroplastic | PAP2_ORYSJ | PAP2 | 4.14 | 66.54 |
| Formate dehydrogenase 1, mitochondrial | FDH1_ORYSJ | Os06g0486800 | 33.95 | 36.16 |
| Glutathione S-transferase, N-terminal domain containing protein | Q67UK9_ORYSJ | Os06g0232600 | 35.45 | 32.97 |
| Uncharacterized protein | A2Y7F9_ORYSI (+1) | OsI_20977 | 53.29 | 14.59 |
| Uncharacterized protein | A2YAZ4_ORYSI (+1) | OsI_22266 | 44.03 | 21.78 |
| Cysteine proteinase inhibitor (Fragment) | A0A0P0V179_ORYSJ (+1) | Os01g0270100 | 44.84 | 20.18 |
| Fiber protein Fb19, putative, expressed | Q2QNV2_ORYSJ | Os12g0552500 | 34.75 | 29.77 |
| Uncharacterized protein | B8AZZ6_ORYSI (+1) | OsI_20631 | 30.39 | 31.35 |
| Os07g0671800 protein (Fragment) | A0A0P0XAA0_ORYSJ | Os07g0671800 | 3.65 | 56.95 |
| Peroxygenase | PXG_ORYSI (+1) | PXG | 35.03 | 24.97 |
| Uncharacterized protein | B8BPQ2_ORYSI | OsI_38365 | 23.02 | 36.77 |
| Uncharacterized protein | A2XMP7_ORYSI (+1) | OsI_13813 | 25.40 | 33.76 |
| Os03g0744600 protein | Q7XXR0_ORYSJ | LOC_Os03g53270 | 34.05 | 24.98 |
| Annexin | A2X9Q4_ORYSI (+1) | Ann2 | 32.59 | 24.98 |
| Lactoylglutathione lyase | Q0DJE6_ORYSJ | Os05g0295800 | 34.70 | 20.18 |
| 16.9 kDa class I heat shock protein 3 | HS16C_ORYSJ | HSP16 | 39.73 | 14.59 |
| Uncharacterized protein | B8AVZ8_ORYSI (+1) | OsI_17824 | 26.12 | 26.58 |
| Proteasome subunit alpha type-4-1 | PSA4A_ORYSI (+2) | OsI_021120 | 26.11 | 23.38 |
| Alpha-galactosidase | B8B656_ORYSI (+1) | OsI_27343 | 24.67 | 23.38 |
| Uncharacterized protein | A2X6K4_ORYSI (+1) | OsI_07846 | 32.58 | 15.38 |
| Os02g0705400 protein | Q6Z2G8_ORYSJ | P0680A05 | 35.44 | 12.19 |
| Cell death associated protein | Q6J657_ORYSJ | Os05g0410200 | 26.89 | 18.59 |
| Os09g0567300 protein | Q652L6_ORYSJ | Os09g0567300 | 23.27 | 21.77 |
| Uncharacterized protein | A2XNF7_ORYSI (+1) | OsI_14096 | 26.07 | 18.59 |
| Os02g0704800 protein | Q6YVI0_ORYSJ | Os02g0704800 | 40.88 | 3.05 |
| Uncharacterized protein | A2YIC9_ORYSI (+1) | OsI_24970 | 23.21 | 20.18 |
| Isocitrate dehydrogenase [NAD] subunit, mitochondrial | Q9SDG5_ORYSJ | Os01g0276100 | 24.62 | 18.58 |
| Uncharacterized protein | A2XY57_ORYSI (+1) | OsI_17640 | 28.24 | 13.78 |
| Os03g0219200 protein (Fragment) | Q0DTX5_ORYSJ | Os03g0219200 | 18.24 | 23.38 |
| Os05g0157200 protein | Q75M01_ORYSJ | Os05g0157200 | 27.60 | 12.19 |
| Uncharacterized protein | A2WWV4_ORYSI | OsI_04384 | 20.41 | 18.58 |
| Os09g0338400 protein | Q6ERL4_ORYSJ | Os09g0338400 | 21.82 | 16.98 |
| Proteasome subunit beta type | A2XA20_ORYSI (+1) | OsI_09094 | 23.29 | 15.39 |
| Citrate synthase | Q7F8R1_ORYSJ | P0437H03 | 23.95 | 14.59 |
| Uncharacterized protein | B8AIX1_ORYSI | OsI_06111 | 29.30 | 9.13 |
| Gamma-aminobutyrate transaminase 1, mitochondrial | GATP1_ORYSI (+1) | OsI_17385 | 25.37 | 12.99 |
| Uncharacterized protein | A2YAR7_ORYSI (+1) | OsI_22183 | 15.37 | 20.97 |
| Armadillo/beta-catenin-like repeat family protein, expressed | Q852A6_ORYSJ | OSJNBb0081B07 | 24.66 | 11.39 |

| | | | | |
|---|---|---|---|---|
| Uncharacterized protein | A2XZJ1_ORYSI (+1) | OsI_18149 | 17.46 | 17.78 |
| Hypersensitive-induced response protein 1 | HIR1_ORYSJ | HIR1 | 15.33 | 19.38 |
| Os06g0531200 protein | Q5Z790_ORYSJ | Os06g0531200 | 18.20 | 15.39 |
| Uncharacterized protein | B8BKA3_ORYSI (+1) | OsI_35959 | 17.53 | 15.38 |
| Uncharacterized protein | A2XZ07_ORYSI (+1) | OsI_17940 | 18.19 | 14.59 |
| Uncharacterized protein | A2X5N7_ORYSI (+1) | OsI_07520 | 16.05 | 16.18 |
| Dihydrolipoyl dehydrogenase | A2WPH0_ORYSI (+1) | OsI_01744 | 16.81 | 15.38 |
| Uncharacterized protein | B8ABY6_ORYSI (+1) | OsI_02921 | 17.49 | 14.59 |
| Ornithine aminotransferase, mitochondrial | OAT_ORYSJ | OAT | 20.42 | 11.39 |
| Anthranilate synthase alpha subunit 2, chloroplastic | ASA2_ORYSJ (+1) | OsASA2 | 15.98 | 15.51 |
| Annexin | A2YAT3_ORYSI (+1) | OsI_22198 | 11.79 | 19.39 |
| Uncharacterized protein | B8APW2_ORYSI (+1) | OsI_11657 | 15.37 | 15.38 |
| Uncharacterized protein | A2YK26_ORYSI (+1) | OsI_25575 | 2.92 | 27.38 |
| Alcohol dehydrogenase 1 | ADH1_ORYSI (+1) | ADH1 | 16.05 | 13.79 |
| Os08g0464000 protein | Q6YUA7_ORYSJ | Os08g0464000 | 16.04 | 13.79 |
| putative late embryogenesis abundant protein, LEA14-A | Q75HZ0_ORYSJ | Os05g0584200 | 18.19 | 11.39 |
| Uncharacterized protein | B8AMJ8_ORYSI | OsI_12624 | 14.64 | 14.59 |
| Os01g0757500 protein | Q5JLZ9_ORYSJ | Os01g0757500 | 17.00 | 11.39 |
| Uncharacterized protein | A2ZJA1_ORYSI (+1) | OsI_37900 | 11.06 | 16.18 |
| Uncharacterized protein | B8B5M9_ORYSI (+1) | OsI_25803 | 14.64 | 12.19 |
| Os01g0528800 protein | Q5QM39_ORYSJ | Os01g0528800 | 14.64 | 12.19 |
| Beta-fructofuranosidase, insoluble isoenzyme 1 | INV1_ORYSJ | CIN1 | 13.64 | 11.21 |
| Argininosuccinate lyase | A0A024FLK4_ORYSJ | OsASL1 | 12.47 | 12.18 |
| Uncharacterized protein | A2X813_ORYSI (+1) | OsI_08367 | 1.81 | 21.77 |
| Chaperone protein ClpB2, chloroplastic | CLPB2_ORYSJ | CLPB2 | 9.88 | 5.32 |
| Dehydroascorbate reductase | Q65XA0_ORYSJ | Os05g0116100 | 7.51 | 5.90 |
| Uncharacterized protein | A2XB19_ORYSI (+1) | OsI_09452 | 6.84 | 3.94 |
| Os05g0519400 protein | Q65X08_ORYSJ | Os05g0519400 | 5.21 | 3.16 |
| Chaperonin | Q69Y99_ORYSJ | P0528E04 | 5.12 | 3.18 |
| Superoxide dismutase [Cu-Zn] 2 | SODC2_ORYSJ | SODCC2 | 4.11 | 2.84 |
| Uncharacterized protein | A2YS08_ORYSI (+1) | OsI_28106 | 3.49 | 2.46 |
| Uncharacterized protein | A2Y3J4_ORYSI (+1) | OsI_19576 | 2.60 | 2.98 |
| Phosphoglycerate kinase | B8AIH2_ORYSI (+1) | OsI_06015 | 3.34 | 2.03 |
| Harpin binding protein 1, putative, expressed | Q2R1S1_ORYSJ | Os11g0595200 | 2.16 | 2.31 |
| Glyceraldehyde-3-phosphate dehydrogenase 1, cytosolic | G3PC1_ORYSJ (+1) | GAPC1 | 2.16 | 1.97 |
| L-ascorbate peroxidase 1, cytosolic | APX1_ORYSJ | APX1 | 2.38 | 1.72 |
| Os08g0379400 protein | Q7EYM8_ORYSJ | Os08g0379400 | 1.54 | 2.41 |
| L-ascorbate peroxidase 2, cytosolic | APX2_ORYSJ (+1) | APX2 | 2.18 | 1.61 |
| Uncharacterized protein | B8A8D4_ORYSI (+1) | OsI_03471 | 1.87 | 1.87 |
| Malate dehydrogenase, cytoplasmic | MDHC_ORYSJ | Os10g0478200 | 1.99 | 1.50 |
| Glyceraldehyde-3-phosphate dehydrogenase | A2XUU7_ORYSI (+1) | OsI_16384 | 1.28 | 1.43 |
| Uncharacterized protein | B8BNI2_ORYSI (+1) | OsI_37718 | 0.55 | 0.75 |
| Ribulose bisphosphate carboxylase small chain, chloroplastic | RBS1_ORYSI (+1) | RBCS | 0.61 | 0.66 |
| Fructose-bisphosphate aldolase | A2ZBX1_ORYSI (+1) | OsI_35277 | 0.47 | 0.62 |
| Uncharacterized protein | A2XFL8_ORYSI (+1) | OsI_11157 | 0.55 | 0.53 |
| ATP synthase epsilon chain, chloroplastic | ATPE_ORYSI (+1) | atpE | 0.48 | 0.59 |
| Os09g0535000 protein | Q69K00_ORYSJ | P0569E11 | 0.45 | 0.55 |
| Chlorophyll a-b binding protein, chloroplastic | A2XU61_ORYSI (+1) | OsI_16135 | 0.39 | 0.57 |
| Ribulose bisphosphate carboxylase/ oxygenase activase, chloroplastic | RCA_ORYSJ | RCA | 0.46 | 0.48 |
| Cold shock domain protein 2 | Q84UR8_ORYSJ | P0582D05 | 0.53 | 0.37 |
| Peroxidase | Q6AVZ8_ORYSJ | prx65 | 0.26 | 0.62 |
| ATP-dependent zinc metalloprotease FTSH 1, chloroplastic | FTSH1_ORYSJ | FTSH1 | 0.43 | 0.43 |
| Fructokinase-2 | SCRK2_ORYSI (+1) | FRK2 | 0.44 | 0.38 |
| Uncharacterized protein | B8A7J7_ORYSI (+1) | OsI_01815 | 0.26 | 0.54 |
| Chlorophyll a-b binding protein, chloroplastic | Q53N83_ORYSJ | Os11g0242800 | 0.27 | 0.48 |
| Phenylalanine ammonia-lyase | A0A0P0YAL3_ORYSJ | Os12g0520200 | 0.55 | 0.19 |
| Uncharacterized protein | B8AF20_ORYSI (+1) | OsI_07973 | 0.33 | 0.38 |
| Os03g0278000 protein | Q8W3J0_ORYSJ | UXS-3 | 0.32 | 0.34 |
| Carbonic anhydrase | A2WT25_ORYSI (+1) | OsI_03015 | 0.33 | 0.30 |
| Ribulose bisphosphate carboxylase large chain | RBL_ORYSI (+1) | rbcL | 0.15 | 0.47 |
| Uncharacterized protein | A2ZAA6_ORYSI (+1) | OsI_34669 | 0.08 | 0.54 |
| Sucrose synthase | A2XHR1_ORYSI | OsI_11950 | 0.36 | 0.22 |
| Os02g0101500 protein | Q6YU90_ORYSJ | B1370C05 | 0.21 | 0.34 |
| Uncharacterized protein | B8ATW7_ORYSI (+1) | OsI_17267 | 0.03 | 0.51 |
| Uncharacterized protein | A2Z2X9_ORYSI (+2) | OsI_28791 | 0.05 | 0.47 |
| Uncharacterized protein | B8ANZ3_ORYSI (+1) | OsI_11442 | 0.04 | 0.44 |
| Cytochrome b6-f complex iron-sulfur subunit | A2YMJ8_ORYSI (+1) | OsI_26450 | 0.17 | 0.23 |
| Alpha-L-arabinofuranosidase C-terminus family protein | Q2QY88_ORYSJ | Os12g0128700 | 0.02 | 0.37 |

| | | | | |
|---|---|---|---|---|
| S-adenosylmethionine synthase 1 | METK1_ORYSI (+1) | SAM1 | 0.21 | 0.16 |
| Dirigent protein | A2Y986_ORYSI | OsI_21624 | 0.03 | 0.32 |
| Ferredoxin--NADP reductase | Q6ZFJ3_ORYSJ | OJ1435_F07 | 0.02 | 0.19 |
| Ferredoxin--NADP reductase, leaf isozyme, chloroplastic | FENR1_ORYSJ | Os06g0107700 | 0.01 | 0.17 |
| Os01g0819400 protein | A0A0P0V9Q4_ORYSJ (+6) | Os01g0819400 | 0.08 | 0.09 |
| Aldo-keto reductase | B8AYU7_ORYSI | AKR4 | 0.08 | 0.09 |
| Uncharacterized protein | A2WV25_ORYSI (+1) | OsI_03735 | 0.09 | 0.08 |
| Uncharacterized protein | A2YVK0_ORYSI (+3) | OsI_29358 | 0.08 | 0.08 |
| Cysteine synthase | Q5UJF9_ORYSI (+1) | CAS | 0.08 | 0.08 |
| Catalase | B8AGH7_ORYSI (+1) | OsI_05576 | 0.07 | 0.09 |
| Peptidylprolyl isomerase | Q653Z1_ORYSJ | Os06g0663800 | 0.09 | 0.07 |
| Thiamine thiazole synthase, chloroplastic | Q7XXS4_ORYSJ | THI1 | 0.07 | 0.08 |
| Uncharacterized protein | B8AU72_ORYSI | OsI_17350 | 0.08 | 0.07 |
| Uncharacterized protein | B8AL26_ORYSI (+1) | OsI_10998 | 0.08 | 0.07 |
| Uncharacterized protein | A2ZK08_ORYSI (+1) | OsI_38160 | 0.07 | 0.08 |
| ATP synthase subunit b, chloroplastic | ATPF_ORYSI (+1) | atpF | 0.07 | 0.08 |
| Os12g0189300 protein | Q0IPL3_ORYSJ | Os12g0189300 | 0.08 | 0.07 |
| Cytochrome b559 subunit alpha | PSBE_ORYSI (+2) | psbE | 0.07 | 0.07 |
| Uncharacterized protein | A2XVB4_ORYSI (+1) | OsI_16554 | 0.08 | 0.06 |
| Uncharacterized protein | A2Z6D8_ORYSI (+1) | OsI_33217 | 0.07 | 0.07 |
| Uncharacterized protein | B8BHC8_ORYSI | OsI_33947 | 0.07 | 0.07 |
| Uncharacterized protein | B8B1F4_ORYSI | OsI_24144 | 0.08 | 0.06 |
| Uncharacterized protein | A2Y5W6_ORYSI | OsI_20389 | 0.08 | 0.06 |
| Glucose-1-phosphate adenylyltransferase large subunit 1, chloroplastic/amyloplastic | GLGL1_ORYSJ | AGPL1 | 0.07 | 0.06 |
| Uncharacterized protein | A2XI59_ORYSI (+1) | OsI_12120 | 0.09 | 0.05 |
| Delta-aminolevulinic acid dehydratase, chloroplastic | HEM2_ORYSJ | HEMB | 0.07 | 0.06 |
| 40S ribosomal protein S24 | B8B3L8_ORYSI | OsI_23353 | 0.07 | 0.06 |
| Uncharacterized protein | A2Y8Y0_ORYSI (+1) | OsI_21509 | 0.07 | 0.06 |
| Uncharacterized protein | A2ZBV1_ORYSI (+1) | OsI_35255 | 0.06 | 0.07 |
| Uncharacterized protein | A2YWS7_ORYSI (+1) | OsI_29793 | 0.08 | 0.04 |
| Uncharacterized protein | A2YVL4_ORYSI | OsI_29372 | 0.06 | 0.07 |
| Os08g0562100 protein | Q6YYW3_ORYSJ | Os08g0562100 | 0.06 | 0.06 |
| Dirigent protein | A2Y992_ORYSI (+1) | OsI_21630 | 0.07 | 0.05 |
| Probable pyridoxal 5'-phosphate synthase subunit PDX1.2 | PDX12_ORYSJ | PDX12 | 0.06 | 0.06 |
| Uncharacterized protein | A2XM46_ORYSI (+1) | OsI_13588 | 0.06 | 0.06 |
| Os09g0252100 protein (Fragment) | A0A0N7KQF3_ORYSJ | Os09g0252100 | 0.06 | 0.06 |
| 60S ribosomal protein L13 | A2Y8K1_ORYSI (+1) | OsI_21382 | 0.06 | 0.06 |
| Ribosomal protein | B7F9R7_ORYSJ | Os01g0860300 | 0.06 | 0.06 |
| Peroxiredoxin-2E-2, chloroplastic | PR2E2_ORYSJ | PRXIIE-2 | 0.04 | 0.07 |
| Protochlorophyllide reductase B, chloroplastic | PORB_ORYSJ | PORB | 0.07 | 0.04 |
| ATP-citrate synthase alpha chain protein 3 | ACLA3_ORYSJ (+1) | ACLA-3 | 0.04 | 0.07 |
| Glucose-1-phosphate adenylyltransferase small subunit 2, chloroplastic/amyloplastic/cytosolic | GLGS2_ORYSJ | AGPS2 | 0.05 | 0.06 |
| 3-oxoacyl-[acyl-carrier-protein] synthase | Q69YA2_ORYSJ | Os06g0196600 | 0.04 | 0.07 |
| Fructose-1,6-bisphosphatase, cytosolic | F16P2_ORYSI (+1) | OsI_04558 | 0.04 | 0.06 |
| Uncharacterized protein | B8BMN2_ORYSI | OsI_38846 | 0.05 | 0.05 |
| Cold shock domain protein 1 | Q6YUR8_ORYSJ | CSP1 | 0.06 | 0.05 |
| 60S ribosomal protein L13 | A2XIT5_ORYSI (+1) | OsI_12345 | 0.06 | 0.05 |
| 60S ribosomal protein L6 | B8AVI5_ORYSI (+1) | OsI_16279 | 0.05 | 0.05 |
| Os10g0461100 protein | Q109K8_ORYSJ (+1) | Os10g0461100 | 0.05 | 0.05 |
| Uncharacterized protein | B8AU70_ORYSI (+1) | OsI_17346 | 0.05 | 0.04 |
| Uncharacterized protein | A2XF65_ORYSI | OsI_11006 | 0.04 | 0.05 |
| Uncharacterized protein | A2Z925_ORYSI (+1) | OsI_34214 | 0.05 | 0.04 |
| Os06g0538900 protein (Fragment) | A0A0P0WXJ2_ORYSJ | Os06g0538900 | 0.05 | 0.05 |
| Uncharacterized protein | A2XHP8_ORYSI (+1) | OsI_11938 | 0.03 | 0.05 |
| Peroxidase | B8APG3_ORYSI | OsI_11487 | 0.05 | 0.04 |
| Uncharacterized protein | B8B5K7_ORYSI (+1) | OsI_27219 | 0.04 | 0.05 |
| Uncharacterized protein | A2Z9K4_ORYSI (+1) | OsI_34414 | 0.05 | 0.04 |
| Cucumisin-like serine protease, putative, expressed | Q75I27_ORYSJ | OSJNBa0004G03 | 0.02 | 0.06 |
| Porphobilinogen deaminase, chloroplastic | HEM3_ORYSJ | HEMC | 0.04 | 0.04 |
| Os02g0196800 protein | Q6H7M1_ORYSJ | Os02g0196800 | 0.03 | 0.05 |
| Os05g0382600 protein | B7E4J4_ORYSJ (+1) | Os05g0382600 | 0.04 | 0.04 |
| Os02g0720900 protein (Fragment) | A0A0N7KG02_ORYSJ (+2) | Os02g0720900 | 0.04 | 0.04 |
| Phenylalanine ammonia-lyase | PAL1_ORYSJ | PAL | 0.02 | 0.05 |
| Os01g0315800 protein | Q75PK7_ORYSJ | UXS-2 | 0.03 | 0.04 |
| Os05g0363200 protein | Q6I683_ORYSJ | UXS-5 | 0.03 | 0.04 |

| | | | | |
|---|---|---|---|---|
| Uncharacterized protein | B8B936_ORYSI | OsI_30021 | 0.04 | 0.03 |
| Uncharacterized protein | A2WJQ6_ORYSI (+1) | OsI_00053 | 0.03 | 0.04 |
| Uncharacterized protein | A2ZLP6_ORYSI (+1) | OsI_38742 | 0.03 | 0.04 |
| Uncharacterized protein | A2ZAT7_ORYSI (+2) | OsI_34873 | 0.04 | 0.04 |
| Probable glutamyl endopeptidase, chloroplastic | CGEP_ORYSJ | GEP | 0.03 | 0.04 |
| Uncharacterized protein | A2XEP1_ORYSI (+1) | OsI_10803 | 0.02 | 0.05 |
| Os09g0279500 protein | Q6H443_ORYSJ | Os09g0279500 | 0.04 | 0.03 |
| Os02g0779200 protein (Fragment) | A0A0P0VQ78_ORYSJ (+1) | Os02g0779200 | 0.03 | 0.04 |
| Ribulose-phosphate 3-epimerase | B8APA6_ORYSI (+1) | OsI_10180 | 0.04 | 0.03 |
| Peroxidase | A2X2T0_ORYSI (+1) | OsI_06495 | 0.03 | 0.03 |
| Os10g0100300 protein | Q10A77_ORYSJ | LOC_Os10g01044 | 0.04 | 0.02 |
| Uncharacterized protein | A2ZN20_ORYSI | OsI_39235 | 0.02 | 0.03 |
| Phospholipase D | Q9LKM3_ORYSI | RPLD3 | 0.02 | 0.03 |
| Pyrophosphate--fructose 6-phosphate 1-phosphotransferase subunit alpha | B8B9Z2_ORYSI (+1) | PFP-ALPHA | 0.03 | 0.03 |
| Protein translocase subunit SecA | A2WP63_ORYSI | OsI_01632 | 0.03 | 0.03 |
| Probable 4-coumarate--CoA ligase 3 | 4CL3_ORYSJ (+1) | 4CL3 | 0.02 | 0.03 |
| Uncharacterized protein | A2YHE6_ORYSI (+1) | OsI_24612 | 0.03 | 0.02 |
| 40S ribosomal protein S8 | B8AHZ6_ORYSI (+1) | OsI_07259 | 0.03 | 0.02 |
| Glycine-rich RNA binding protein | Q6ASX7_ORYSJ | Os03g0670700 | 0.02 | 0.02 |
| Os10g0492300 protein | Q0IWS0_ORYSJ | Os10g0492300 | 0.03 | 0.02 |
| Uncharacterized protein | B8B8E9_ORYSI (+1) | OsI_25360 | 0.03 | 0.02 |
| Serine hydroxymethyltransferase | A0A0P0Y248_ORYSJ | Os11g0455800 | 0.02 | 0.02 |
| Uncharacterized protein | A2XDB9_ORYSI (+1) | OsI_10302 | 0.02 | 0.02 |
| Acylamino-acid-releasing enzyme 1 | AARE1_ORYSJ (+1) | Os10g0415600 | 0.02 | 0.02 |
| Nucleoid DNA-binding-like protein | Q8GSB5_ORYSJ | OJ1477_F01 | 0.02 | 0.02 |
| Alpha-1,4 glucan phosphorylase | Q8LQ33_ORYSJ | Os01g0851700 | 0.02 | 0.02 |
| Glycosyltransferase | Q5VME5_ORYSJ | Os06g0289900 | 0.01 | 0.01 |
| Flavone 3'-O-methyltransferase 1 | OMT1_ORYSJ | COMT | 0.01 | 0.01 |
| Uncharacterized protein | B8AIS2_ORYSI (+1) | OsI_08964 | 0.01 | 0.01 |
| S-adenosylmethionine synthase 2 | METK2_ORYSJ | SAM2 | 0.01 | 0.01 |
| Uncharacterized protein | B8AJW3_ORYSI (+1) | OsI_13516 | 0.01 | 0.01 |
| Cytochrome f | CYF_ORYSI (+1) | petA | 0.01 | 0.01 |
| Phenylalanine ammonia-lyase | A2XVK1_ORYSI (+1) | OsI_16658 | 0.00 | 0.00 |

**Proteins found in both Koshihikari and Samnam under recovery after heat stress**

221 and 278 proteins in Koshihikari and 235 and 170 proteins in Samnam were respectively up- and downregulated (**Figure 2-3D**). Among those, there were 113 upregulated and 127 downregulated proteins found in common between Koshihikari and Samnam (**Table 2-5**). The major differentially expressed proteins found in both cultivars were involved in metabolic process (28%), oxidation-reduction process (18%) and response to stimulus (8). A decrease in

abundance was observed mostly in metabolic process (37%), oxidation-reduction process (16%). In contrast, an increase in abundance was observed in oxidation-reduction process (21%), metabolic process (19%), and response to stimulus (12%). Among these proteins, DnaK family proteins and a number of heat shock proteins were mostly increased in both cultivars which were showing similar patterns as heat stress response.

**Table 2-5** DEPs found in both Koshihikari and Samnam under recovery after heat stress

| Identified Proteins | Accession Number | Alternate ID | dHRK | dHRS |
|---|---|---|---|---|
| DnaK family protein, putative, expressed | Q6L509_ORYSJ | Os05g0460000 | 663.81 | 623.29 |
| 70 kDa heat shock protein | Q10SR3_ORYSJ | LOC_Os03g02260 | 371.39 | 400.72 |
| 26.7 kDa heat shock protein, chloroplastic | HS26P_ORYSJ | HSP26 | 288.81 | 89.02 |
| Uncharacterized protein | A2Y2C8_ORYSI (+1) | OsI_19158 | 334.16 | 8.08 |
| DnaK family protein, putative, expressed | B9G4B3_ORYSJ | Os09g0491772 | 216.04 | 98.56 |
| Heat shock protein 81-3 | HSP83_ORYSJ | HSP81-3 | 201.71 | 53.98 |
| Uncharacterized protein | A2X036_ORYSI (+1) | OsI_05577 | 193.84 | 61.76 |
| Hsp90 protein, expressed | Q0IN14_ORYSJ | Os12g0514500 | 146.05 | 104.26 |
| Uncharacterized protein | A2X9T6_ORYSI (+1) | OsI_09007 | 156.15 | 85.42 |
| Ubiquinol oxidase | A2XX54_ORYSI (+1) | OsI_17254 | 178.99 | 50.76 |
| Uncharacterized protein | A2XPL8_ORYSI | OsI_14582 | 198.45 | 28.92 |
| Ubiquinol oxidase | A2XX55_ORYSI (+1) | OsI_17255 | 199.17 | 19.28 |
| Aldehyde dehydrogenase | Q69P84_ORYSJ | OJ1344_B01 | 129.85 | 79.33 |
| Glutathione S-transferase, N-terminal domain containing protein, expressed | Q945W6_ORYSJ | Os10g0527800 | 178.19 | 23.79 |
| Isocitrate lyase | ACEA_ORYSJ | ICL | 21.93 | 160.60 |
| WD40-like Beta Propeller Repeat family protein, expressed | Q6AVR6_ORYSJ | LOC_Os03g62370 | 81.49 | 92.54 |
| Uncharacterized protein | B8AJS5_ORYSI (+1) | OsI_11975 | 114.83 | 55.18 |
| Uncharacterized protein | B8BGM4_ORYSI | OsI_33417 | 66.05 | 82.38 |
| Hsp18.0 | A2XEW8_ORYSI (+1) | Hsp18 | 110.16 | 33.79 |
| Uncharacterized protein | A2X753_ORYSI (+1) | OsI_08047 | 94.45 | 48.65 |
| secretory protein, putative, expressed | Q9FWU4_ORYSJ | Os10g0491000 | 114.48 | 24.99 |
| Uncharacterized protein | A2Y534_ORYSI (+1) | OsI_20107 | 83.21 | 55.99 |
| Uncharacterized protein | A2XEW1_ORYSI (+1) | OsI_10878 | 95.71 | 36.77 |
| Uncharacterized protein | A2XEW6_ORYSI (+2) | OsI_10881 | 97.03 | 33.01 |
| Uncharacterized protein | A2XE02_ORYSI (+1) | OsI_10547 | 103.59 | 21.63 |
| glycosyl hydrolases family 17, putative, expressed | Q8GT15_ORYSJ | Os01g0947000 | 94.09 | 20.52 |
| Thioredoxin H1 | TRXH1_ORYSJ (+1) | TRXH | 76.87 | 27.81 |
| Uncharacterized protein | B8AXV2_ORYSI | OsI_18377 | 52.06 | 51.29 |
| Uncharacterized protein | B8AMC4_ORYSI (+1) | OsI_14111 | 59.36 | 38.62 |
| Uncharacterized protein | A2YY23_ORYSI (+1) | OsI_30244 | 66.59 | 28.12 |
| Uncharacterized protein | A2WKD5_ORYSI (+1) | OsI_00285 | 66.36 | 27.56 |
| Uncharacterized protein | B8ACF1_ORYSI | OsI_04454 | 77.03 | 13.57 |
| monodehydroascorbate reductase, putative, expressed | Q652L6_ORYSJ | Os09g0567300 | 51.43 | 39.12 |
| 18.0 kDa class II heat shock protein | HSP18_ORYSJ (+1) | HSP18 | 51.91 | 32.95 |
| Catalase | B8B2L5_ORYSI (+2) | OsI_24526 | 35.43 | 47.38 |
| Probable plastid-lipid-associated protein 2, chloroplastic | PAP2_ORYSJ | PAP2 | 4.78 | 78.03 |
| Uncharacterized protein | A2X9V8_ORYSI | OsI_09029 | 37.83 | 43.61 |
| Chitinase 1, putative, expressed | Q7XEL9_ORYSJ | Os10g0416800 | 75.70 | 3.70 |
| Sucrose synthase | B8APD5_ORYSI (+1) | OsI_11498 | 47.40 | 29.06 |
| Mitochondrial Rho GTPase | A2XN85_ORYSI (+1) | OsI_14016 | 60.16 | 14.00 |

| | | | | |
|---|---|---|---|---|
| Uncharacterized protein | B8AI32_ORYSI (+1) | OsI_08851 | 32.99 | 40.50 |
| Superoxide dismutase [Mn], mitochondrial | SODM_ORYSJ | SODA | 41.44 | 30.94 |
| Formate dehydrogenase 1, mitochondrial | FDH1_ORYSJ | Os06g0486800 | 31.88 | 39.44 |
| V-type proton ATPase subunit C | B8AXG9_ORYSI (+1) | OsI_21221 | 45.80 | 25.17 |
| Os12g0478100 protein (Fragment) | C7JA48_ORYSJ | Os12g0478200 | 52.43 | 17.40 |
| Uncharacterized protein | B8AZZ6_ORYSI (+1) | OsI_20631 | 48.74 | 20.75 |
| Fiber protein Fb19, putative, expressed | Q2QNV2_ORYSJ | Os12g0552500 | 44.91 | 24.48 |
| Uncharacterized protein | A2X5N7_ORYSI (+1) | OsI_07520 | 45.58 | 23.20 |
| Uncharacterized protein | A2Z9M2_ORYSI (+1) | OsI_34432 | 23.14 | 39.72 |
| Uncharacterized protein | A2XKX3_ORYSI (+2) | OsI_13113 | 19.45 | 42.26 |
| Peroxygenase | PXG_ORYSI (+1) | PXG | 33.04 | 24.30 |
| Uncharacterized protein | A2Y402_ORYSI (+1) | OsI_19732 | 51.15 | 3.85 |
| NADPH-dependent FMN reductase domain containing protein, expressed | Q8LQN2_ORYSJ | Os01g0784800 | 30.14 | 24.67 |
| Uncharacterized protein | A2XCU8_ORYSI (+1) | OsI_10133 | 13.14 | 37.43 |
| Uncharacterized protein | B8AM92_ORYSI (+1) | OsI_14045 | 27.73 | 22.69 |
| Uncharacterized protein | B8B537_ORYSI (+1) | OsI_27057 | 37.27 | 13.07 |
| stem-specific protein TSJT1, putative, expressed | Q7XXR0_ORYSJ | LOC_Os03g53270 | 23.36 | 25.55 |
| Uncharacterized protein | A2WYZ8_ORYSI (+1) | OsI_05163 | 34.96 | 12.10 |
| Uncharacterized protein | A2YDY6_ORYSI (+1) | OsI_23327 | 33.76 | 13.29 |
| Proteasome subunit beta type | A2XA20_ORYSI (+1) | OsI_09094 | 29.16 | 16.83 |
| Uncharacterized protein | B8AIH6_ORYSI | OsI_06005 | 32.53 | 11.31 |
| Uncharacterized protein | A2XNF7_ORYSI (+1) | OsI_14096 | 19.68 | 23.10 |
| Glutathione reductase, cytosolic | GSHRC_ORYSJ | GRC2 | 4.10 | 37.84 |
| 4-hydroxy-4-methyl-2-oxoglutarate aldolase | Q6Z6H0_ORYSJ | Os02g0761900 | 19.75 | 18.87 |
| WIP5 - Wound-induced protein precursor, expressed | Q941F5_ORYSJ | PR4 | 15.01 | 23.61 |
| Alpha-galactosidase | B8B656_ORYSI (+1) | OsI_27343 | 20.73 | 17.02 |
| Uncharacterized protein | B8AVZ8_ORYSI (+1) | OsI_17824 | 12.67 | 24.67 |
| Proteasome subunit alpha type-4-1 | PSA4A_ORYSI (+2) | OsI_021120 | 23.14 | 14.17 |
| Succinate--CoA ligase [ADP-forming] subunit beta, mitochondrial | A2X7C5_ORYSI (+1) | OsI_08117 | 21.03 | 15.91 |
| Isocitrate dehydrogenase [NAD] subunit, mitochondrial | Q9SDG5_ORYSJ | Os01g0276100 | 14.61 | 21.94 |
| Proteasome subunit alpha type | B8AB88_ORYSI (+1) | OsI_04163 | 18.47 | 17.02 |
| Glutamate dehydrogenase 2, mitochondrial | DHE2_ORYSI (+1) | GDH2 | 17.27 | 17.99 |
| Lactoylglutathione lyase | Q0DJE6_ORYSJ | Os05g0295800 | 20.95 | 14.17 |
| Gamma-aminobutyrate transaminase 1, mitochondrial | GATP1_ORYSI (+1) | OsI_17385 | 12.42 | 22.13 |
| 60S acidic ribosomal protein P0 | RLA0_ORYSJ | Os08g0130500 | 11.39 | 23.01 |
| Plasma membrane ATPase | A2XYF8_ORYSI (+1) | OsI_17734 | 19.81 | 13.90 |
| Uncharacterized protein | A2Z3I6_ORYSI (+1) | OsI_32190 | 14.86 | 16.61 |
| Uncharacterized protein | A2WRY9_ORYSI (+1) | OsI_02626 | 16.14 | 14.86 |
| NAD dependent epimerase/dehydratase family protein, putative, expressed | Q5QM39_ORYSJ | Os01g0528800 | 16.68 | 13.48 |
| Alcohol dehydrogenase 1 | ADH1_ORYSI (+1) | ADH1 | 12.67 | 16.11 |
| Uncharacterized protein | A2YAR7_ORYSI (+1) | OsI_22183 | 13.80 | 14.76 |
| cysteine desulfurase 1, mitochondrial precursor, putative, expressed | Q6ERL4_ORYSJ | Os09g0338400 | 15.31 | 12.60 |
| Uncharacterized protein | A2XY57_ORYSI (+1) | OsI_17640 | 12.82 | 12.60 |
| Glutathione peroxidase | Q0JB49_ORYSJ | Os04g0556300 | 13.73 | 11.41 |
| Arginase 1, mitochondrial | ARGI1_ORYSJ | ARG1 | 11.54 | 13.16 |
| Uncharacterized protein | A2XMP7_ORYSI (+1) | OsI_13813 | 13.11 | 11.22 |
| rRNA N-glycosidase | Q9LGK6_ORYSJ | Os01g0160800 | 12.75 | 11.22 |
| Pyruvate dehydrogenase E1 component subunit beta | B8B945_ORYSI (+1) | OsI_30042 | 1.56 | 21.63 |
| Uncharacterized protein | B8APW2_ORYSI (+1) | OsI_11657 | 11.62 | 11.31 |
| Uncharacterized protein | A2X813_ORYSI (+1) | OsI_08367 | 2.08 | 18.09 |
| Uncharacterized protein | B8AIX1_ORYSI | OsI_06111 | 14.30 | 3.65 |
| Uncharacterized protein | A2XB19_ORYSI (+1) | OsI_09452 | 8.72 | 6.02 |
| Dehydroascorbate reductase | Q65XA0_ORYSJ | Os05g0116100 | 9.06 | 5.49 |
| Uncharacterized protein | A2YZX0_ORYSI (+1) | OsI_30905 | 2.12 | 11.13 |
| Chaperonin | Q69Y99_ORYSJ | P0528E04 | 6.92 | 2.20 |
| Chaperone protein ClpB2, chloroplastic | CLPB2_ORYSJ | CLPB2 | 4.93 | 2.91 |
| Uncharacterized protein | A2WLZ0_ORYSI (+1) | OsI_00859 | 2.92 | 3.92 |
| Superoxide dismutase [Cu-Zn] 2 | SODC2_ORYSJ | SODCC2 | 3.86 | 2.41 |
| Phosphoglycerate kinase | B8AIH2_ORYSI (+1) | OsI_06015 | 4.20 | 1.84 |
| Phosphoglycerate kinase | A2YG06_ORYSI (+1) | OsI_24050 | 3.61 | 1.90 |
| Uncharacterized protein | A2YE33_ORYSI | OsI_23378 | 2.92 | 2.31 |
| Uncharacterized protein | A2YS08_ORYSI (+1) | OsI_28106 | 3.16 | 2.06 |
| Harpin binding protein 1, putative, expressed | Q2R1S1_ORYSJ | Os11g0595200 | 3.37 | 1.84 |
| Glyceraldehyde-3-phosphate dehydrogenase 1, cytosolic | G3PC1_ORYSJ (+1) | GAPC1 | 2.40 | 2.28 |
| OSJNBa0072K14.5 protein | Q7XVM2_ORYSJ | Os04g0394200 | 2.49 | 1.84 |
| Carboxymethylenebutenolidase-like protein | Q8LQS5_ORYSJ | Os01g0531500 | 2.13 | 1.84 |
| Malate dehydrogenase | A2Y7R4_ORYSI (+1) | OsI_21084 | 2.20 | 1.31 |

| | | | | |
|---|---|---|---|---|
| 6-phosphogluconate dehydrogenase, decarboxylating 1 | 6PGD1_ORYSJ | G6PGH1 | 1.86 | 1.52 |
| Fructose-bisphosphate aldolase | Q94JJ0_ORYSJ | Os01g0118000 | 2.02 | 1.31 |
| UDP-glucose pyrophosphorylase | A3QQQ3_ORYSI | UGP | 1.92 | 1.25 |
| Malate dehydrogenase, cytoplasmic | MDHC_ORYSJ | Os10g0478200 | 1.87 | 1.27 |
| Glyceraldehyde-3-phosphate dehydrogenase | A2XUU7_ORYSI (+1) | OsI_16384 | 1.54 | 1.35 |
| 2-Cys peroxiredoxin BAS1, chloroplastic | BAS1_ORYSJ | BAS1 | 1.61 | 1.08 |
| DnaK family protein, putative, expressed | B8ARU3_ORYSI (+1) | OsI_18017 | 0.67 | 0.70 |
| 70 kDa heat shock protein | Q5QMK7_ORYSJ | Os01g0817700 | 0.49 | 0.65 |
| 26.7 kDa heat shock protein, chloroplastic | B8A8L8_ORYSI (+1) | OsI_02088 | 0.49 | 0.63 |
| Uncharacterized protein | A2XU61_ORYSI (+1) | OsI_16135 | 0.47 | 0.64 |
| DnaK family protein, putative, expressed | A2YA91_ORYSI | OsI_22003 | 0.44 | 0.54 |
| Heat shock protein 81-3 | RCA_ORYSJ | RCA | 0.51 | 0.46 |
| Uncharacterized protein | A2X6N1_ORYSI (+1) | OsI_07870 | 0.41 | 0.56 |
| Hsp90 protein, expressed | A2WT25_ORYSI (+1) | OsI_03015 | 0.46 | 0.43 |
| Uncharacterized protein | Q5KQH5_ORYSJ | Os05g0482700 | 0.45 | 0.43 |
| Ubiquinol oxidase | A2YML1_ORYSI (+1) | OsI_26463 | 0.37 | 0.40 |
| Uncharacterized protein | A2XME9_ORYSI (+1) | OsI_13699 | 0.30 | 0.45 |
| Ubiquinol oxidase | Q6AVZ8_ORYSJ | prx65 | 0.12 | 0.61 |
| Aldehyde dehydrogenase | Q53N83_ORYSJ | Os11g0242800 | 0.25 | 0.44 |
| Glutathione S-transferase, N-terminal domain containing protein, expressed | B8AK72_ORYSI (+1) | OsI_13603 | 0.28 | 0.41 |
| Isocitrate lyase | A2YG12_ORYSI (+1) | OsI_24055 | 0.23 | 0.45 |
| WD40-like Beta Propeller Repeat family protein, expressed | PSBQ_ORYSI (+1) | OsI_025465 | 0.27 | 0.35 |
| Uncharacterized protein | B8ANZ3_ORYSI (+1) | OsI_11442 | 0.04 | 0.55 |
| Uncharacterized protein | SCRK2_ORYSI (+1) | FRK2 | 0.22 | 0.29 |
| Hsp18.0 | FTSH1_ORYSJ | FTSH1 | 0.11 | 0.39 |
| Uncharacterized protein | B8BPH4_ORYSI (+1) | OsI_38224 | 0.01 | 0.46 |
| secretory protein, putative, expressed | A2Z764_ORYSI (+1) | OsI_33538 | 0.04 | 0.43 |
| Uncharacterized protein | B8A6V4_ORYSI | OsI_03121 | 0.40 | 0.05 |
| Uncharacterized protein | ATPE_ORYSI (+1) | atpE | 0.01 | 0.43 |
| Uncharacterized protein | FENR1_ORYSJ | Os06g0107700 | 0.13 | 0.31 |
| Uncharacterized protein | Q6YU90_ORYSJ | B1370C05 | 0.02 | 0.41 |
| glycosyl hydrolases family 17, putative, expressed | B8APA6_ORYSI (+1) | OsI_10180 | 0.04 | 0.32 |
| Thioredoxin H1 | A2YMJ8_ORYSI (+1) | OsI_26450 | 0.01 | 0.35 |
| Uncharacterized protein | A2YHE6_ORYSI (+1) | OsI_24612 | 0.03 | 0.32 |
| Uncharacterized protein | B8AWG8_ORYSI (+1) | OsI_20926 | 0.14 | 0.18 |
| Uncharacterized protein | CHLI_ORYSI (+1) | CHLI | 0.04 | 0.28 |
| Uncharacterized protein | Q6ZFJ3_ORYSJ | OJ1435_F07 | 0.02 | 0.29 |
| Uncharacterized protein | METK1_ORYSI (+1) | SAM1 | 0.01 | 0.29 |
| monodehydroascorbate reductase, putative, expressed | OMT1_ORYSJ | COMT | 0.01 | 0.22 |
| 18.0 kDa class II heat shock protein | Q8S1N3_ORYSJ | Os01g0868900 | 0.19 | 0.02 |
| Catalase | Q8W3J0_ORYSJ | UXS-3 | 0.01 | 0.18 |
| Probable plastid-lipid-associated protein 2, chloroplastic | CYF_ORYSI (+1) | petA | 0.01 | 0.17 |
| Uncharacterized protein | A0A0P0V9Q4_ORYSJ (+6) | Os01g0819400 | 0.08 | 0.09 |
| Chitinase 1, putative, expressed | B8AYU7_ORYSI | AKR4 | 0.08 | 0.09 |
| Sucrose synthase | A2WV25_ORYSI (+1) | OsI_03735 | 0.09 | 0.08 |
| Mitochondrial Rho GTPase | A2XHR1_ORYSI | OsI_11950 | 0.11 | 0.05 |
| Uncharacterized protein | A2YVK0_ORYSI (+3) | OsI_29358 | 0.08 | 0.08 |
| Superoxide dismutase [Mn], mitochondrial | Q5UJF9_ORYSI (+1) | CAS | 0.08 | 0.08 |
| Formate dehydrogenase 1, mitochondrial | Q653Z1_ORYSJ | Os06g0663800 | 0.09 | 0.07 |
| V-type proton ATPase subunit C | B8BAC6_ORYSI (+1) | OsI_27610 | 0.07 | 0.08 |
| Os12g0478100 protein (Fragment) | Q7XXS4_ORYSJ | THI1 | 0.07 | 0.08 |
| Uncharacterized protein | B8AU72_ORYSI | OsI_17350 | 0.08 | 0.07 |
| Fiber protein Fb19, putative, expressed | B8AL26_ORYSI (+1) | OsI_10998 | 0.08 | 0.07 |
| Uncharacterized protein | A2ZK08_ORYSI (+1) | OsI_38160 | 0.07 | 0.08 |
| Uncharacterized protein | ATPF_ORYSI (+1) | atpF | 0.07 | 0.08 |
| Uncharacterized protein | PAL1_ORYSJ | PAL | 0.01 | 0.13 |
| Peroxygenase | PSBE_ORYSI (+2) | psbE | 0.07 | 0.07 |
| Uncharacterized protein | A2XVB4_ORYSI (+1) | OsI_16554 | 0.08 | 0.06 |
| NADPH-dependent FMN reductase domain containing protein, expressed | B8B1F4_ORYSI | OsI_24144 | 0.08 | 0.06 |
| Uncharacterized protein | A2Y5W6_ORYSI | OsI_20389 | 0.08 | 0.06 |
| Uncharacterized protein | GLGL1_ORYSJ | AGPL1 | 0.07 | 0.06 |
| Uncharacterized protein | A2XI59_ORYSI (+1) | OsI_12120 | 0.09 | 0.05 |
| stem-specific protein TSJT1, putative, expressed | HEM2_ORYSJ | HEMB | 0.07 | 0.06 |
| Uncharacterized protein | A2ZBV1_ORYSI (+1) | OsI_35255 | 0.06 | 0.07 |
| Uncharacterized protein | A2YWS7_ORYSI (+1) | OsI_29793 | 0.08 | 0.04 |
| Proteasome subunit beta type | A2YVL4_ORYSI | OsI_29372 | 0.06 | 0.07 |

| | | | | |
|---|---|---|---|---|
| Uncharacterized protein | A2Y992_ORYSI (+1) | OsI_21630 | 0.07 | 0.05 |
| Uncharacterized protein | PDX12_ORYSJ | PDX12 | 0.06 | 0.06 |
| Glutathione reductase, cytosolic | A2XM46_ORYSI (+1) | OsI_13588 | 0.06 | 0.06 |
| 4-hydroxy-4-methyl-2-oxoglutarate aldolase | A2Y715_ORYSI (+1) | OsI_20825 | 0.06 | 0.06 |
| WIP5 - Wound-induced protein precursor, expressed | Q6YZI2_ORYSJ | Os08g0559200 | 0.05 | 0.07 |
| Alpha-galactosidase | Q6K6A4_ORYSJ | Os02g0816800 | 0.06 | 0.06 |
| Uncharacterized protein | A0A0N7KQF3_ORYSJ | Os09g0252100 | 0.06 | 0.06 |
| Proteasome subunit alpha type-4-1 | A2Y8K1_ORYSI (+1) | OsI_21382 | 0.06 | 0.06 |
| Succinate--CoA ligase [ADP-forming] subunit beta, mitochondrial | B8B9N6_ORYSI | OsI_30253 | 0.05 | 0.06 |
| Isocitrate dehydrogenase [NAD] subunit, mitochondrial | B7F9R7_ORYSJ | Os01g0860300 | 0.06 | 0.06 |
| Proteasome subunit alpha type | PR2E2_ORYSJ | PRXIIE-2 | 0.04 | 0.07 |
| Glutamate dehydrogenase 2, mitochondrial | A2YQP2_ORYSI (+1) | OsI_27611 | 0.05 | 0.06 |
| Lactoylglutathione lyase | PORB_ORYSJ | PORB | 0.07 | 0.04 |
| Gamma-aminobutyrate transaminase 1, mitochondrial | Q69YA2_ORYSJ | Os06g0196600 | 0.04 | 0.07 |
| 60S acidic ribosomal protein P0 | F16P2_ORYSI (+1) | OsI_04558 | 0.04 | 0.06 |
| Plasma membrane ATPase | B8BMN2_ORYSI | OsI_38846 | 0.05 | 0.05 |
| Uncharacterized protein | Q6YUR8_ORYSJ | CSP1 | 0.06 | 0.05 |
| Uncharacterized protein | A2XNE7_ORYSI (+1) | OsI_14085 | 0.05 | 0.05 |
| NAD dependent epimerase/dehydratase family protein, putative, expressed | A2XIT5_ORYSI (+1) | OsI_12345 | 0.06 | 0.05 |
| Alcohol dehydrogenase 1 | B8AVI5_ORYSI (+1) | OsI_16279 | 0.05 | 0.05 |
| Uncharacterized protein | B8AU70_ORYSI (+1) | OsI_17346 | 0.05 | 0.04 |
| cysteine desulfurase 1, mitochondrial precursor, putative, expressed | Q6ER67_ORYSJ | Os02g0321900 | 0.05 | 0.05 |
| Uncharacterized protein | A2XF65_ORYSI | OsI_11006 | 0.04 | 0.05 |
| Glutathione peroxidase | IF4G1_ORYSJ | Os04g0499300 | 0.05 | 0.04 |
| Arginase 1, mitochondrial | A0A0P0WXJ2_ORYSJ | Os06g0538900 | 0.05 | 0.05 |
| Uncharacterized protein | A2Z2X9_ORYSI (+2) | OsI_28791 | 0.05 | 0.04 |
| rRNA N-glycosidase | GLU2A_ORYSJ | Os03g0216600 | 0.03 | 0.06 |
| Pyruvate dehydrogenase E1 component subunit beta | A2XHP8_ORYSI (+1) | OsI_11938 | 0.03 | 0.05 |
| Uncharacterized protein | B8APG3_ORYSI | OsI_11487 | 0.05 | 0.04 |
| Uncharacterized protein | B8B5K7_ORYSI (+1) | OsI_27219 | 0.04 | 0.05 |
| Uncharacterized protein | A2Z9K4_ORYSI (+1) | OsI_34414 | 0.05 | 0.04 |
| Uncharacterized protein | Q75I27_ORYSJ | OSJNBa0004G03 | 0.02 | 0.06 |
| Dehydroascorbate reductase | HEM3_ORYSJ | HEMC | 0.04 | 0.04 |
| Uncharacterized protein | B8A8C8_ORYSI (+1) | OsI_03466 | 0.04 | 0.04 |
| Chaperonin | B7E4J4_ORYSJ (+1) | Os05g0382600 | 0.04 | 0.04 |
| Chaperone protein ClpB2, chloroplastic | A0A0N7KG02_ORYSJ (+2) | Os02g0720900 | 0.04 | 0.04 |
| Uncharacterized protein | Q75PK7_ORYSJ | UXS-2 | 0.03 | 0.04 |
| Superoxide dismutase [Cu-Zn] 2 | A2WJQ6_ORYSI (+1) | OsI_00053 | 0.03 | 0.04 |
| Phosphoglycerate kinase | A2ZLP6_ORYSI (+1) | OsI_38742 | 0.03 | 0.04 |
| Phosphoglycerate kinase | A2ZAT7_ORYSI (+2) | OsI_34873 | 0.04 | 0.04 |
| Uncharacterized protein | CGEP_ORYSJ | GEP | 0.03 | 0.04 |
| Uncharacterized protein | A2XEP1_ORYSI (+1) | OsI_10803 | 0.02 | 0.05 |
| Harpin binding protein 1, putative, expressed | B8BFP6_ORYSI (+1) | OsI_32713 | 0.04 | 0.03 |
| Glyceraldehyde-3-phosphate dehydrogenase 1, cytosolic | A2X2T0_ORYSI (+1) | OsI_06495 | 0.03 | 0.03 |
| OSJNBa0072K14.5 protein | Q10A77_ORYSJ | LOC_Os10g01044 | 0.04 | 0.02 |
| Carboxymethylenebutenolidase-like protein | Q9LKM3_ORYSI | RPLD3 | 0.02 | 0.03 |
| Malate dehydrogenase | B8B9Z2_ORYSI (+1) | PFP-ALPHA | 0.03 | 0.03 |
| 6-phosphogluconate dehydrogenase, decarboxylating 1 | A2WP63_ORYSI | OsI_01632 | 0.03 | 0.03 |
| Fructose-bisphosphate aldolase | 4CL3_ORYSJ (+1) | 4CL3 | 0.02 | 0.03 |
| UDP-glucose pyrophosphorylase | A2Y986_ORYSI | OsI_21624 | 0.03 | 0.03 |
| Malate dehydrogenase, cytoplasmic | Q6ASX7_ORYSJ | Os03g0670700 | 0.02 | 0.02 |
| Glyceraldehyde-3-phosphate dehydrogenase | Q0IWS0_ORYSJ | Os10g0492300 | 0.03 | 0.02 |
| 2-Cys peroxiredoxin BAS1, chloroplastic | B8B8E9_ORYSI (+1) | OsI_25360 | 0.03 | 0.02 |
| DnaK family protein, putative, expressed | B8AEL6_ORYSI | OsI_06421 | 0.03 | 0.02 |
| 70 kDa heat shock protein | A0A0P0Y248_ORYSJ | Os11g0455800 | 0.02 | 0.02 |
| 26.7 kDa heat shock protein, chloroplastic | A2XDB9_ORYSI (+1) | OsI_10302 | 0.02 | 0.02 |
| Uncharacterized protein | Q8GSB5_ORYSJ | OJ1477_F01 | 0.02 | 0.02 |
| DnaK family protein, putative, expressed | B8AHL5_ORYSI (+1) | PFP-ALPHA | 0.02 | 0.02 |
| Heat shock protein 81-3 | Q8LQ33_ORYSJ | Os01g0851700 | 0.02 | 0.02 |
| Uncharacterized protein | DPE1_ORYSJ | DPE1 | 0.02 | 0.01 |
| Hsp90 protein, expressed | Q5VME5_ORYSJ | Os06g0289900 | 0.01 | 0.01 |
| Uncharacterized protein | A2X345_ORYSI | OsI_06628 | 0.02 | 0.01 |
| Ubiquinol oxidase | B8AIS2_ORYSI (+1) | OsI_08964 | 0.01 | 0.01 |
| Uncharacterized protein | B8AJW3_ORYSI (+1) | OsI_13516 | 0.01 | 0.01 |
| Ubiquinol oxidase | B8AQE5_ORYSI (+1) | OsI_13267 | 0.01 | 0.01 |
| Aldehyde dehydrogenase | ACT2_ORYSJ | ACT2 | 0.01 | 0.01 |
| Glutathione S-transferase, N-terminal domain containing protein, | A2XVK1_ORYSI (+1) | OsI_16658 | 0.00 | 0.00 |

| | | | | |
|---|---|---|---|---|
| expressed | | | | |
| Isocitrate lyase | A2YI66_ORYSI | OsI_24900 | 2.51 | 0.08 |
| WD40-like Beta Propeller Repeat family protein, expressed | Q6Z8F4_ORYSJ (+1) | Os02g0698000 | 1.48 | 0.72 |
| Uncharacterized protein | A2XKY8_ORYSI (+1) | OsI_13132 | 0.71 | 19.78 |
| Uncharacterized protein | IMA1A_ORYSJ | Os01g0253300 | 0.09 | 14.51 |
| Hsp18.0 | Q688M9_ORYSJ | Os05g0399100 | 0.09 | 11.82 |
| Uncharacterized protein | A2XSR2_ORYSI (+1) | OsI_15649 | 0.09 | 14.26 |
| secretory protein, putative, expressed | A2ZJA6_ORYSI (+1) | OsI_37905 | 0.06 | 16.65 |
| Uncharacterized protein | Q0DEF1_ORYSJ | KMK0024M20 | 0.06 | 2.71 |
| Uncharacterized protein | B8B9C4_ORYSI (+1) | OsI_30128 | 0.04 | 3.22 |
| Uncharacterized protein | A2XZP5_ORYSI (+2) | OsI_18204 | 0.04 | 1.61 |

**Trends in abundance of proteins in rice subjected to temperature stresses and recovery**

To identify the statistical significance of expression changes, a series of separate comparisons of expression proteins between chosen condition pairs in Koshihikari and Samnam were performed, respectively.

**1) Normal condition versus cold stress treatment**

Pairwise comparison of leaves under normal condition and cold stressed leaves resulted in identification of cold stress responsive proteins. More proteins were differentially expressed in response to cold stress in Koshihikari than in Samnam (**Figure 2-3A**). The most notably differentially expressed proteins in both cultivars exposed to cold stress were involved in metabolic process and oxidation-reduction process (**Figure 2-4**).

**2) Normal condition versus recovery after cold stress**

Pairwise comparison of leaves under normal condition and recovery after cold stress resulted in identification of recovery related proteins. More proteins were differentially expressed under recovery after cold stress in Koshihikari than in Samnam (**Figure 2-3B**). The most notably differentially expressed proteins in both cultivars under recovery after cold stress were involved in metabolic process and oxidation-reduction process (**Figure 2-5**).

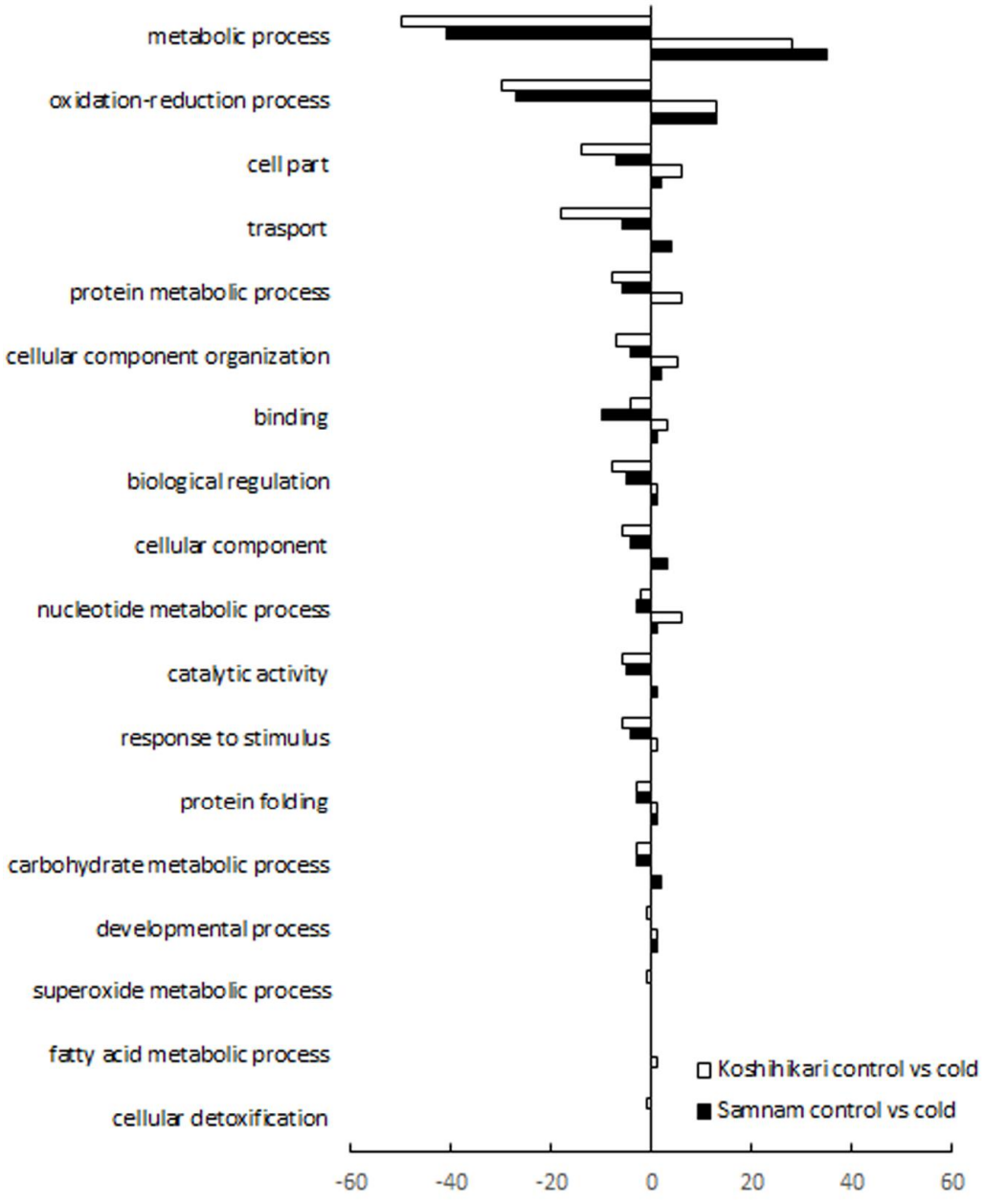


**Figure 2-4. Comparison and classification of unique proteins expressed in Koshihikari or Samnam of control condition with cold stress.**

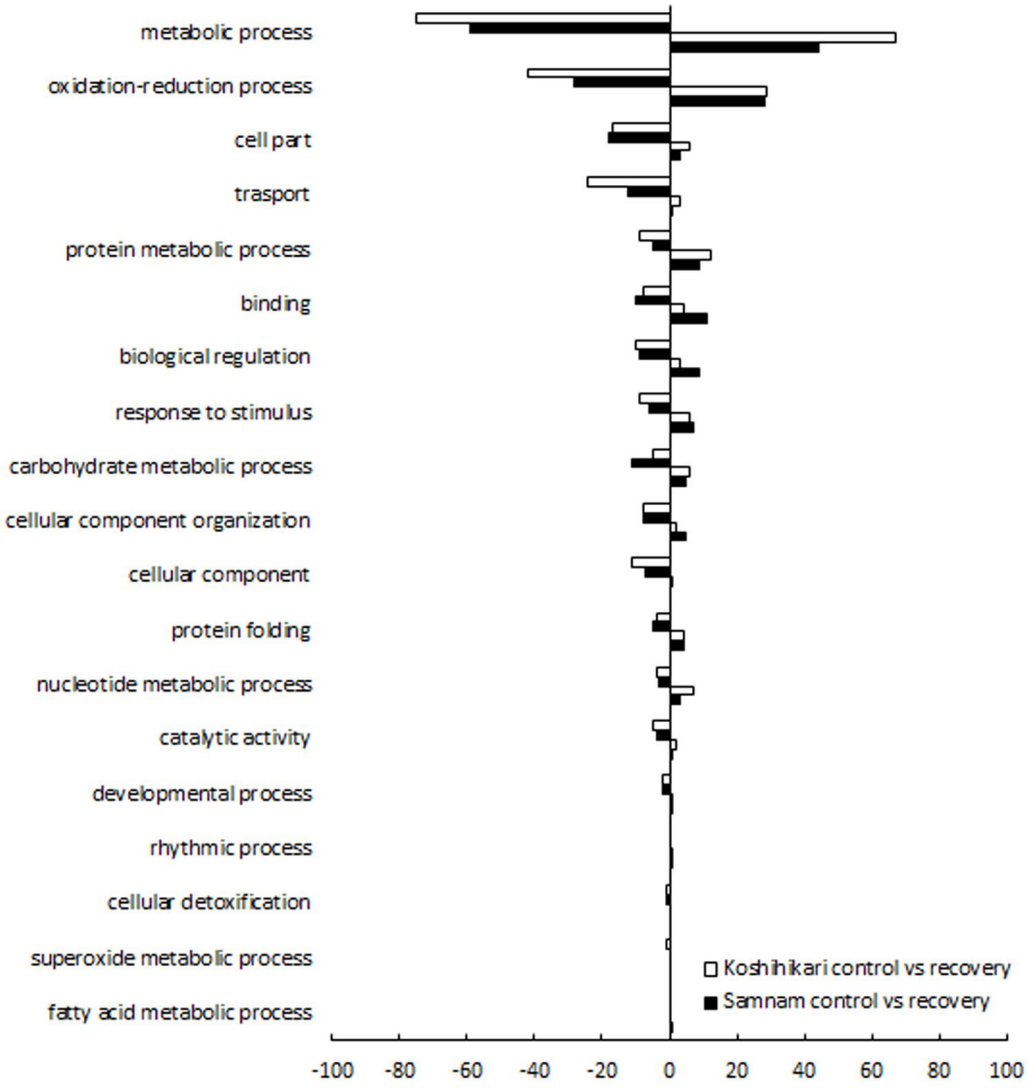


**Figure 2-5. Comparison and classification of unique proteins expressed in Koshihikari or Samnam of control condition with recovery after cold stress.**

**3) Cold stress versus recovery after cold stress**

Pairwise comparisons using cold stress as a reference were carried out to identify the proteins differentially expressed under the recovery condition. The number of differentially expressed proteins increased more than 1.6-fold in both cultivars after 5 days of recovery (**Figure 2-3A, B**). The differentially expressed proteins were grouped into 12 classes by the expression patterns of cold stress and subsequence recovery condition (**Figure 2-6, 2-7**). Some downregulated proteins under cold stress were found upregulated during recovery, while the upregulated proteins showed low abundance. Peroxidases, ribosomal proteins, peptidase and oryzain, which were upregulated under cold stress in Koshihikari, were found to be reduced after 5 days of recovery. On the other hand, proteins involved in photosynthesis and translation such as photosystem II, chlorophyll a-b binding proteins, ribosomal proteins, eukaryotic translation initiation factor, elongation factor 1-alpha, which showed less abundance under cold stress, were found upregulated after recovery. In Samnam, decreased abundance of peroxidases and ribosomal proteins, which were upregulated under cold stress, were observed after recovery. Proteins involved in photosynthesis that were downregulated in cold stress, such as photosystem I and II, and plastid specific 30S ribosomal protein 2, showed increased abundance during recovery. However, no such changes or more severer decrease were observed in proteins, such as ribosomal

proteins, elongation factors, Mg-protoporphyrin IX monomethyl ester cyclase, and TOC75. These difference in observed protein abundance between Koshihikari and Samnam suggested that Koshihikari could adjust to environmental change efficiently than Samnam. When plants were subjected to normal condition after cold stress, Koshihikari seems to be able to rapidly modulate the expression of proteins involved in translation, chlorophyll biosynthesis and translocation targeted to chloroplast, returning them within a relatively short period to a similar level to that in the controls.

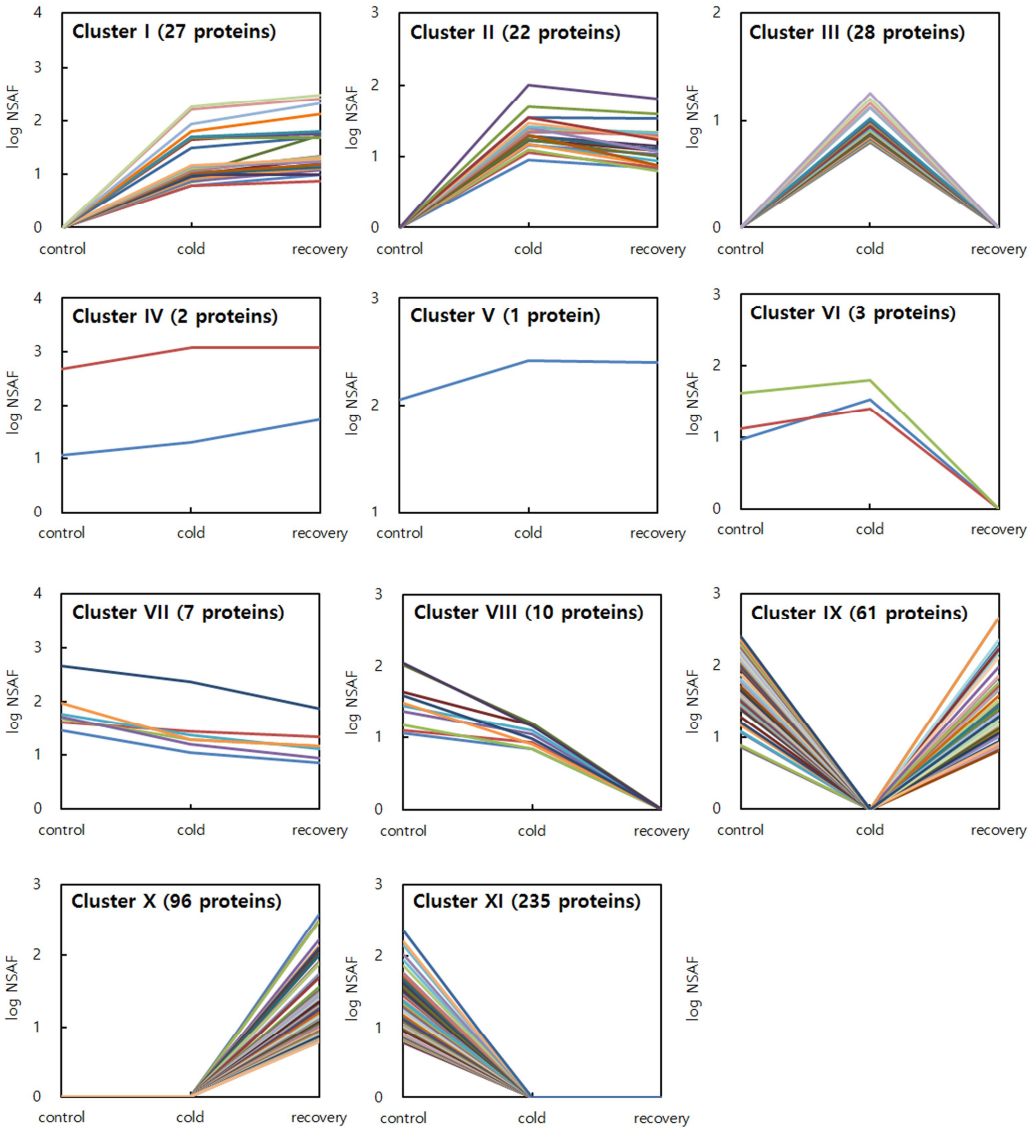


**Figure 2-6. 11 clusters identified in the analysis of proteins expressed exposed to cold stress and subsequent recovery in Koshihikari.** The log NSAF values were used for clustering.

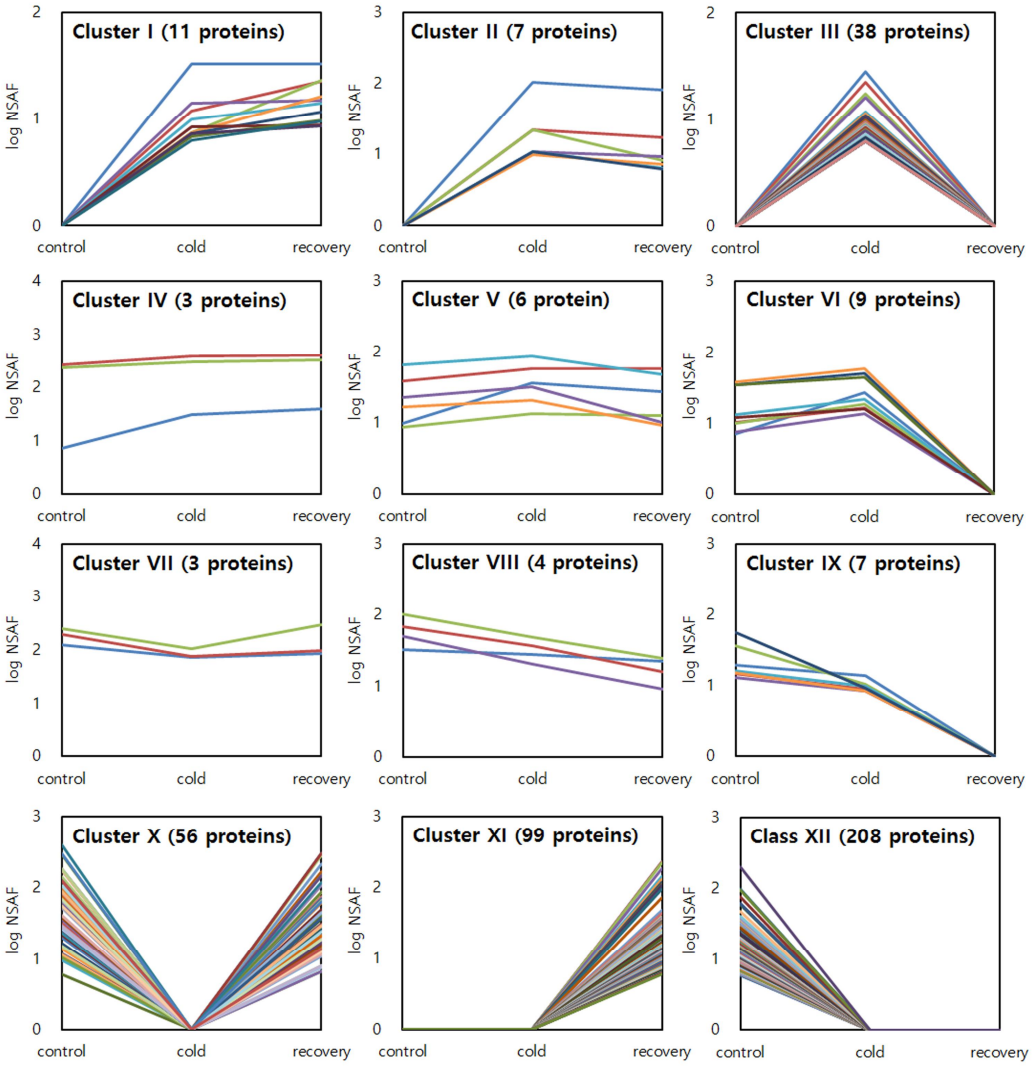


**Figure 2-7. 12 clusters identified in the analysis of proteins expressed exposed to cold stress and subsequent recovery in Samnam.** The log NSAF values were used for clustering.

**4) Normal condition versus heat stress treatment**

Pairwise comparison of leaves under normal condition and heat stressed leaves resulted in identification of heat stress responsive proteins. Although Samnam showed tolerance to heat stress, more proteins were differentially expressed in response to heat stress in Koshihikari than in Samnam (**Figure 2-3C**). The most notably differentially expressed proteins in both cultivars exposed to heat stress were involved in metabolic process, oxidation-reduction process and response to stimulus (**Figure 2-8**).

**5) Normal condition versus recovery after heat stress**

Pairwise comparison of leaves under normal condition and recovery after heat stress resulted in identification of recovery related proteins. More proteins were upregulated under recovery after heat stress in Samnam than in Koshihikari. However, more downregulated proteins were shown in Koshihikari than in Samnam (**Figure 2-3D**). The most notably differentially expressed proteins in both cultivars under recovery after heat stress were involved in metabolic process, oxidation-reduction process, and response to stimulus (**Figure 2-9**).

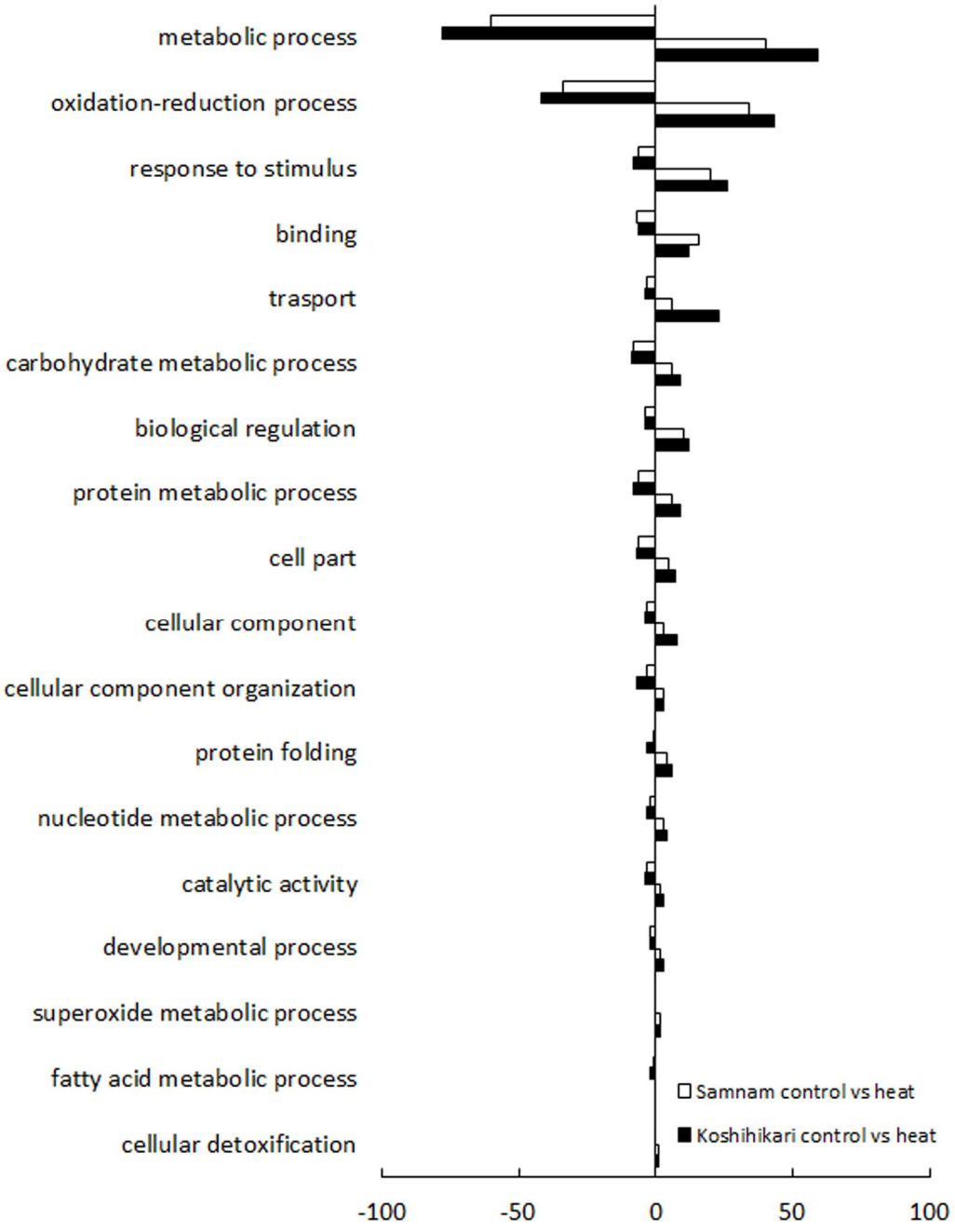


**Figure 2-8. Comparison and classification of unique proteins expressed in Koshihikari or Samnam of control condition with heat stress.**

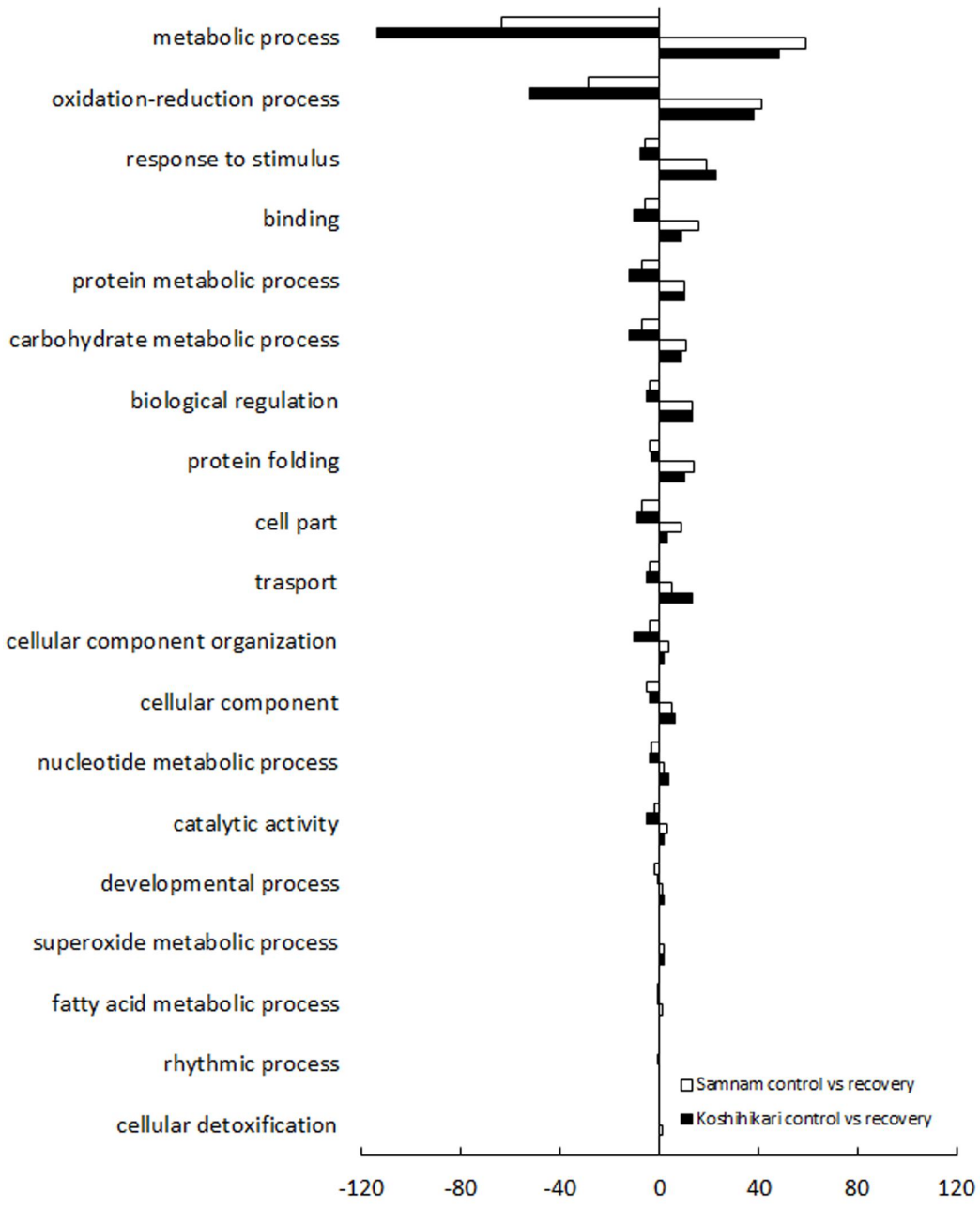


**Figure 2-9. Comparison and classification of unique proteins expressed in Koshihikari or Samnam of control condition with recovery after heat stress.**

**6) Heat stress versus recovery after heat stress**

Pairwise comparisons using heat stress as a reference were carried out to identify the proteins differentially expressed under the recovery condition. The number of differentially expressed proteins were slightly increased in both cultivars after 5 days of recovery (**Figure 2-3C, D**). The differentially expressed proteins were grouped into 12 classes by the expression patterns of heat stress and subsequence recovery condition (**Figure 2-10, 2-11**). Some downregulated proteins under heat stress were found upregulated during recovery, while the upregulated proteins showed low abundance. Heat shock proteins (HSPs), such as 18.0 kDa class II HSP, 16.9 kDa class I HSP, 17.7 kDa class I HSP, chaperonins and stress-related protein, which were upregulated under heat stress in Samnam, were found to be reduced after 5 days of recovery. On the other hand, proteins involved in photosynthesis, such as ferredoxin-dependent glutamate synthase, chlorophyll a-b binding protein, and oxygen-evolving enhancer protein 3, which showed less abundance under heat stress, were found upregulated after recovery. In Koshihikari, decreased abundance of heat shock proteins, chaperonins, and stress-related proteins, which were upregulated under heat stress, were observed after recovery similar to that of Samnam. On the other hand, proteins photosynthesis-related proteins that were downregulated in heat stress showed increased abundance during recovery similar to that of Samnam. However, no

such changes or even severer decrease were observed in proteins involved in oxidation-reduction process and energy metabolic process, such as peroxidase, cytochrome f, ferredoxin-NADP reductase, 2,3-bisphosphoglycerate-independent phosphoglycerate mutase, phosphoribulokinase, UDP-glucose pyrophosphorylase, ribulose-phosphate 3-epimerase, and fructose-bisphosphate aldolase. Moreover, a severer decrease were also shown in a number of photosynthesis-related proteins. These difference in observed protein abundance between Samnam and Koshihikari suggested that Samnam could adjust to heat stress efficiently than Koshihikari. When plants were subjected to normal condition after heat stress, Samnam seems to be able to rapidly modulate the expression of proteins involved in oxidation-reduction process and energy metabolism process, returning them within a relatively short period to a similar level to that in the controls.

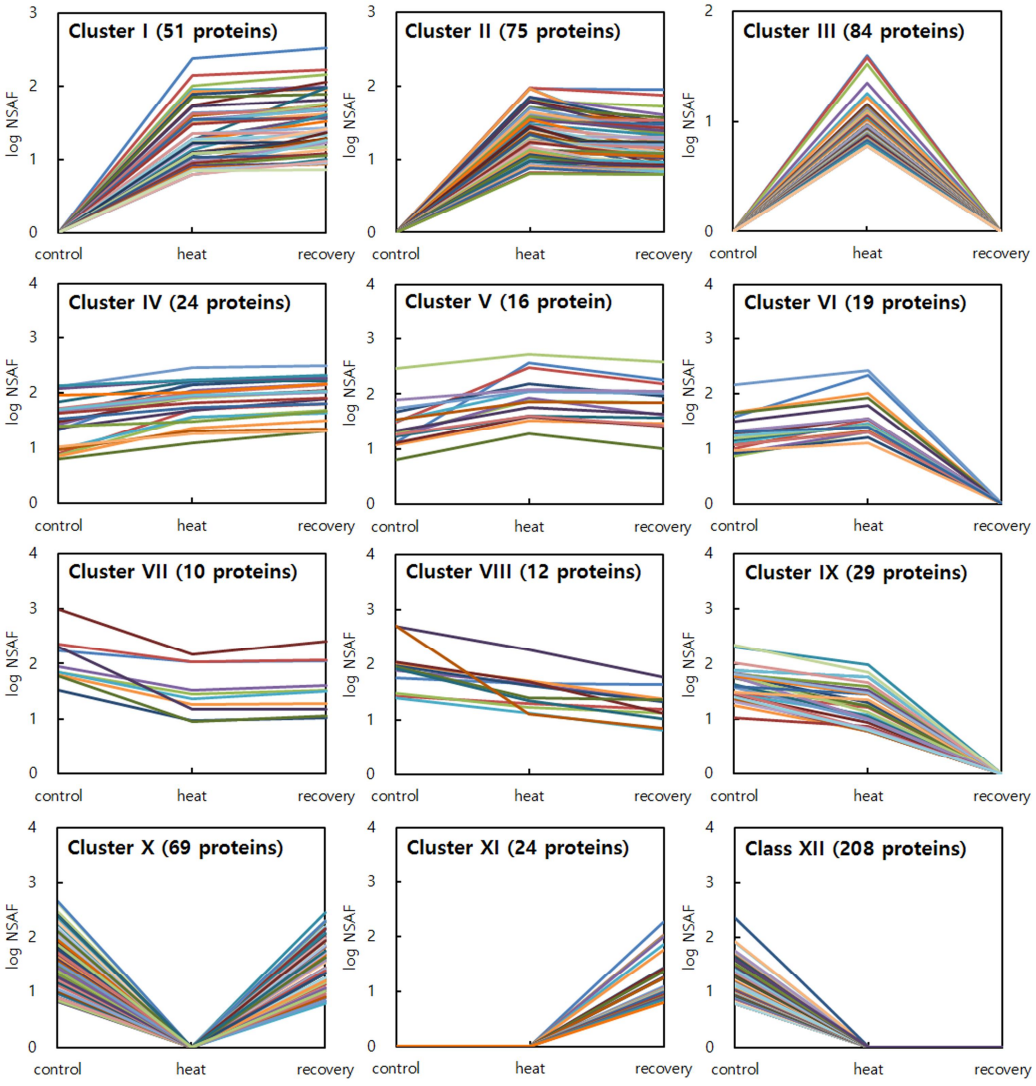


**Figure 2-10. 12 clusters identified in the analysis of proteins expressed exposed to heat stress and subsequent recovery in Koshihikari.** The log NSAF values were used for clustering.

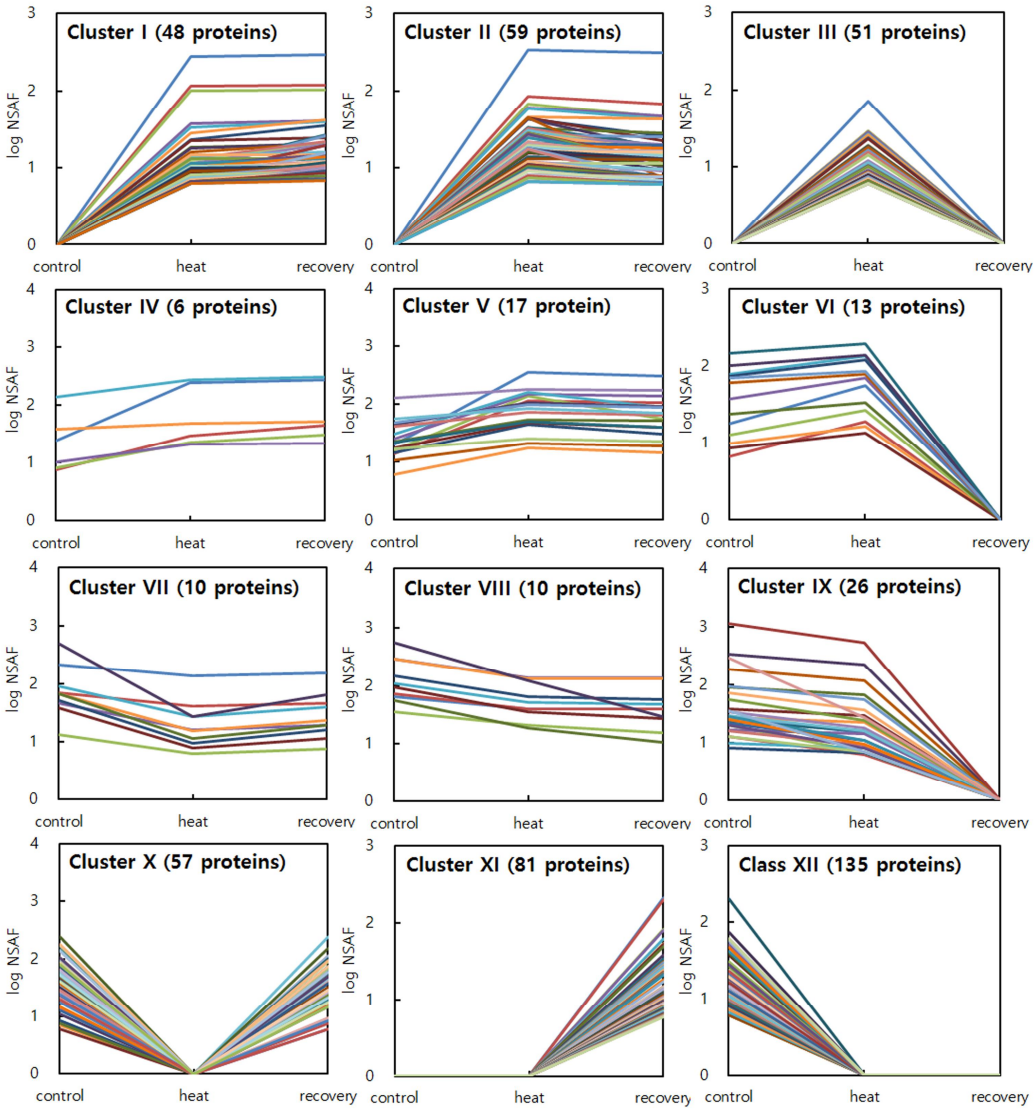


**Figure 2-11. 12 clusters identified in the analysis of proteins expressed exposed to heat stress and subsequent recovery in Samnam.** The log NSAF values were used for clustering.

# CONCLUDING REMARKS

The objective of this study was to analyze proteins and biochemical pathways involved in temperature stress response in two contrasting rice cultivars. Proteomic analysis were employed to investigate differential protein abundance patterns in response to temperature stresses, including cold and heat, followed by recovery. In this study, specific molecular responses related to translation and photosynthesis were clearly recognized in Koshihikari exposed to cold stress. On the other hand, specific molecular responses related to oxidation-reduction and energy metabolism process were clearly recognized in Samnam expose to heat stress. In summary, the results of our study have allowed us to perform a detailed comparison of differentially expressed proteins between two contrasting cultivars exposed to cold and heat stress conditions. This study has provided a number of valuable molecular insights into temperature stress responses in rice and generated large number of candidate proteins that can form the basis of further detailed study.

`

# REFERENCE


Agrawal, G. K., Jwa, N.-S., and Rakwal, R. (2000). A novel rice (Oryza sativa L.) acidic PR1 gene highly responsive to cut, phytohormones, and protein phosphatase inhibitors. *Biochemical and biophysical research communications* 274, 157–165.

Arnon, D. (1949). Estimation of Total chlorophyll. *Plant Physiology* 24, 1–15.

Asai, T., Tena, G., Plotnikova, J., Willmann, M. R., Chiu, W.-L., Gomez-Gomez, L., et al. (2002). MAP kinase signalling cascade in Arabidopsis innate immunity. *Nature* 415, 977.

Badowiec, A., and Weidner, S. (2014). Proteomic changes in the roots of germinating Phaseolus vulgaris seeds in response to chilling stress and post-stress recovery. *Journal of plant physiology* 171, 389–398.

Boch, J., Verbsky, M. L., Robertson, T. L., Larkin, J. C., and Kunkel, B. N. (1998). Analysis of resistance gene-mediated defense responses in Arabidopsis thaliana plants carrying a mutation in CPR5. *Molecular Plant-Microbe Interactions* 11, 1196–1206.

Bowling, S. A., Clarke, J. D., Liu, Y., Klessig, D. F., and Dong, X. (1997). The cpr5 mutant of Arabidopsis expresses both NPR1-dependent and NPR1-independent resistance. *The plant cell* 9, 1573–1584.

Bryngelsson, T., and Green, B. (1989). Characterization of a pathogenesis-related, thaumatin-like protein isolated from barley challenged with an incompatible race of mildew. *Physiological and molecular plant pathology* 35, 45–52.

Carriger, S., and Vallée, D. (2007). More crop per drop. *Rice Today* 6, 10–13.

Change, I. P. O. C. (2007). Climate change 2007: The physical science basis. *Agenda* 6, 333.

Chen, C., Song, Y., Zhuang, K., Li, L., Xia, Y., and Shen, Z. (2015). Proteomic analysis of copper-binding proteins in excess copper-stressed roots of two rice (Oryza sativa L.) varieties with different Cu tolerances. *PLoS One* 10, e0125367.

Chen, X., Hao, L., Pan, J., Zheng, X., Jiang, G., Jin, Y., et al. (2012). SPL5, a cell death and defense-related gene, encodes a putative splicing factor 3b subunit 3 (SF3b3) in rice. *Molecular breeding* 30, 939–949.

Chin, J.-H., Kim, J.-H., Jiang, W., Chu, S.-H., Woo, M.-O., Han, L., et al. (2007). Identification of subspecies-specific STS markers and their association with segregation distortion in rice (Oryza sativa L.). *J Crop Sci Biotech* 10, 175–184.

Cohen, J., Screen, J. A., Furtado, J. C., Barlow, M., Whittleston, D., Coumou, D., et al. (2014). Recent Arctic amplification and extreme mid-latitude weather. *Nature geoscience* 7, 627.

Cui, S., Huang, F., Wang, J., Ma, X., Cheng, Y., and Liu, J. (2005). A proteomic analysis of cold stress responses in rice seedlings. *Proteomics* 5, 3162–3172.

Dangl, J. L., and Jones, J. D. (2001). Plant pathogens and integrated defence responses to infection. *nature* 411, 826.

Datta, K., Velazhahan, R., Oliva, N., Ona, I., Mew, T., Khush, G. S., et al. (1999). Over-expression of the cloned rice thaumatin-like protein (PR-5) gene in transgenic rice plants enhances environmental friendly resistance to Rhizoctonia solani causing sheath blight disease. *Theoretical and Applied Genetics* 98, 1138–1145.

de Abreu, C. E. B., dos Santos Araújo, G., de Oliveira Monteiro-Moreira, A. C., Costa, J. H., de Brito Leite, H., Moreno, F. B. M. B., et al. (2014). Proteomic analysis of salt stress and recovery in leaves of Vigna unguiculata cultivars differing in salt tolerance. *Plant cell reports* 33, 1289–

1306.

del Pozo, O., Pedley, K. F., and Martin, G. B. (2004). MAPKKKα is a positive regulator of cell death associated with both plant immunity and disease. *The EMBO Journal* 23, 3072–3082.

Dietrich, R. A., Delaney, T. P., Uknes, S. J., Ward, E. R., Ryals, J. A., and Dangl, J. L. (1994). Arabidopsis mutants simulating disease resistance response. *Cell* 77, 565–577.

Echevarría-Zomeño, S., Ariza, D., Jorge, I., Lenz, C., Del Campo, A., Jorrín, J. V., et al. (2009). Changes in the protein profile of Quercus ilex leaves in response to drought stress and recovery. *Journal of plant physiology* 166, 233–245.

Fang, H., Meng, Q., Xu, J., Tang, H., Tang, S., Zhang, H., et al. (2015). Knock-down of stress inducible OsSRFP1 encoding an E3 ubiquitin ligase with transcriptional activation activity confers abiotic stress tolerance through enhancing antioxidant protection in rice. *Plant molecular biology* 87, 441–458.

Frye, C. A., Tang, D., and Innes, R. W. (2001). Negative regulation of defense responses in plants by a conserved MAPKK kinase. *Proceedings of the National Academy of Sciences* 98, 373–378.

Gammulla, C. G., Pascovici, D., Atwell, B. J., and Haynes, P. A. (2010). Differential metabolic response of cultured rice (Oryza sativa) cells exposed to high-and low-temperature stress. *Proteomics* 10, 3001–3019.

Gammulla, C. G., Pascovici, D., Atwell, B. J., and Haynes, P. A. (2011). Differential proteomic response of rice (Oryza sativa) leaves exposed to high-and low-temperature stress. *Proteomics* 11, 2839–2850.

Gao, L., and Xiang, C.-B. (2008). The genetic locus At1g73660 encodes a putative MAPKKK and negatively regulates salt tolerance in Arabidopsis.

*Plant molecular biology* 67, 125–134.

Gao, Y., Stebbing, J., Tubei, K., Tian, L. N., Li, X. Q., and Xing, T. (2016). Response of TaFLR MAPKKK to wheat leaf rust and Fusarium head blight and the activation of downstream components. *Tropical Plant Pathology* 41, 15–23.

Gazanchian, A., Hajheidari, M., Sima, N. K., and Salekdeh, G. H. (2007). Proteome response of Elymus elongatum to severe water stress and recovery. *Journal of Experimental Botany* 58, 291–300.

Gould, K. L., Cooper, J. A., and Hunter, T. (1984). The 46,000-dalton tyrosine protein kinase substrate is widespread, whereas the 36,000-dalton substrate is only expressed at high levels in certain rodent tissues. *The Journal of cell biology* 98, 487–497.

Gray, J., Close, P. S., Briggs, S. P., and Johal, G. S. (1997). A novel suppressor of cell death in plants encoded by the Lls1 gene of maize. *Cell* 89, 25–31.

Greenberg, J. T., Guo, A., Klessig, D. F., and Ausubel, F. M. (1994). Programmed cell death in plants: a pathogen-triggered response activated coordinately with multiple defense functions. *Cell* 77, 551–563.

Greenberg, J. T., Silverman, F. P., and Liang, H. (2000). Uncoupling salicylic acid-dependent cell death and defense-related responses from disease resistance in the Arabidopsis mutant acd5. *Genetics* 156, 341–350.

Grumm, R. H. (2011). The central European and Russian heat event of July–August 2010. *Bulletin of the American Meteorological Society* 92, 1285–1296.

Gygi, S. P., Rochon, Y., Franza, B. R., and Aebersold, R. (1999). Correlation between protein and mRNA abundance in yeast. *Molecular and cellular biology* 19, 1720–1730.

Hamel, L.-P., Nicole, M.-C., Sritubtim, S., Morency, M.-J., Ellis, M., Ehlting, J.,

et al. (2006). Ancient signals: comparative genomics of plant MAPK and MAPKK gene families. *Trends in plant science* 11, 192–198.

Han, F., Chen, H., Li, X.-J., Yang, M.-F., Liu, G.-S., and Shen, S.-H. (2009). A comparative proteomic analysis of rice seedlings under various high-temperature stresses. *Biochimica et Biophysica Acta (BBA)-Proteins and Proteomics* 1794, 1625–1634.

Hanks, S. K., and Quinn, A. M. (1991). "[2] Protein kinase catalytic domain sequence database: Identification of conserved features of primary structure and classification of family members," in *Methods in enzymology* (Elsevier), 38–62.

Hao, P., Zhu, J., Gu, A., Lv, D., Ge, P., Chen, G., et al. (2015). An integrative proteome analysis of different seedling organs in tolerant and sensitive wheat cultivars under drought stress and recovery. *Proteomics* 15, 1544–1563.

Hashimoto, M., and Komatsu, S. (2007). Proteomic analysis of rice seedlings during cold stress. *Proteomics* 7, 1293–1302.

Ishikawa, A., Okamoto, H., Iwasaki, Y., and Asahi, T. (2001). A deficiency of coproporphyrinogen III oxidase causes lesion formation in Arabidopsis. *The Plant Journal* 27, 89–99.

Jagadish, S. V. K., Muthurajan, R., Oane, R., Wheeler, T. R., Heuer, S., Bennett, J., et al. (2009). Physiological and proteomic approaches to address heat tolerance during anthesis in rice (Oryza sativa L.). *Journal of experimental botany* 61, 143–156.

Jambunathan, N., Siani, J. M., and McNellis, T. W. (2001). A humidity-sensitive Arabidopsis copine mutant exhibits precocious cell death and increased disease resistance. *The Plant Cell* 13, 2225–2240.

Ji, L., Zhou, P., Zhu, Y., Liu, F., Li, R., and Qiu, Y. (2017). Proteomic Analysis of

Rice Seedlings Under Cold Stress. *The protein journal* 36, 299–307.

Jin, H., Axtell, M. J., Dahlbeck, D., Ekwenna, O., Zhang, S., Staskawicz, B., et al. (2002). NPK1, an MEKK1-like mitogen-activated protein kinase kinase kinase, regulates innate immunity and development in plants. *Developmental cell* 3, 291–297.

Jwa, N.-S., Agrawal, G. K., Rakwal, R., Park, C.-H., and Agrawal, V. P. (2001). Molecular cloning and characterization of a novel jasmonate inducible pathogenesis-related class 10 protein gene, JIOsPR10, from rice (Oryza sativa L.) seedling leaves. *Biochemical and biophysical research communications* 286, 973–983.

Kaneda, C. (1974). Response of indica japonica rice hybrids to low temperature. *SABRAO J.* 6, 17–32.

Keller, A., Nesvizhskii, A. I., Kolker, E., and Aebersold, R. (2002). Empirical statistical model to estimate the accuracy of peptide identifications made by MS/MS and database search. *Analytical chemistry* 74, 5383–5392.

Kieber, J. J., Rothenberg, M., Roman, G., Feldmann, K. A., and Ecker, J. R. (1993). CTR1, a negative regulator of the ethylene response pathway in Arabidopsis, encodes a member of the raf family of protein kinases. *Cell* 72, 427–441.

Kim, T.-W., Michniewicz, M., Bergmann, D. C., and Wang, Z.-Y. (2012). Brassinosteroid regulates stomatal development by GSK3-mediated inhibition of a MAPK pathway. *Nature* 482, 419.

Koga, H., Dohi, K., Nakayachi, O., and Mori, M. (2004). A novel inoculation method of Magnaporthe grisea for cytological observation of the infection process using intact leaf sheaths of rice plants. *Physiological and molecular plant pathology* 64, 67–72.

Krysan, P. J., Jester, P. J., Gottwald, J. R., and Sussman, M. R. (2002). An

Arabidopsis mitogen-activated protein kinase kinase kinase gene family encodes essential positive regulators of cytokinesis. *The Plant Cell* 14, 1109–1120.

Kusaba, M., Ito, H., Morita, R., Iida, S., Sato, Y., Fujimoto, M., et al. (2007). Rice NON-YELLOW COLORING1 is involved in light-harvesting complex II and grana degradation during leaf senescence. *The Plant Cell* 19, 1362–1375.

Lam, E., Kato, N., and Lawton, M. (2001). Programmed cell death, mitochondria and the plant hypersensitive response. *Nature* 411, 848.

Langebartels, C., Wohlgemuth, H., Kschieschan, S., Grün, S., and Sandermann, H. (2002). Oxidative burst and cell death in ozone-exposed plants. *Plant Physiology and Biochemistry* 40, 567–575.

Lee, D.-G., Ahsan, N., Lee, S.-H., Kang, K. Y., Bahk, J. D., Lee, I.-J., et al. (2007). A proteomic approach in analyzing heat-responsive proteins in rice leaves. *Proteomics* 7, 3369–3383.

Lee, R.-H., Wang, C.-H., Huang, L.-T., and Chen, S.-C. G. (2001). Leaf senescence in rice plants: cloning and characterization of senescence up-regulated genes. *Journal of Experimental Botany* 52, 1117–1121.

Lewis, T. S., Shapiro, P. S., and Ahn, N. G. (1998). "Signal transduction through MAP kinase cascades," in *Advances in cancer research* (Elsevier), 49–139.

Li, Z., Zhang, Y., Liu, L., Liu, Q., Bi, Z., Yu, N., et al. (2014). Fine mapping of the lesion mimic and early senescence 1 (lmes1) in rice (Oryza sativa). *Plant physiology and biochemistry* 80, 300–307.

Lim, P. O., Kim, H. J., and Gil Nam, H. (2007). Leaf senescence. *Annu. Rev. Plant Biol.* 58, 115–136.

Lin, B., and De Wit, P. J. G. (1999). Identification and characterization of a novel Arabidopsis mutant, svn1, exhibiting aberrant regulation of cell death.

*Biology of Plant–Microbe Interactions* 2, 416–421.

Lin, L.-L., Wartmann, M., Lin, A. Y., Knopf, J. L., Seth, A., and Davis, R. J. (1993). cPLA2 is phosphorylated and activated by MAP kinase. *Cell* 72, 269–278.

Liu, G.-T., Ma, L., Duan, W., Wang, B.-C., Li, J.-H., Xu, H.-G., et al. (2014). Differential proteomic analysis of grapevine leaves by iTRAQ reveals responses to heat stress and subsequent recovery. *BMC plant biology* 14, 110.

Lorrain, S., Vailleau, F., Balagué, C., and Roby, D. (2003). Lesion mimic mutants: keys for deciphering cell death and defense pathways in plants? *Trends in plant science* 8, 263–271.

Mach, J. M., Castillo, A. R., Hoogstraten, R., and Greenberg, J. T. (2001). The Arabidopsis-accelerated cell death gene ACD2 encodes red chlorophyll catabolite reductase and suppresses the spread of disease symptoms. *Proceedings of the National Academy of Sciences* 98, 771–776.

Mirzaei, M., Pascovici, D., Atwell, B. J., and Haynes, P. A. (2012). Differential regulation of aquaporins, small GTPases and V-ATPases proteins in rice leaves subjected to drought stress and recovery. *Proteomics* 12, 864–877.

Mirzaei, M., Soltani, N., Sarhadi, E., Pascovici, D., Keighley, T., Salekdeh, G. H., et al. (2011). Shotgun proteomic analysis of long-distance drought signaling in rice roots. *Journal of proteome research* 11, 348–358.

Mitin, A. (2009). Documentation of selected adaptation strategies to climate change in rice cultivation. *East Asia Rice Working Group*, 8.

Mittler, R., Vanderauwera, S., Gollery, M., and Van Breusegem, F. (2004). Reactive oxygen gene network of plants. *Trends in plant science* 9, 490–498.

Mizobuchi, R., Hirabayashi, H., Kaji, R., Nishizawa, Y., Yoshimura, A., Satoh, H., et al. (2002). Isolation and characterization of rice lesion-mimic mutants

with enhanced resistance to rice blast and bacterial blight. *Plant Science* 163, 345–353.

Mizoguchi, T., Ichimura, K., Irie, K., Morris, P., Giraudat, J., Matsumoto, K., et al. (1998). Identification of a possible MAP kinase cascade in Arabidopsis thaliana based on pairwise yeast two-hybrid analysis and functional complementation tests of yeast mutants. *FEBS letters* 437, 56–60.

Morita, R., Sato, Y., Masuda, Y., Nishimura, M., and Kusaba, M. (2009). Defect in non-yellow coloring 3, an α/β hydrolase-fold family protein, causes a stay-green phenotype during leaf senescence in rice. *The Plant Journal* 59, 940–952.

Mosher, S., Moeder, W., Nishimura, N., Jikumaru, Y., Joo, S.-H., Urquhart, W., et al. (2010). The lesion-mimic mutant cpr22 shows alterations in abscisic acid signaling and abscisic acid insensitivity in a salicylic acid-dependent manner. *Plant Physiology* 152, 1901–1913.

MURAI, M., HIROSE, S., SATo, S., and TAKEBE, M. (1991). Effects of dwarfing genes from Dee-Geo-Woo-Gen and other varieties on cool temperature tolerance at booting stage in rice. *Japanese Journal of Breeding* 41, 241–254.

Navabpour, S., Morris, K., Allen, R., Harrison, E., A-H-Mackerness, S., and Buchanan-Wollaston, V. (2003). Expression of senescence-enhanced genes in response to oxidative stress. *Journal of Experimental Botany* 54, 2285–2292.

Neilson, K. A., Ali, N. A., Muralidharan, S., Mirzaei, M., Mariani, M., Assadourian, G., et al. (2011a). Less label, more free: approaches in label-free quantitative mass spectrometry. *Proteomics* 11, 535–553.

Neilson, K. A., Mariani, M., and Haynes, P. A. (2011b). Quantitative proteomic analysis of cold-responsive proteins in rice. *Proteomics* 11, 1696–1706.

Nesvizhskii, A. I., Keller, A., Kolker, E., and Aebersold, R. (2003). A statistical model for identifying proteins by tandem mass spectrometry. *Analytical chemistry* 75, 4646–4658.

Nishihama, R., Ishikawa, M., Araki, S., Soyano, T., Asada, T., and Machida, Y. (2001). The NPK1 mitogen-activated protein kinase kinase kinase is a regulator of cell-plate formation in plant cytokinesis. *Genes & Development* 15, 352–363.

Noutoshi, Y., Kuromori, T., Wada, T., Hirayama, T., Kamiya, A., Imura, Y., et al. (2006). Loss of necrotic spotted lesions 1 associates with cell death and defense responses in Arabidopsis thaliana. *Plant molecular biology* 62, 29–42.

Park, S.-Y., Yu, J.-W., Park, J.-S., Li, J., Yoo, S.-C., Lee, N.-Y., et al. (2007). The senescence-induced staygreen protein regulates chlorophyll degradation. *The Plant Cell* 19, 1649–1664.

Prasad, P. V. V., Boote, K. J., Allen Jr, L. H., Sheehy, J. E., and Thomas, J. M. G. (2006). Species, ecotype and cultivar differences in spikelet fertility and harvest index of rice in response to high temperature stress. *Field crops research* 95, 398–411.

Qiao, Y., Jiang, W., Lee, J., Park, B., Choi, M.-S., Piao, R., et al. (2010). SPL28 encodes a clathrin-associated adaptor protein complex 1, medium subunit μ1 (AP1M1) and is responsible for spotted leaf and early senescence in rice (Oryza sativa). *New Phytologist* 185, 258–274.

Rao, K. P., Richa, T., Kumar, K., Raghuram, B., and Sinha, A. K. (2010). In silico analysis reveals 75 members of mitogen-activated protein kinase kinase kinase gene family in rice. *DNA research* 17, 139–153.

Rustérucci, C., Aviv, D. H., Holt, B. F., Dangl, J. L., and Parker, J. E. (2001). The disease resistance signaling components EDS1 and PAD4 are essential

regulators of the cell death pathway controlled by LSD1 in Arabidopsis. *The Plant Cell* 13, 2211–2224.

Sagor, G. H. M., Zhang, S., Kojima, S., Simm, S., Berberich, T., and Kusano, T. (2016). Reducing cytoplasmic polyamine oxidase activity in Arabidopsis increases salt and drought tolerance by reducing reactive oxygen species production and increasing defense gene expression. *Frontiers in plant science* 7, 214.

Salekdeh, G. H., Siopongco, J., Wade, L. J., Ghareyazie, B., and Bennett, J. (2002). Proteomic analysis of rice leaves during drought stress and recovery. *PROTEOMICS: International Edition* 2, 1131–1145.

Salinger, M. J. (2005). "Climate variability and change: past, present and future—an overview," in *Increasing Climate Variability and Change* (Springer), 9–29.

Sarhadi, E., Bazargani, M. M., Sajise, A. G., Abdolahi, S., Vispo, N. A., Arceta, M., et al. (2012). Proteomic analysis of rice anthers under salt stress. *Plant Physiology and Biochemistry* 58, 280–287.

Sarkar, N. K., Kim, Y.-K., and Grover, A. (2014). Coexpression network analysis associated with call of rice seedlings for encountering heat stress. *Plant molecular biology* 84, 125–143.

Sarowar, S., Kim, Y. J., Kim, E. N., Kim, K. D., Hwang, B. K., Islam, R., et al. (2005). Overexpression of a pepper basic pathogenesis-related protein 1 gene in tobacco plants enhances resistance to heavy metal and pathogen stresses. *Plant cell reports* 24, 216–224.

SATAKE, T. (1989). Male sterility caused by cooling treatment at the young microspore stage in rice plants: XXIX. The mechanism of enhancement in cool tolerance by raising water temperature before the critical stage. *Japanese Journal of Crop Science* 58, 240–245.

Sato, Y., Morita, R., Katsuma, S., Nishimura, M., Tanaka, A., and Kusaba, M. (2009). Two short-chain dehydrogenase/reductases, NON-YELLOW COLORING 1 and NYC1-LIKE, are required for chlorophyll b and light-harvesting complex II degradation during senescence in rice. *The Plant Journal* 57, 120–131.

Sekiguchi, Y. (1965). On a rice mutant showing particular reaction to some spotting diseases. *Preliminary report. Ann. Phytopathol. Soc. Jpn.* 30, 71–72.

Sengupta, D., Kannan, M., and Reddy, A. R. (2011). A root proteomics-based insight reveals dynamic regulation of root proteins under progressive drought stress and recovery in Vigna radiata (L.) Wilczek. *Planta* 233, 1111–1127.

Sengupta, S., and Majumder, A. L. (2009). Insight into the salt tolerance factors of a wild halophytic rice, Porteresia coarctata: a physiological and proteomic approach. *Planta* 229, 911–929.

Smith, P., and Gregory, P. J. (2013). Climate change and sustainable food production. *Proceedings of the Nutrition Society* 72, 21–28.

Song, Y., Cui, J., Zhang, H., Wang, G., Zhao, F.-J., and Shen, Z. (2013). Proteomic analysis of copper stress responses in the roots of two rice (Oryza sativa L.) varieties differing in Cu tolerance. *Plant and soil* 366, 647–658.

Sturgill, T. W., and Ray, L. B. (1986). Muscle proteins related to microtubule associated protein-2 are substrates for an insulin-stimulatable kinase. *Biochemical and biophysical research communications* 134, 565–571.

Suarez-Rodriguez, M. C., Adams-Phillips, L., Liu, Y., Wang, H., Su, S.-H., Jester, P. J., et al. (2007). MEKK1 is required for flg22-induced MPK4 activation in Arabidopsis plants. *Plant physiology* 143, 661–669.

Tanaka, R., and Tanaka, A. (2011). Chlorophyll cycle regulates the construction

and destruction of the light-harvesting complexes. *Biochimica et Biophysica Acta (BBA)-Bioenergetics* 1807, 968–976.

Tian, X., Li, X., Zhou, W., Ren, Y., Wang, Z., Liu, Z., et al. (2017). Transcription factor OsWRKY53 positively regulates brassinosteroid signaling and plant architecture. *Plant physiology*, pp–00946.

Van Loon, L. C., and Van Strien, E. A. (1999). The families of pathogenesis-related proteins, their activities, and comparative analysis of PR-1 type proteins. *Physiological and molecular plant pathology* 55, 85–97.

Vara Prasad, P. V., Craufurd, P. Q., Summerfield, R. J., and Wheeler, T. R. (2000). Effects of short episodes of heat stress on flower production and fruit-set of groundnut (Arachis hypogaea L.). *Journal of Experimental Botany* 51, 777–784.

Voelckel, C., Mirzaei, M., Reichelt, M., Luo, Z., Pascovici, D., Heenan, P. B., et al. (2010). Transcript and protein profiling identify candidate gene sets of potential adaptive significance in New Zealand Pachycladon. *BMC evolutionary biology* 10, 151.

Wang, L., Pei, Z., Tian, Y., and He, C. (2005). OsLSD1, a rice zinc finger protein, regulates programmed cell death and callus differentiation. *Molecular Plant-Microbe Interactions* 18, 375–384.

Wang, S.-H., Lim, J.-H., Kim, S.-S., Cho, S.-H., Yoo, S.-C., Koh, H.-J., et al. (2015). Mutation of SPOTTED LEAF3 (SPL3) impairs abscisic acid-responsive signalling and delays leaf senescence in rice. *Journal of experimental botany* 66, 7045–7059.

Wei, Q., Cao, H., Li, Z., Kuai, B., and Ding, Y. (2013). Identification of an AtCRN1-like chloroplast protein BeCRN1 and its distinctive role in chlorophyll breakdown during leaf senescence in bamboo (Bambusa emeiensis ‘Viridiflavus’). *Plant Cell, Tissue and Organ Culture (PCTOC)*

114, 1–10.

Wu, C., Bordeos, A., Madamba, M. R. S., Baraoidan, M., Ramos, M., Wang, G., et al. (2008). Rice lesion mimic mutants with enhanced resistance to diseases. *Molecular Genetics and Genomics* 279, 605–619.

Wu, J., Kim, S. G., Kang, K. Y., Kim, J.-G., Park, S.-R., Gupta, R., et al. (2016a). Overexpression of a pathogenesis-related protein 10 enhances biotic and abiotic stress tolerance in rice. *The plant pathology journal* 32, 552.

Wu, X.-C., Fang, C.-X., Chen, J.-Y., Wang, Q.-S., Chen, T., Lin, W.-X., et al. (2011). A proteomic analysis of leaf responses to enhanced ultraviolet-B radiation in two rice (Oryza sativa L.) cultivars differing in UV sensitivity. *Journal of Plant Biology* 54, 251.

Wu, Y., Mirzaei, M., Pascovici, D., Chick, J. M., Atwell, B. J., and Haynes, P. A. (2016b). Quantitative proteomic analysis of two different rice varieties reveals that drought tolerance is correlated with reduced abundance of photosynthetic machinery and increased abundance of ClpD1 protease. *Journal of proteomics* 143, 73–82.

Xing, Y., Du, D., Xiao, Y., Zhang, T., Chen, X., Feng, P., et al. (2016). Fine Mapping of a New Lesion Mimic and Early Senescence 2 (lmes2) Mutant in Rice. *Crop Science* 56, 1550–1560.

Xu, C., and Huang, B. (2008). Root proteomic responses to heat stress in two Agrostis grass species contrasting in heat tolerance. *Journal of Experimental Botany* 59, 4183–4194.

Yamanouchi, U., Yano, M., Lin, H., Ashikari, M., and Yamada, K. (2002). A rice spotted leaf gene, Spl7, encodes a heat stress transcription factor protein. *Proceedings of the National Academy of Sciences* 99, 7530–7535.

Yang, C.-M., Heilman, J. L., and Heilman, J. L. (1993). (42 (1): 1-11) Response of Rice (Oryza Sativa L.) to Short-term High Temperature: Growth,

Development, and Yield. *Journal of Agricultural Research of China* 42, 1–11.

Yang, P.-F., Li, X.-J., Liang, Y., Jing, Y.-X., Shen, S.-H., and Kuang, T.-Y. (2006). Proteomic analysis of the response of Liangyoupeijiu (super high-yield hybrid rice) seedlings to cold stress. *Journal of Integrative Plant Biology* 48, 945–951.

Yin, J., Zhu, X., Yuan, C., Wang, J., Li, W., Wang, Y., et al. (2015). Characterization and fine mapping of a novel vegetative senescence lethal mutant locus in rice. *Journal of Genetics and Genomics* 42, 511–514.

Zeng, L.-R., Qu, S., Bordeos, A., Yang, C., Baraoidan, M., Yan, H., et al. (2004). Spotted leaf11, a negative regulator of plant cell death and defense, encodes a U-box/armadillo repeat protein endowed with E3 ubiquitin ligase activity. *The Plant Cell* 16, 2795–2808.

Zentgraf, U., and Hemleben, V. (2008). "Molecular cell biology: are reactive oxygen species regulators of leaf senescence?," in *Progress in botany* (Springer), 117–138.

Zhong, L. J., Cheng, F. M., Wen, X., Sun, Z. X., and Zhang, G. P. (2005). The deterioration of eating and cooking quality caused by high temperature during grain filling in early-season indica rice cultivars. *Journal of Agronomy and Crop Science* 191, 218–225.

Zhou, Y., Huang, W., Liu, L., Chen, T., Zhou, F., and Lin, Y. (2013). Identification and functional characterization of a rice NAC gene involved in the regulation of leaf senescence. *BMC plant biology* 13, 132.

Zou, J., Liu, C., and Chen, X. (2011). Proteomics of rice in response to heat stress and advances in genetic engineering for heat tolerance in rice. *Plant cell reports* 30, 2155–2165.

Zurbriggen, M. D., Carrillo, N., and Hajirezaei, M.-R. (2010). ROS signaling in

the hypersensitive response: when, where and what for? *Plant signaling & behavior* 5, 393–396.

# 잎집 병반 (*SPOTTED LEAF SHEATH*) 유전자 동정 및 온도 스트레스 처리에 따른 단백질체 분석

## 초 록

식물은 생장 과정 중 다양한 스트레스에 노출된다. 동물과 달리 식물은 스트레스를 유동적으로 피할 수 없으며, 경미하고 일시적인 환경 변화에도 식물체내 생리적, 생화학적 조성이 크게 변하여 생육 전반에 악영향을 미쳐 작물 생산량 감소로 이어지기도 한다. 따라서 다양한 스트레스에 대한 저항성 품종을 육성하기 위해서는 생물적, 무생물적 스트레스의 분자적 메커니즘에 대한 이해가 필요하다.

본 실험에서는 mitogen activated protein kinase kinase kinase (MAPKKK)에 해당하며 벼 도열병균 저항성에 관여하는 *SPOTTED LEAF SHEATH* (*SLES*) 유전자를 동정하였다. 병원균 접종 이틀 후 균사의 생장 정도를 비교한 결과 정상형에서는 균사가 접종 세포뿐만 아니라 그 주위까지 널리 퍼져 있었으나 돌연변이체에서는 균사가 접종 세포 주위로 뻗어나가지 못하고 세포 내로 생장이 국한되었으며 세포 내에 암갈색 과립이 축적되어 있었다. 돌연변이체에서 활성산소

생성에 관여하는 NADPH 산화효소 유전자의 발현이 높게 나타났으며, 세포 내 활성산소 농도 또한 높게 나타났다. 일반적으로 lesion mimic mutants (LMMs)는 잎에 병반이 나타나는데 반해 *sles* mutant는 잎집에서 병반이 나타나는 특징을 보였다. 또한 *sles* mutant에서는 엽록소 분해 관련 유전자와 노화 관련 유전자의 높은 발현과 함께 잎집 내 엽육세포가 많이 손상되어 있었고, 엽록소 함량 또한 감소하였으며, 잎이 노랗게 변색되고 있는 현상을 통해 노화가 촉진되고 있음을 알 수 있었다. 이러한 사실들로부터 *SLES* 유전자가 활성산소 항상성에 관여하고 있을 것이라고 생각되며, 따라서 *sles* mutant에서는 이 유전자가 제 기능을 수행하지 못하기 때문에 세포 내 활성산소 농도가 높게 나타났으며, 이로 인해 병반을 동반한 세포 사멸이 촉진되어 도열병 균사의 생장이 억제되는 결과를 초래하였을 것이다.

생물적 스트레스 기작 연구에 이어 저온 및 고온 스트레스 그리고 스트레스 처리 후 회복 과정 중 발현되는 단백질을 동정하기 위한 실험이 진행되었다. 상대적으로 저온 저항성을 보이는 고시히까리와 상대적으로 고온 저항성을 보이는 삼남을 재료로 이용하였으며, 3 엽기 때 각각의 온도 스트레스를 처리하고 스트레스 처리에 따른 단백질

발현 양상을 관찰하였다. 스트레스 처리 전 까지 모든 벼 실생은 28/25°C에서 재배되었으며, 저온은 4°C, 고온은 42°C에서 각각 5일간 스트레스를 처리하였고, 이어서 5일간 회복 과정을 거쳤다. 각 단계별로 성숙한 잎을 수확하여 단백질 추출 및 Triple TOF MS/MS 분석을 진행하였다. 총 1192개의 단백질이 동정되었으며 이 중 500개 이상이 온도 스트레스 반응 및 회복 관련 단백질로 판명되었다. 저온 처리, 저온 처리 후 회복, 고온 처리, 고온 처리 후 회복 과정 중 고시히까리와 삼남 공통으로 발현된 단백질은 각각 82, 159, 254 그리고 250개였다. 저온 처리 및 회복 과정에서는 저온 저항성 품종인 고시히까리에서 특이적으로 발현 단백질이 각각 197, 278개였으며, 고온 스트레스 및 회복 과정 중 고온 저항성 품종인 삼남에서는 각각 104, 155개의 단백질이 특이적으로 발현하였다. 본 실험결과는 온도 스트레스 반응에 따른 단백질체 정보를 구명한 것으로서 벼의 온도 스트레스 반응에 대한 분자적 메커니즘의 이해를 넓혔으며 스트레스 저항성 품종을 육종하기 위한 중요한 자료들을 제공하고 있다.